İSTANBUL TECHNICAL UNIVERSITY ★ INSTITUTE OF SCIENCE AND TECHNOLOGY

EFFECTS OF MODE LOCALIZATION AND CURVE VEERING ON INPUT-OUTPUT DIRECTIONAL PROPERTIES OF ROTATIONALLY PERIODIC STRUCTURES

M.Sc. Thesis by

Özgür UYAR, Mechanical Eng.

Department : Mechanical Engineering

Programme: Solid Mechanics

JULY 2006

İSTANBUL TECHNICAL UNIVERSITY ★ INSTITUTE OF SCIENCE AND TECHNOLOGY

EFFECTS OF MODE LOCALIZATION AND CURVE VEERING ON INPUT-OUTPUT DIRECTIONAL PROPERTIES OF ROTATIONALLY PERIODIC STRUCTURES

M.Sc. Thesis by

Özgür UYAR, Mechanical Eng.

(503031513)

Date of submission : 8 May 2006

Date of defence examination: 14 June 2006

Supervisor (Chairman): Assoc. Prof. Dr. Ata MUĞAN

Members of the Examining Committee Prof.Dr. Tuncer TOPRAK (İTÜ)

Assoc. Prof.Dr. Haluk EROL (İTÜ)

JULY 2006

ACKNOWLEDGEMENTS

First and foremost, I would like to thank my family for always being there when I needed them. They have always believed in me. Their love, strength, and guidance have sustained me through many difficult times.

I would also like to extend my sincerest appreciation to Assoc. Prof. Ata Muğan for his hard work and dedication. He made the work here not only challenging, but also interesting. I learned a lot from him.The research topic presented here in was his idea. He guided me along the way, and yet he let me find my own path. His help, and patience, made this thesis possible. The most important thing I learned here at ITU was about the trials and tribulations of research.

Finally, I would like to thank my friends for constantly reminding me that there was life outside of ITU. You were always there when I needed to talk to someone.

Thank you.

May 2006 Özgür UYAR

Mechanical Engineer

TABLE OF CONTENTS

ABBREVIATIONS

SVD	: Singular Value Decomposition
RPS	: Rotationally Periodic Structure
HCF	: High Cycle Fatigue
DOF	: Degree of Freedom

LIST OF TABLES

No. of Page

LIST OF FIGURES

No. of Page

LIST OF SYMBOLS

k_i	**:** Stiffness of ith element
R	**:** Dimensionless coupling ratio
m	**:** Mass
g	**:** acceleration of Gravity
l	**:** Length
Δl	**:** Length deviation
λ	**:** Eigenvalue
f_i	**:** Force
θ	**:** Angle
ω	**:** Excitation frequency
F	**:** Force vector
$s = j\omega$	**:** Complex frequency
v_i	**:** Components of right singular vectors
u_i	**:** Components of left singular vectors
σ_i	**:** ith singular value
ω_{ri}, ω_{bi}	**:** ith natural frequency
A	**:** Matrix
A^H	**:** Hermitian transpose of matrix
A^T	**:** Transpose of matrix
S	**:** Real symmetric matrix, Singular value matrix
Q	**:** Orthonormal vectors
U	**:** Unitary matrix, Right singular vector matrix
V	**:** Left singular vector matrix
a	**:** Non-zero scalar number
$\Re$	**:** Real numbers
δ_{ij}	**:** Kronecker delta function
$\tilde{v}_i$	**:** Orthonormal pair of right singular vectors
$\tilde{u}_i$	**:** Orthonormal pair of left singular vectors

e_i, w_k	**:** Unit vector
Λ	**:** Positive singular value matrix
$\ddot{q}$	**:** Acceleration
$\dot{q}$	**:** Velocity
q	**:** Displacement
ς	**:** Viscous damping ratio
Δf_i	**:** Dimensionless mistuning strength for the ith component system
ϕ	**:** Phase angle
n	**:** nth blade
N	**:** Number of blades
b	**:** Viscous damping coefficent
k_b	**:** Blade stiffness
k_c	**:** Coupling stiffness
ω_b	**:** Natural frequency
G	**:** Transfer function
M	**:** Mass matrix
C	**:** Damping matrix
K	**:** Stiffness matrix
smax	**:** Max. singular value
smin	**:** Min. singular value
Ui	**:** ith left vector
Vi	**:** ith right vector
Uij	**:** ith component of jth left vector
Vij	**:** ith component of jth right vector
ε	**:** Perturbation
B	**:** Arbitrary
z	**:** Generalized eigenvector
P_i	**:** ith eigenvector

MODE LOKALLEŞMESİ VE EĞRİ YÖN DEĞİŞİMİNİN DÖNEN PERİYODİK YAPILARIN GİRDİ-ÇIKTI ÖZELLİKLERİ ÜZERİNDEKİ ETKİLERİ

ÖZET

Bu çalışmada, ilk kez tekil vektör ayrıştırma yöntemi ile yapısal sistemlerdeki düzensizliklerden kaynaklanan mod lokalleşmesi ve eğri yöndeğişiminin uçak motoru türbini gibi dönen periyodik yapıların girdi-çıktı yönsel özellikleri üzerindeki etkileri araştırılmıştır.

Çalışmanın mode localization and curve veering bölümünde, mode lokalleşmesi ve eğri yön değişimi hakkında teorik bilgiler verilmiş ve bu olaylar daha önce yapılan çalışmalardan alınan örnekler ile gösterilmiştir.

Singular value decomposition bölümünde, tekil değerler, sol tekil vektörler ve sağ tekil vektörler matematiksel olarak örneklerle açıklanmış, daha sonra tekil değer ayrıştırma yöntemi ve özellikleri anlatılmıştır. Bu bölümde yine ilk kez tekil değerler ile yapıların doğal frekansları arasındaki ilişki matematiksel olarak ispatlanmıştır. En son olarak tekil vektörlerin, girdi-çıktı yönsel özellikler ile ilişkisi açıklanmıştır.

Input-otput properties of a turbine bölümünde, üç kanatlı bir türbin modeli alınarak hareket denklemi çıkarılmış ve tekil değer ayrıştırma yönteminin uygulanacağı transfer fonksiyonu elde edilmiştir. Dönen periyodik yapılara tekil değer ayrıştırma yöntemi uygulandığında, tekil değerlerin birbirini tekrarladığı, bu tekrarlamadan kaynaklanan problemler ve çözümleri gösterilmiştir. Bu problemler giderildikten sonra türbinin analizleri düzenli ve düzensiz zayıf bağlı ve kuvvetli bağlı modeller için yapılmıştır.

Son bölüm olan sonuç bölümünde ise elde edilen sonuçlar yorumlanmıştır.

EFFECTS OF MODE LOCALIZATION AND CURVE VEERING ON INPUT-OUTPUT DIRECTIONAL PROPERTIES OF ROTATIONALLY PERIODIC STRUCTURES

SUMMARY

In this study, effects of mode localization which is caused by disorders on structures and curve veering, on input-otput directional properties of rotationally periodic structures such as jet engine turbine are examined as first.

In mode localization and curve veering section, theoritical informations about mode localization and curve veering are explained by the examples which are taken from early studies about this subject.

In singular value decomposition section, singular values, left and right singular vectors are explained as mathematically, then singular value decomposition method and properties are told. As first, mathematical proof of the relationship between singular values and structures' resonance frequencies is done. As last, relationship between singular vectors and directional properties are explained.

In input-otput properties of a turbine section, equation of motion of a three bladed turbine model is obtained and transfer function which is applied singular value decomposition method is calculated. It is shown that, repeated eigenvalue phenomena occurs, when singular value decomposition method is applied to rotationally periodic structures. It is also shown that the problems which are caused because of the repeated singular values and solution of these problems. After these problems are solved, analysis of the turbine model is done for tuned and mistuned weak coupled models and strongly coupled models.

In last section, results which are obtained from the analyses are interpreted.

1. INTRODUCTION

All mechanical systems work under dynamic loads and because of these loads, systems show various vibration movements. Vibration response of structures are related to system's phsical properties and applied forces. Hence, when a new mechanical system is designed, all of the environmental effects and physical properties of structures, such as mass, stifness, material properties, are considered constant. However, in many cases these properties are not constant and systems are not homogen. If we think about a turbine, although it is assumed that all blades have the same properties with each other, they do not. Because of the many reasons such as manufacturing defects, assembly defects, material irregularities, homogen structures becomes disordered and this disorder causes mode localization and curve veering phenomena. So, when a mechanical system is designed these effects need to be considered.

Effects of mode localization and curve veering on structures are studied in various fields from the physics to structural dynamics. Leissa [2] showed that curve veering phenomena occurs because of the mode localization. Many researches studied the effects of these phenomenas on eigenvalues and corresponding mode shapes of structures[1,3,5,10]. Muğan showed that these phenomenas also effect the input-output directional properties of periodic structures such as osscilators.

In this study, in second section mode localization and curve veering phenomenas are explained with examples. In third section theory of singular value decomposition, directional properties of singular vectors and relationship between singular values and resonance frequencies are examined mathematically. In forth section, repeated eigenvalue problem and effects of disorder, mode localization, curve veering on input-output directional properties of a turbine examined. In last section results are evaluated and new analysis techniques are obtained.

2. MODE LOCALIZATION AND CURVE VEERING

Because of defects in manufacturing and assembly, no structures designed as a periodic structure can be perfectly periodic. Disorder can occur in the geometry of configuration and material properties of the structure. The dynamical behaviour of a disordered periodic system could be significantly different from that of a perfectly periodic structure. For a perfectly periodic structure, the vibration modes are of wavy shapes and extend through the structure, whereas when the structure is disordered, vibration is confined to a small region, with the amplitudes of vibration decaying exponentially away from a center. This phenomenon is known as vibration mode localization [1].

Generally speaking, the dependence of the eigenvalues often a system parameter is often of interest in structural dynamics. This leads to a group of loci when the eigenvalues are plotted versus the system parameter. Such eigenvalue loci are known to have fascinating characteristics, which were first discovered by Leissa [2] in a pioneer paper. When two eigenvalue loci approach each other, they either cross or do not cross. Often in the latter case, even though the loci nearly intersect, in fact they do not but rather veer away from each other with high local curvature. This phenomenon, referred to as eigenvalue loci veering, or curve veering, has been throughly studied in both dynamics and physics [3].

The frequencies at which singular value veering phenomenon occurs have a special meaning as follows: two singular values are almost equal to each other at such frequencies whereas their singular vectors are completely different. It means that while the system has almost the same power and energy transmission ratios at these frequencies, forced response characteristics are quite different. Subsequently, these frequencies will be called isopower frequencies [4].

Bladed disks often feature very high mistuning sensivity for operational conditions corresponding to tuned natural frequency veering regions. Thus, special attention is given to extract tuned free response information from natural frequency veering

regions in order to model the structural system and efficiently predict the increase in forced response levels due to mistuning [5].

2.1 Examples of Mode Localization and Curve Veering

Mode localization effects of nearly periodic structures is investigated by using eigenvalue based perturbation methods and singular value decomposition method. While the eigenvalue based analyses give information about the resonance frequencies and vibration modes of a structure, singular values of the structure are related to the forced response characteristics and give the dynamic behaviour in the frequency domain. Both examples can be seen below.

2.1.1 Eigenvalue Based Analyses of Mode Localization & Curve Veering Effects

The system of two coupled ossilators shown in figue 2.1 is considered. The two important parameters are the dimensionless coupling between pendulums, $R^2 = (k/m)/(g/l)$, and the dimensionless length deviation, Δl. For $\Delta l = 0$, the system is tuned, or ordered; otherwise, it is mistuned or disordered [3].

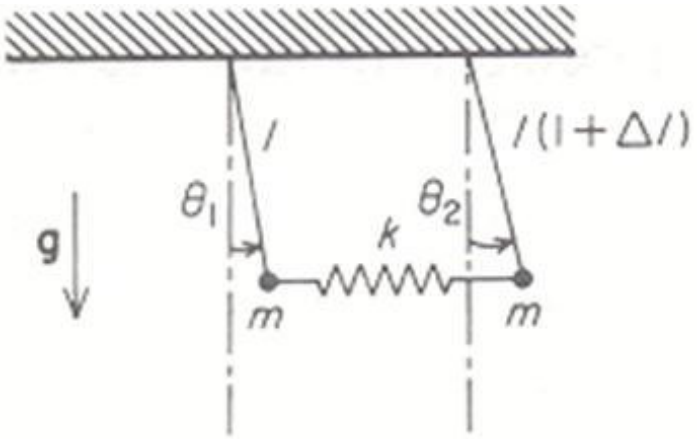

Figure 2.1 : Two coupled oscillators [3].

Figure 2.2 and 2.3 represents the loci of the two dimensionless eigenvalues versus disorder, Δl. Mode shapes of angular amplitudes are also displayed for both tuned and mistuned systems. Figure 2.2 is for a strongly coupled system such thar R=0.5. Observe that small disorder does not have much effect on both the eigenvalues and the mode shapes, as the modes of the mistuned system are merely perturbations of those of the tuned system. Also note that two eigenvalues are far apart. Now consider

figure 2.3, which is for weak coupling, R=0.025. while the mode shapes of the ordered system are still extended (in fact, this is the case for arbitrarily small coupling), the modes of the mistuned system become strongly localized about one pendulum when small disorder is intruduced, a well known phenomenon. Indeed, these localized modes are perturbations of those of the decoupled tuned system. Perhaps, less expected, the behaviour of the eigenvalues in figure 2.3 is also quite different from that in figure 2.2. One observes that for small coupling the loci seem to cross at the ordered state, although in fact they do not cross but veer abruptly from each other with high local curvatures. The loci cannnot cross becausethere is no multiple eigenvalue for the system, which results in a mutual repulsion of both loci, or curve veering. For strong interpendulum coupling no such drastic phenomenon is observed. One concludes that both strong mode localization and eigenvalue loci veering occur for weak coupling between oscillators, that is, when the eigenvalues of the ordered system are close [3].

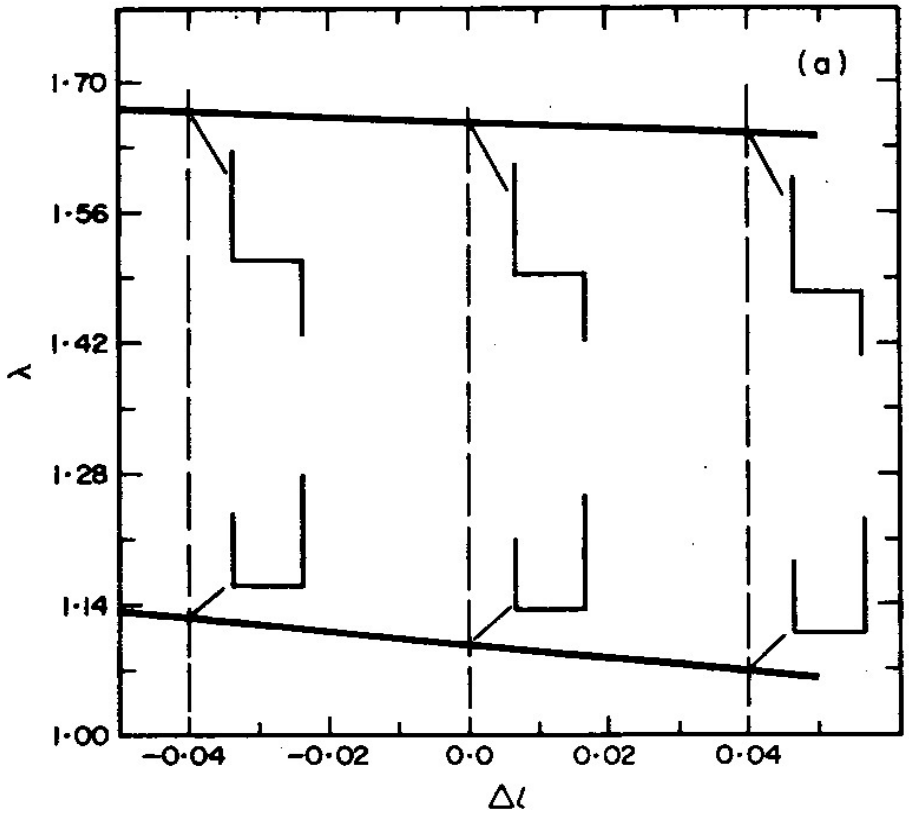

Figure 2.2 : The strong interpendulum coupling case, R=0.5; neither eigenvalue loci veering nor mode localization occur [3].

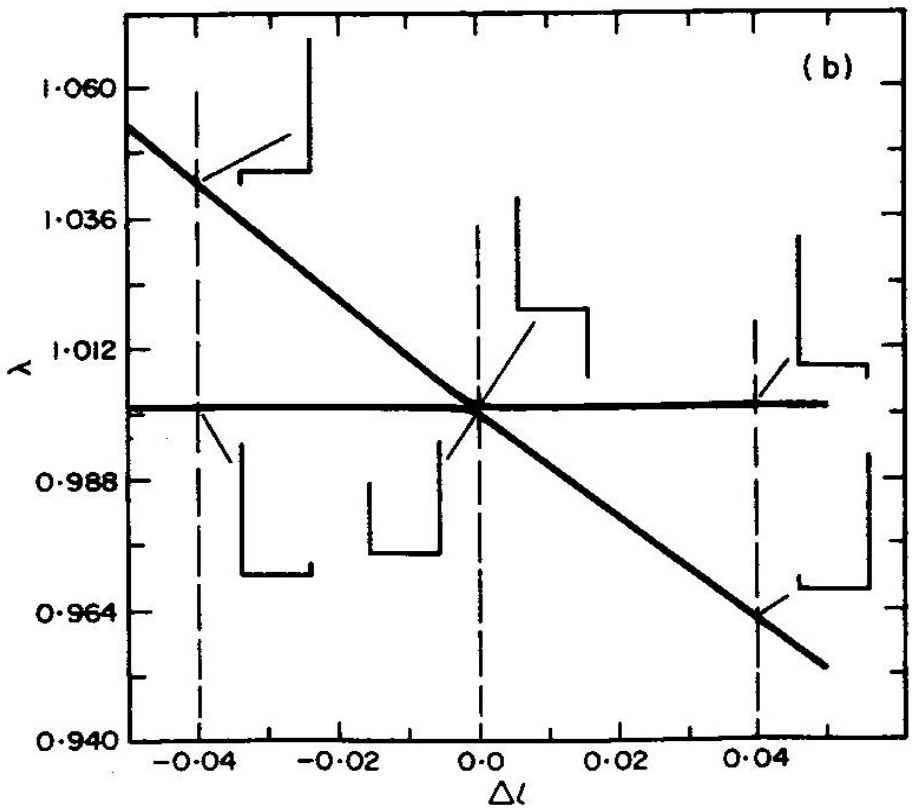

Figure 2.3 : The weak interpendulum coupling case, R=0.025; both eigenvalue loci veering and strong localization occur [3].

2.1.2 SVD Based Analyses of Mode Localization & Curve Veering Effects

Consider the disordered system of two coupled oscillators shown in figure 2.4. by using the SVD, forced response characteristics of the coupled oscillators are studied in this section. [4]

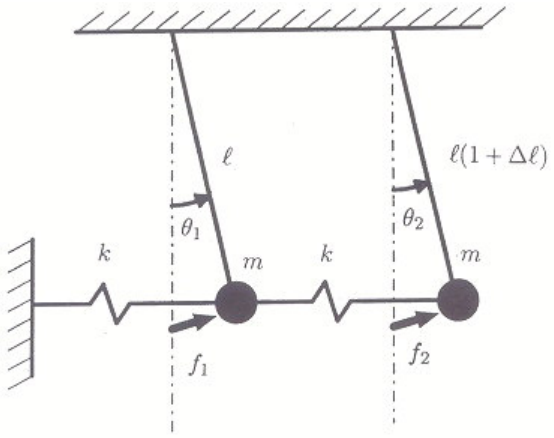

Figure 2.4 : Two coupled oscillators [4].

The governing equations of motion for small angles are as follows

$$ml^2\ddot{\theta}_1 = f_1 l - kl^2\dot{\theta}_1 - k\left(l\theta_1 - l(1+\Delta l)\theta_2\right)l - mgl\theta_1 \quad \textbf{(2.1)}$$

$$ml^2(1+\Delta l)^2\ddot{\theta}_2 = f_2 l(1+\Delta l) + k\left(l\theta_1 - l(1+\Delta l)\theta_2\right)l(1+\Delta l) - mgl(1+\Delta l)\theta_2 \quad \textbf{(2.2)}$$

By taking the laplace transform of both equations and arranging them, one gets

$$\left(\frac{l}{g}\right)s^2\theta_1(s) + \left(1+2R^2\right)\theta_1(s) - R^2(1+\Delta l)\theta_2(s) = \frac{F_1(s)}{mg} \quad \textbf{(2.3)}$$

$$\left(\frac{l}{g}\right)(1+\Delta l)s^2\theta_2(s) + \left(1+R^2(1+\Delta l)\right)\theta_2(s) - R^2\theta_1(s) = \frac{F_2(s)}{mg} \quad \textbf{(2.4)}$$

By defining $\tilde{\theta}_1 = \theta_1/(1+\Delta l)$ and $\tilde{\theta}_2 = \theta_2$ to obtain symmetric system matrices, equations 2.3 and 2.4 can be cast into the following form,

$$\tilde{\Theta}(s) = \left(Ms^2 + K\right)^{-1} F(s) \quad \textbf{(2.5)}$$

where M and K are symmetric, l is the nominal length of the pendulums, Δl the second pendulum's dimensionless length deviation from the nominal length, ω the excitation frequency, $\lambda = \omega^2/(g/l)$ the dimensionless eigenvalue, $R^2 = (k/m)/(g/l)$ the dimensionless coupling, $\tilde{\Theta}(s) = \left[\tilde{\theta}_1(s)\tilde{\theta}_2(s)\right]^T$, and $F(s) = \left[F_1(s)/(mg)\,F_1(s)/(mg)\right]^T$ For $\Delta l = 0$, the system is called tuned or ordered; otherwise, it is mistuned or disordered. Free vibration modes, mode localization and eigenvalue loci veering phenomena of this system are seen first example, where in the existence of small disorder strong mode localization is reported for weakly coupled systemswhereas mode shapes and eigenvalues of strongly coupled system do not manifest localization. Similar phenomana are observed in input-output reliationships of this system as well. [4].

The following parameter values are used in the numerical studies: $g = 10, l = 1, k = 1, m = 640$ for a weakly coupled system (R=0.0125) and k=1600 for a strongly coupled system (R=0.5). Since the system matrices M and K are symmetric in equation 2.5, right singular vectors v_i are equal to u_i. Considering the SVD of the matrix transfer function $G(s) = \left(Ms^2 + K\right)^{-1}$ of the weakly coupled system, the singular value loci σ_1 is presented in figure 2.5 and the components of

the associated left singular vectors u_1 are given in figures 2.6 and 2.7, where ω_{ri} are the natural frequencies and $u_{i,j}$ denotes the jth component of u_1. Note that while u_1 is the worst possible load case and the corresponding structural response ($u_1=v_1$ in this problem) , σ_1 is the corresponding structural power and energy transmission ratios. The peaks in singular value loci correspond to resonance frequencies. These plots show the way the system will respond to a sinusoidal excitation of frequency ω at steady state. Since there is no damping in the system, components of the singular vectors exhibit jumps at resonance frequencies [4].

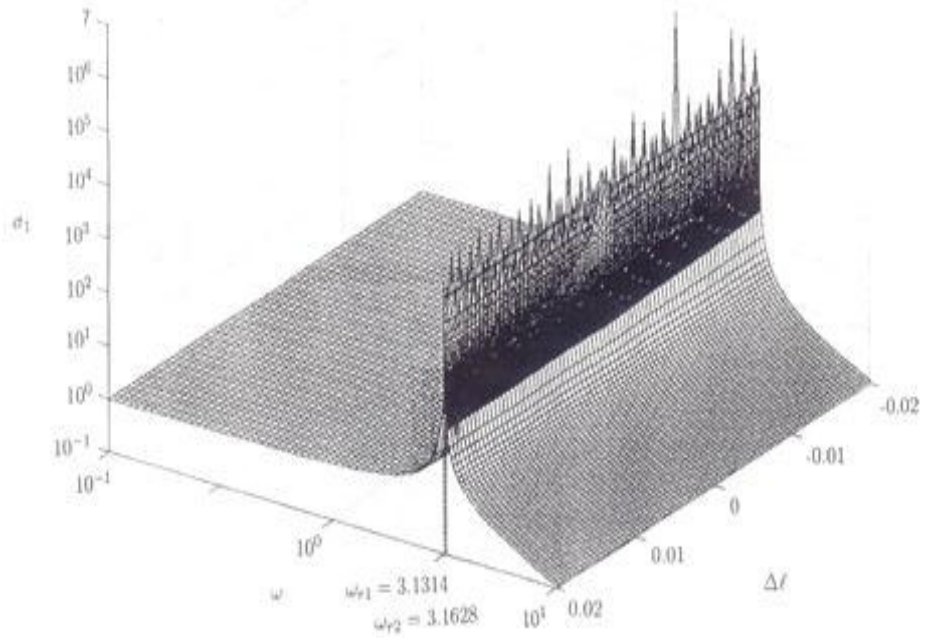

Figure 2.5 : The singular value σ_1 where R=0.0125 [4].

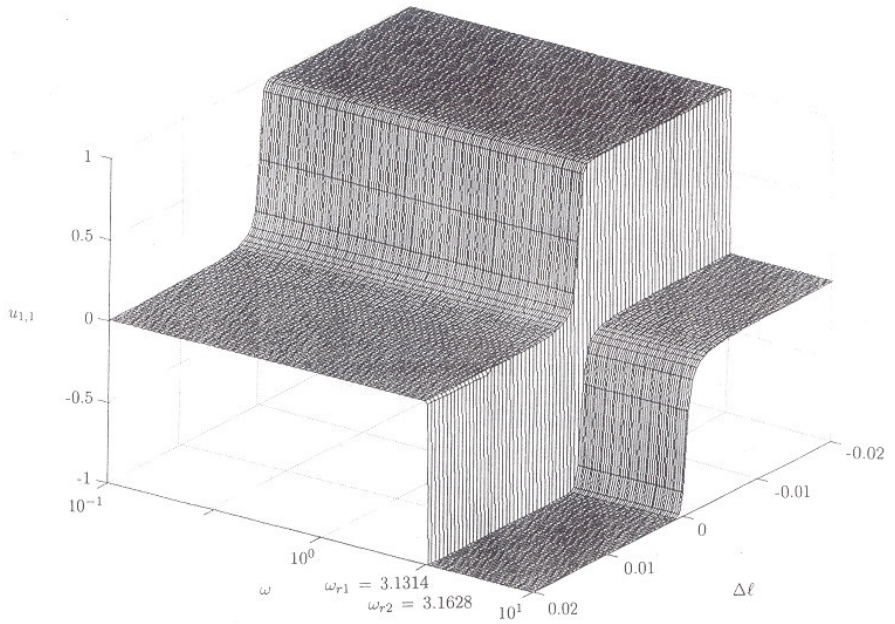

Figure 2.6 : The left singular vector component $u_{1,1}$ where R=0.0125 [4].

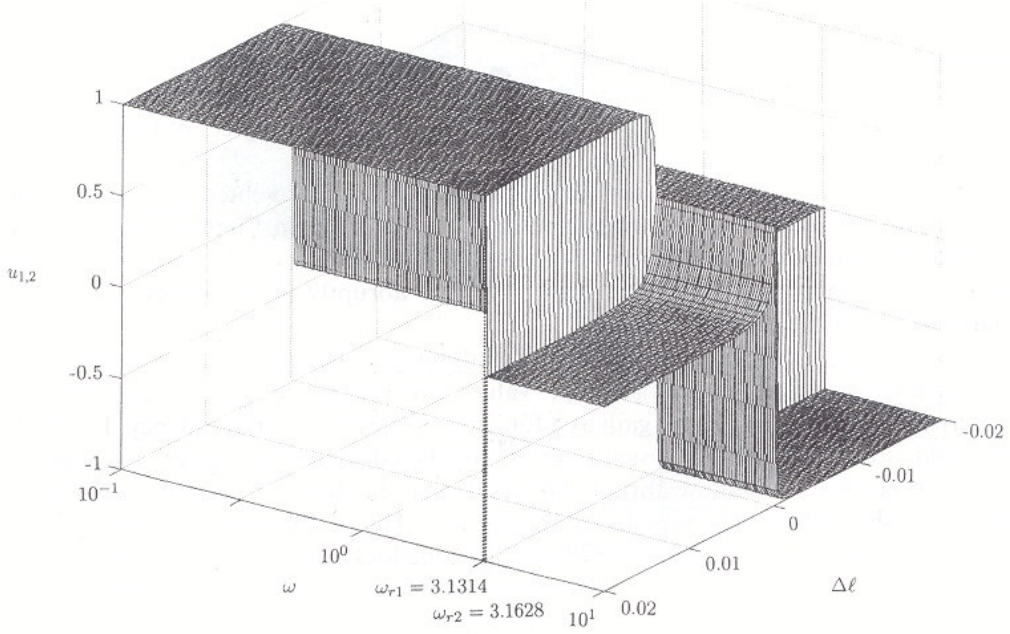

Figure 2.7 : The left singular vector component $u_{1,2}$ where R=0.0125 [4].

The singular value loci of the weakly coupled oscillators in figure 2.4 are almost insensitive to changes in disorder Δl . As singular values of a system are the bounds of the system's energy and power transmission ratios, it means that the system's power and energy transmissions are almost insensitive to changes in the disorder Δl in all

frequencies. The loci of both singular values of the weakly coupled system are shown in figure 2.8 for Δl=0.005 in which one can observe the singular value veering phenomena about ω=3.158 rad/s. As the amount of disorder Δl increases, the gap between the two peak of σ_1 corresponding to resonance frequencies of the system increases having a curve veering in the middle of the peaks. Components of singular vectors change abruptly at resonance frequencies, ω=3.158 rad/s and Δl=0 whereas the corresponding changes in singular values are smooth. This result means the power and energy transmission ratios are smooth; however, distribution of the total energy among different degrees of freedom may change abruptly as determined by the left singular vector u_i. [4].

For the strongly coupled system, the singular value plot σ_1 is presented in figure 2.9, and components of the associated left singular vector u_1 are given in figures 2.10 and 2.11. For Δl=0.005, the singular value veering phenomena occurs about ω=3.71 rad/s as shown in figure 2.12. Components of singular vectors change abruptly at the peaks of σ_1(i.e., resonances), ω=3.71 rad/s and Δl=0 [4].

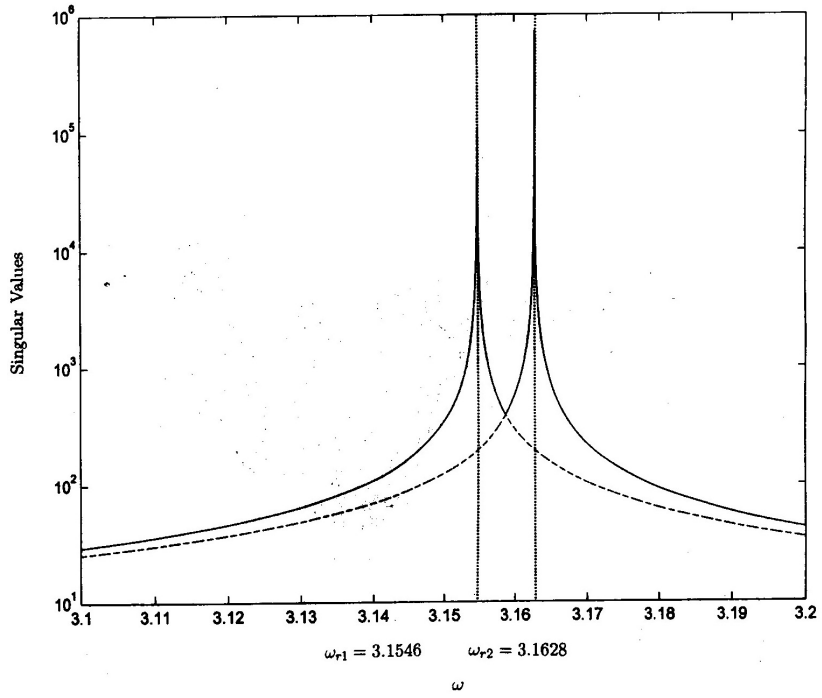

Figure 2.8 : The singular value veering phenomea for weakly coupled system for R=0.0125 and Δl=0.005. (—— σ_1 ;----- σ_2) [4]

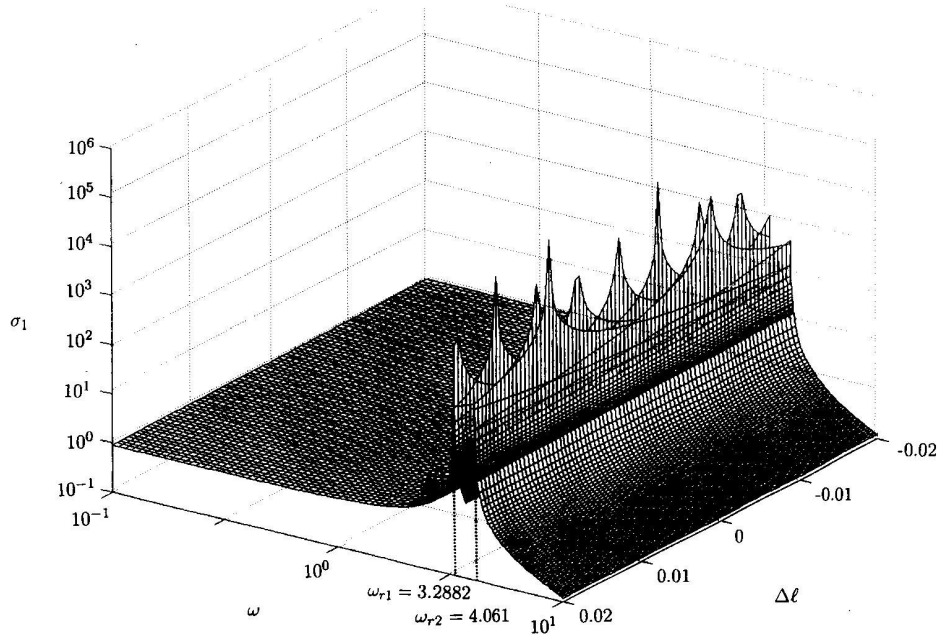

Figure 2.9 : The singular value σ_1 where R=0.5 [4]

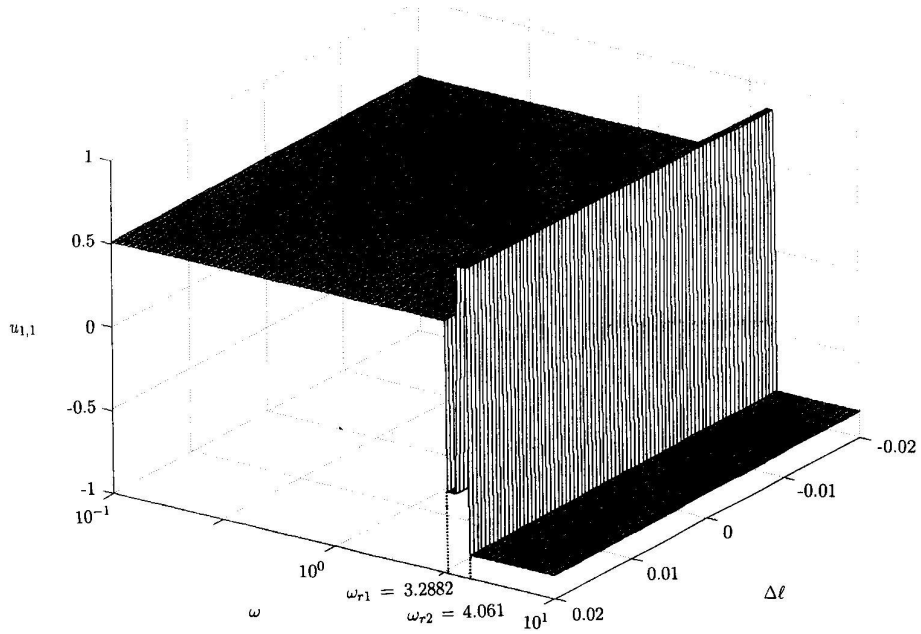

Figure 2.10 : The left singular vector component $u_{1,1}$ where R=0.5 [4]

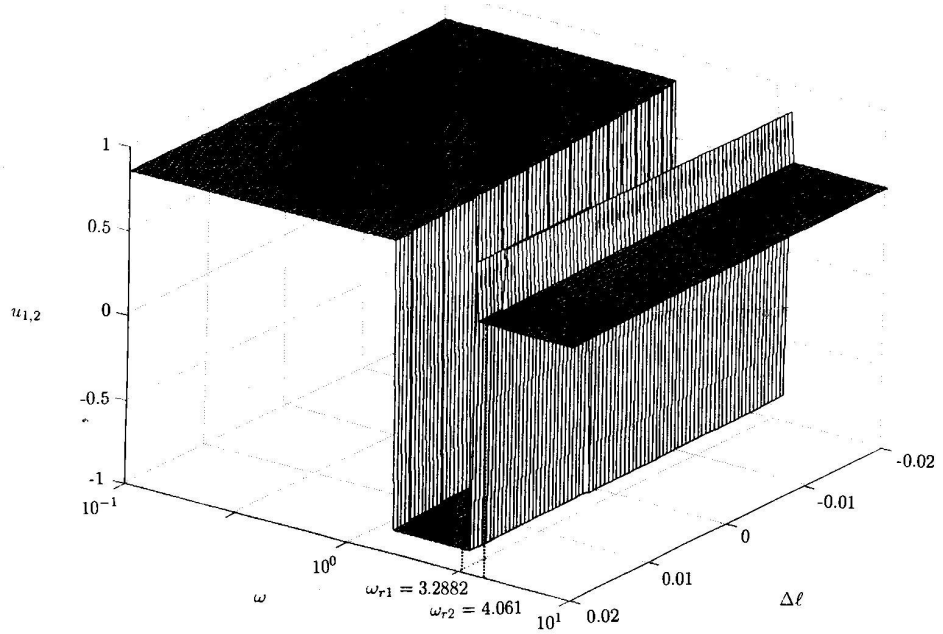

Figure 2.11 : The left singular vector component $u_{1,2}$ where R=0.5 [4]

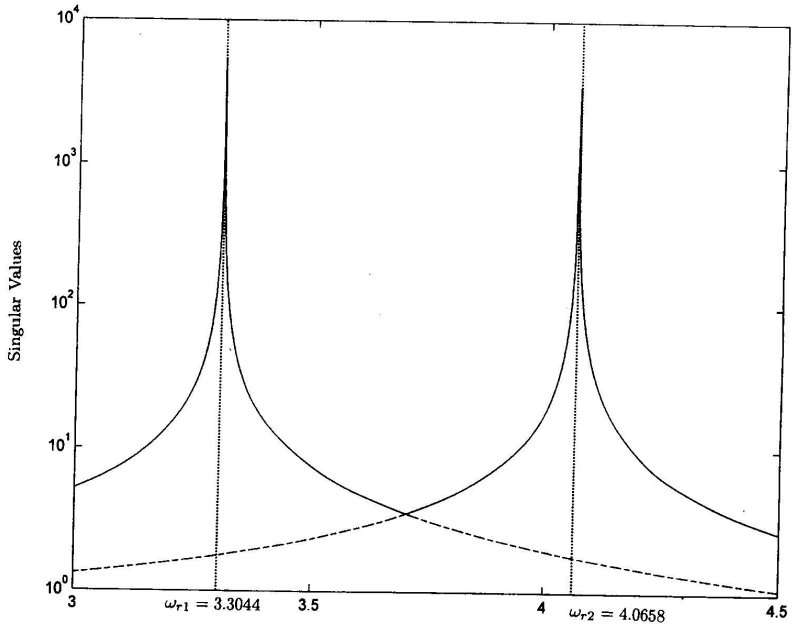

Figure 2.8 : The singular value veering phenomea for strongly coupled system for R=0.5 and Δl =0.005. ($\overline{\quad}$ σ_1 ;----- σ_2) [4]

It is noteworthy that while the eigenvalue based analyses give information about the resonance frequencies and vibration modes of a structure, singular values of the structure are related to the forced response characteristics and give the system gain as a function of excitation frequency. For both weakly and strongly coupled systems, it

is concluded that the power and energy transmission ratios do not show abrupt changes due to disorder because the singular values do not show abrupt changes due to disorder. Hence, the power and energy of the system is not dissipated in the existence of strong mode localization but just concentrated at certain degrees of freedom which are determined by the singular vectors. While these power and energy transmission ratios may be large at certain excitation frequencies as a result of resonance, they may be small t some other excitation frequencies, e.g., see σ_i loci. The frequencies at which singular value veering phenomenon occurs have a special meaning as follows: two singular values are almost equal to each other at such frequencies whereas their singular vectors are completely different. It means that while the system has almost the same power and energy transmission ratios at these frequencies, forced response characteristics are quite different. Subsequently, these frequencies will be called isopower frequencies [4].

3. SINGULAR VALUE DECOMPOSITION

3.1 Singular Values and Vectors

First of all assume that A is a complex m x n matrix and rank(A) = r. Then recall that A^HA and AA^H are hermitian and positive semidefinite, and that the positive eigenvalues of A^HA and AA^H are the same and have equal geometric multiplicities. Since A^HA is positive semidefinite, $(A^HA)^{1/2}$ exists, and its eigenvalues are the nonnegative square roots of the eigenvalues of A^HA. Call the positive eigenvalues of $(A^HA)^{1/2}$ the singular values of A. So if σ is singular value of A, σ is a positive eigenvalue of $(A^HA)^{1/2}$ and σ^2 is an eigenvalue of A^HA and of AA^H. The multiplicity of the singular value σ is the algebraic (and geometric) multiplicity of σ as an eigenvalue of $(A^HA)^{1/2}$. [6]

If we give an example ,

$$A = \begin{bmatrix} 1 & 0 \\ 0 & 0 \\ 1 & 1 \end{bmatrix} \qquad \textbf{(3.1)}$$

Since the matrix is real, singular values are obtained by computing the eigenvalues of A^TA,

$$A^TA = \begin{bmatrix} 2 & 1 \\ 1 & 1 \end{bmatrix} \qquad \textbf{(3.2)}$$

The eigenvalues of A^TA are $\left(3 \pm \sqrt{5}\right)/2$ and therefore, the singular values of A are $\sqrt{\left(3 \pm \sqrt{5}\right)/2}$.

The eigenvalues of $(A^H)^HA^H = AA^H$ are those of A^HA. Because of this, the singular values of A^H are those of A. [6].

The singular values of the real symmetric matrix S are the absolute values of its nonzero eigenvalues. Recall that S is unitarily similar to a diagonal matrix of its eigenvalues. Since S is real, the diagonalizing matrix can be chosen with real orthonormal vectors. That is, there exists Q orthogonal such that $Q^TSQ = \Lambda$ and

$Q^TS^TQ = \Lambda$. Hence, $Q^TS^TSQ = (Q^TS^TQ)(Q^TSQ) = \Lambda^2$. It then follows that if $\lambda \neq 0$ is an eigenvalue of S, $|\lambda|$ is an eigenvalue of $(S^TS)^{1/2}$ and therefore a singular value of S. [6].

One of the main uses of singular value decomposition of A is to provide a numerically sound means for determining rank(A). Rank(A) is the number of singular values of A. First we prove that rank(A) = rank(A^HA). If $x \in null(A)$, $A^HAx = 0$ shows that $x \in null(A)$. Hence, $null(A) \subseteq null(A^HA)$. On the other hand, $A^HAx = 0$ implies $x^HA^HAx = 0$. However, $x^HA^HAx = \|Ax\|^2 = 0$ shows that $Ax = 0$. Hence, $null(A^HA) \subseteq null(A)$. Thus the null spaces of A and A^HA are the same, so rank(A) = rank(A^HA). Suppose Λ is the diagonal matrix of eigenvalues of A^HA. Then, since A^HA is symmetric, there exists a unitary matrix U such that $U^HA^HAU = \Lambda$. So, rank(A) = rank(A^HA) = rank(U^HA^HAU) = rank(Λ) implies that rank (A) is the number of nonzero entries in Λ, which is the number of singular values of A. [6].

Suppose σ is a singular value of A repeated k times. Then there exist k linearly independent eigenvectors $\{v_1, v_2, \ldots, v_k\}$ of A^HA corresponding to the eigenvalue σ^2. Call each such v_i a right singular vector of A corresponding to σ and (σ, v_i) a right singular pair. Similarly there exist k linearly independent eigenvectors $\{u_1, u_2, \ldots, u_k\}$ of AA^H corresponding to the eigenvalue σ^2 of AA^H. These eigenvectors are called left singular vectors of A corresponding to the singular value σ, and (σ, u_i) is a right singular pair. This terminology is motivated by the fact that $Av_i = \sigma u$, where u is some left singular vector of A corresponding to the singular value σ, and also $u^HA = \sigma v^H$, where v is some right singular vector of A corresponding to the singular value σ. By definition, if v is a right singular value of A corresponding to σ, so is av for all nonzero scalars a (similarly for au). [6].

If (σ, v) is a right singular pair of A, then there exists $u \in \Re^m$ such that (σ, u) is a left singular pair of A. Moreover,

$$Av = \sigma u \tag{3.3}$$

$$A^Hu = \sigma v \tag{3.4}$$

By definition and hypothesis, $A^H Av = \sigma^2 v$. Define u by $Av = \sigma u$. Thus, $Av = \sigma u$ holds by definition of u. By multiplying $Av = \sigma u$ by A^H, we obtain

$$A^H Av = A^H(\sigma u) = \sigma A^H u \quad \textbf{(3.5)}$$

Thats is, $A^H Av = \sigma A^H u$. However, $A^H Av = \sigma^2 v$. Hence, $\sigma A^H u = \sigma^2 v$ and $A^H u = \sigma v$ holds. Finally, from $A^H u = \sigma v$ and $Av = \sigma u$, it follows that

$$A^H Au = \sigma Av = \sigma(\sigma u) = \sigma^2 u \quad \textbf{(3.6)}$$

and, thus, (σ^2, u) is an eigenpair of AA^H. [6].

Same theorem is also neccessary for left singular vectors. If If (σ, u) is a left singular pair of A, then there exists $v \in \Re^n$ such that (σ, v) is a right singular pair of A and equation (3.3) holds. [6].

If $\{v_1, v_2, \ldots, v_k\}$ is an orthonormal set of right singular vectors of A corresponding to the singular value σ, then $\{u_1 = (1/\sigma_1)Av_i, u_2 = (1/\sigma_2)Av_2, \ldots, u_k = (1/\sigma_k)Av_k\}$ is a set of orthonormal left singular vectors of A coreresponding to σ. By definition $A^H Av_i = \sigma^2 v_i$, and by hypothesis $\langle v_i, v_j \rangle = \delta_{ij}$. Therefore, $\langle Av_i, Av_j \rangle = \sigma^2 \delta_{ij}$ follows from

$$\langle Av_i, Av_j \rangle = \langle v_i, A^H Av_j \rangle = \langle v_i, \sigma^2 v_j \rangle = \sigma^2 \langle v_i, v_j \rangle \sigma^2 \delta_{ij} \quad \textbf{(3.7)}$$

On the other hand,

$$\sigma^2 \delta_{ij} = \langle Av_i, Av_j \rangle = \langle \sigma u_i, \sigma u_j \rangle = \sigma^2 \langle u_i, u_j \rangle \quad \textbf{(3.8)}$$

Since $\sigma \neq 0, \langle u_i, u_j \rangle = \delta_{ij}$ **(3.9)**

As an example let's find the left and right singular vectors for the matrix, [6]

$$A = \begin{bmatrix} 1 & 0 & -1 \\ 1 & 1 & 1 \end{bmatrix} \quad \textbf{(3.10)}$$

$$A^T A = \begin{bmatrix} 2 & 1 & 0 \\ 1 & 1 & 1 \\ 0 & 1 & 2 \end{bmatrix} \Rightarrow \tag{3.11}$$

Eigenpairs of the A^TA are,

$$\left(2, v_1 = \begin{bmatrix} 1 \\ 0 \\ -1 \end{bmatrix} \right) ; \qquad \left(3, v_2 = \begin{bmatrix} 1 \\ 1 \\ 1 \end{bmatrix} \right) ; \qquad \left(0, v_3 = \begin{bmatrix} 1 \\ -2 \\ 1 \end{bmatrix} \right) \tag{3.12}$$

Hence, the singular values of A are $\sqrt{2}$ and $\sqrt{3}$. The corresponding right singular vectors are v_1 and v_2, respectively. To determine the left singular vectors, compute u=Av;

$$u_1 = Av_1 = \begin{bmatrix} 1 & 0 & -1 \\ 1 & 1 & 1 \end{bmatrix} \begin{bmatrix} 1 \\ 0 \\ -1 \end{bmatrix} = \begin{bmatrix} 2 \\ 0 \end{bmatrix}, \tag{3.13}$$

$$u_2 = Av_2 = \begin{bmatrix} 1 & 0 & -1 \\ 1 & 1 & 1 \end{bmatrix} \begin{bmatrix} 1 \\ 1 \\ 1 \end{bmatrix} = \begin{bmatrix} 0 \\ 3 \end{bmatrix} \tag{3.14}$$

It is easy to verify that

$$AA^T = \begin{bmatrix} 2 & 0 \\ 0 & 3 \end{bmatrix} \tag{3.15}$$

And trivial to see that $(2,u_1)$ and $(3,u_2)$ are eigenpairs of AA^T. An orthonormal pair of right singular vectors are

$$\tilde{v}_1 = \frac{\sqrt{2}}{2} \begin{bmatrix} 1 \\ 0 \\ -1 \end{bmatrix} , \qquad \tilde{v}_2 = \frac{\sqrt{3}}{3} \begin{bmatrix} 1 \\ 1 \\ 1 \end{bmatrix} \tag{3.16}$$

Now,

$$\tilde{u}_1 = \sigma^{-1} A \tilde{v}_1 = \begin{bmatrix} 1 \\ 0 \end{bmatrix} \quad \textit{and} \quad \tilde{u}_2 = \sigma^{-1} A \tilde{v}_2 = \begin{bmatrix} 0 \\ 1 \end{bmatrix} \tag{3.17}$$

3.2 The Singular Value Decomposition of A

Suppose A is m x n. Then there exist unitary matrices U_{mxm} and V_{mxm} such that

$$A = USV^H \tag{3.18}$$

where S is an m x n matrix with the singular values of A displayed along its diagonal and zeros elsewhere. Here are the ideas and conclusions relevant to the proof and construction of S, V and U. Suppose rank(A) = r,

1. The matrices $A^H A$ and AA^H are hermitian and therefore have a complete set of orthonormal eigenvectors. The coloumns of U are the eigenvectors of AA^H; the coloumns of V are the eigenvectors of $A^H A$. It is for this reason that U and V are m x m and n x n unitary matrices, respectively.
2. The coloumns of V are ordered so that the first r coloums contain the right singular vectors of A, and the remaining coloumns are eigenvectors corresponding to the zero eigenvalues of $A^H A$.
3. For $i = 1,2,\ldots,r$

   $$u_i = (1/\sigma_i)Av_i \tag{3.19}$$

   defines the ith coloumn of U. The remaining m – r coloumns of U are eigenvectors corresponding to the zero eigenvalues of $A^H A$. [6]. The matrices U and V contain orthonormal bases for all four subspaces [7].:

   first r columns of V : rowspace of A

   last n-r columns of V : nullspace of A

   first r columns of U : column space of A

   last m-r columns of U : nullspace of A^T

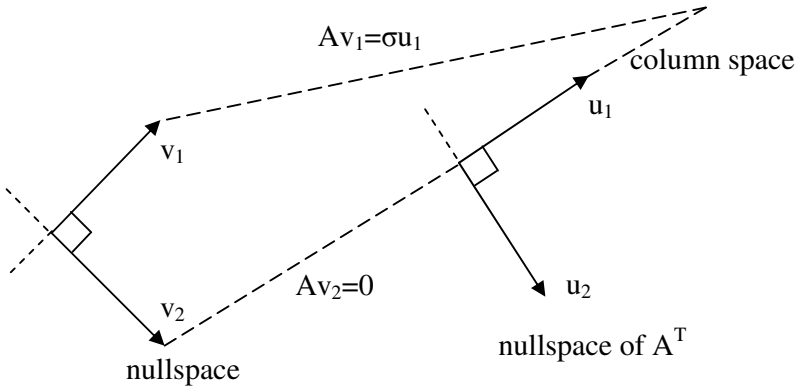

Figure 3.1 : SVD chooses orthonormal bases so that $Av_i = \sigma_i u_i$. [7]

4. The diagonal of the m x n matrix S is composed of the singular values of A and sufficiently many zeros to complete the diagonal. We call S a singular value matrix of A. Thus, S has the following form:

$$S = \begin{bmatrix} \Sigma & 0 \\ 0 & 0 \end{bmatrix} = \begin{bmatrix} \sigma_1 & & & & & & 0 \\ & \sigma_2 & & & & & \\ & & \ddots & & & & \\ & & & \sigma_r & & & \\ & & & & 0 & & \\ & & & & & 0 & \\ 0 & & & & & & \ddots \end{bmatrix}_{mxn} \quad \textbf{(3.20)}$$

If rank(A)=r=m=n, then A is nonsingular and $S = \Sigma$. If r=m<n, then A has full row rank and $S = [\Sigma \quad 0]$. On the other hand, if r=n<m, then A has full coloumn rank and

$$S = \begin{bmatrix} \Sigma \\ 0 \end{bmatrix} \quad \textbf{(3.21)}$$

Since $A^H A$ and AA^H are hermitian and are positive semidefinite matrices, their nonzero eigenvalues are positive and equal, and the positive square roots of these eigenvalues are defined as the singular values of A. These eigenvectors of $A^H A$ may be chosen to form an orthonormal basis for ℓ^n. Let

$$V = \begin{bmatrix} v_1 & v_2 & \dots & v_r & v_{r+1} & \dots & \end{bmatrix} \quad \textbf{(3.22)}$$

be the n x n matrix whose coloumns are these orthonormal vectors. Suppose that rank(A)=r. We may assume that the first r coloumns of V are eigenvectors associated with the eigenvalues of $A^H A$; that is, $A^H A v_i = \sigma_i^2 v_i$, for $i = 1,2,\dots,r$. (These r vectors are the right singular vectors of A by definition.) The remaining n-r coloumns in V are the eigenvectors of $A^H A$ corresponding to its zero eigenvalue. Since the coloumns of V are orthonormal, V is unitary. This completes the construction of V. [6]

We now define U as follows: For $i = 1,2,\dots,r$, set

$$u_i = (1/\sigma_i) A v_i \quad \textbf{(3.23)}$$

Next consider any two vectors u_i and u_j in this set. From equation (3.23),

$$\langle u_i, u_j \rangle = (1/\sigma_i)(1/\sigma_j)\langle Av_i, Av_j \rangle = (1/\sigma_i)(1/\sigma_j)\langle v_i, A^H A v_j \rangle \quad \textbf{(3.24a)}$$

$$= (1/\sigma_i)(1/\sigma_j)\langle v_i, \sigma_j^2 v_j \rangle = (\sigma_j/\sigma_i)\langle v_i, v_j \rangle = (\sigma_j/\sigma_i)\delta_{ij} \quad \textbf{(3.24b)}$$

Hence, the set $\{u_1, u_2, \dots, u_r\}$ is orthonormal. These r orthonormal vectors compose the first r coloumns of U. The remaining m - r coloumns of U are orthonormal vectors that form a basis for $null(AA^H)$, the eigenspace of AA^H corresponding to $\lambda = 0$.

Now the last step. Consider

$$U^H A V = U^H A \begin{bmatrix} v_1 & \dots & v_r & v_{r+1} & \dots & v_n \end{bmatrix} \quad \textbf{(3.25a)}$$

$$= U^H \begin{bmatrix} Av_1 & \dots & Av_r & Av_{r+1} & \dots & Av_n \end{bmatrix} \quad \textbf{(3.25b)}$$

$$= U^H \begin{bmatrix} \sigma_1 u_1 & \dots & \sigma_r u_r 0 & \dots & 0 \end{bmatrix} \quad \textbf{(3.25c)}$$

$$= \begin{bmatrix} \sigma_1 U^H u_1 & \dots & \sigma_r U^H u_r 0 & \dots & 0 \end{bmatrix} \quad \textbf{(3.25d)}$$

$$= \begin{bmatrix} \sigma_1 e_1 & \dots & \sigma_r e_r 0 & \dots & 0 \end{bmatrix} \quad \textbf{(3.25e)}$$

Clearly,

$$S = \begin{bmatrix} \sigma_1 e_1 & \dots & \sigma_r e_r & 0 & \dots & 0 \end{bmatrix} \quad \textbf{(3.26)}$$

is the matrix given in equation (3.20), the singular value matrix of A. [6]

For each matrix A there exist unitary matrices U and V such that

$$U^H A V = S \quad \textbf{(3.27)}$$

Equation (3.27) follows from equation (3.18) and the fact that U and V are unitary matrices. [6]

If $A \neq 0$ is positive semidefinite, then $S = \Lambda$ and we may choose $U = V$. Positive semidefinite matrices have nonnegative eigenvalues λ_i, and since $\sigma_i = |\lambda_i| = \lambda_i$ for each i, $S = \Lambda$ for some ordering of the diagonal entries of S. Because $A^H = A, A^H A = A^2 = AA^H$, and because A^2 has the same eigenvectors as A, the right and left singular vectors of A are the eigenvectors of A that correspond to its nonzero eigenvalues. Now, by equation (3.19),

$$\lambda_i u_i = \sigma_i u_i = A v_i = \sigma_i v_i \quad \textbf{(3.28)}$$

so that $u_i = v_i$ for $i = 1,2,\dots,r$. The remaining vectors in U and V are eigenvectors of A corresponding to the eigenvalue 0. We choose the same eigenvectors for U as for V and arrange that they form an orthonormal set. As an example [6] let's find SVD of

$$A = \begin{bmatrix} 0 & 4 & 3 \\ 4 & 0 & 0 \\ 3 & 0 & 0 \end{bmatrix} \quad \textbf{(3.29)}$$

Eigenpairs of

$$A^T A = \begin{bmatrix} 25 & 0 & 0 \\ 0 & 16 & 12 \\ 0 & 12 & 9 \end{bmatrix} \quad \textbf{(3.30)}$$

are $(25,v_1)$, $(25,v_2)$ and $(0,v_3)$, where

$$v_1 = \begin{bmatrix} 1 \\ 0 \\ 0 \end{bmatrix} \quad , \quad v_2 = \begin{bmatrix} 0 \\ 4/5 \\ 3/5 \end{bmatrix} \quad , \quad v_1 = \begin{bmatrix} 0 \\ 3/5 \\ -4/5 \end{bmatrix} \tag{3.31}$$

Hence, $\sigma_1 = \sigma_2 = 5$. Setting $V = [v_1 \quad v_2 \quad v_3]$ leads to

$$V = \begin{bmatrix} 1 & 0 & 0 \\ 0 & 4/5 & 3/5 \\ 0 & 3/5 & -4/5 \end{bmatrix} \tag{3.32}$$

now u_3 is orthonormal solution of $AA^Tu_3 = A^TAu_3 = A^2u_3 = 0$, namely, v_3.

$$U = \begin{bmatrix} \frac{Av_1}{5} & \frac{Av_2}{5} & u_3 \end{bmatrix} = \begin{bmatrix} 0 & 1 & 0 \\ 4/5 & 0 & 3/5 \\ 3/5 & 0 & -4/5 \end{bmatrix} \tag{3.33}$$

As another example [7], let's find the SVD of ,

$$A = \begin{bmatrix} 2 & 2 \\ -1 & 1 \end{bmatrix} \tag{3.34}$$

Compute A^HA and its eigenvectors. Then make them unit vectors:

$$A^HA = \begin{bmatrix} 5 & 3 \\ 3 & 5 \end{bmatrix} \text{ has unit eigenvectors } v_1 = \begin{bmatrix} 1/\sqrt{2} \\ 1/\sqrt{2} \end{bmatrix} \text{ and } v_2 = \begin{bmatrix} -1/\sqrt{2} \\ 1/\sqrt{2} \end{bmatrix} \tag{3.35}$$

The eigenvalues of A^HA are 8 and 2. The v's are perpendicular because eigenvalues of every symmetric matrix are perpendicular and A^HA is automatically symmetric.

u_1 and u_2 are quick to find, because Av_1 is in the direction of u_1 and Av_2 is in the direction of u_2 :

$$Av_1 = \begin{bmatrix} 2 & 2 \\ -1 & 1 \end{bmatrix} \begin{bmatrix} 1/\sqrt{2} \\ 1/\sqrt{2} \end{bmatrix} = \begin{bmatrix} 2\sqrt{2} \\ 0 \end{bmatrix}. \text{ The unit vector is } u_1 = \begin{bmatrix} 1 \\ 0 \end{bmatrix} \tag{3.36}$$

Clearly Av_1 is the same as $2\sqrt{2}u_1$. The first singular value is $\sigma_1 = 2\sqrt{2}$. Then $\sigma_1^2 = 8$, which is the eigenvalue of A^HA. We have $Av_1 = \sigma_1 u_1$ exactly as required. Similarly,

$$Av_2 = \begin{bmatrix} 2 & 2 \\ -1 & 1 \end{bmatrix} \begin{bmatrix} -1/\sqrt{2} \\ 1/\sqrt{2} \end{bmatrix} = \begin{bmatrix} 0 \\ \sqrt{2} \end{bmatrix}. \text{ The unit vector is } u_2 = \begin{bmatrix} 0 \\ 1 \end{bmatrix} \tag{3.37}$$

Now Av_2 is $\sqrt{2}u_2$. The second singular value is $\sigma_2 = \sqrt{2}$. And σ_2^2 agrees with the other eigenvalue 2 of $A^H A$. We have completed the SVD:

$$A = USV^H \text{ is } \begin{bmatrix} 2 & 2 \\ -1 & 1 \end{bmatrix} = \begin{bmatrix} 1 & 0 \\ 0 & 1 \end{bmatrix} \begin{bmatrix} 2\sqrt{2} & 0 \\ 0 & \sqrt{2} \end{bmatrix} \begin{bmatrix} 1/\sqrt{2} & 1/\sqrt{2} \\ -1/\sqrt{2} & 1/\sqrt{2} \end{bmatrix} \quad \textbf{(3.38)}$$

This matrix and every invertible 2 by 2 matrix , trnsform the unit circle to an ellipse. You can see that in the figure 3.2.

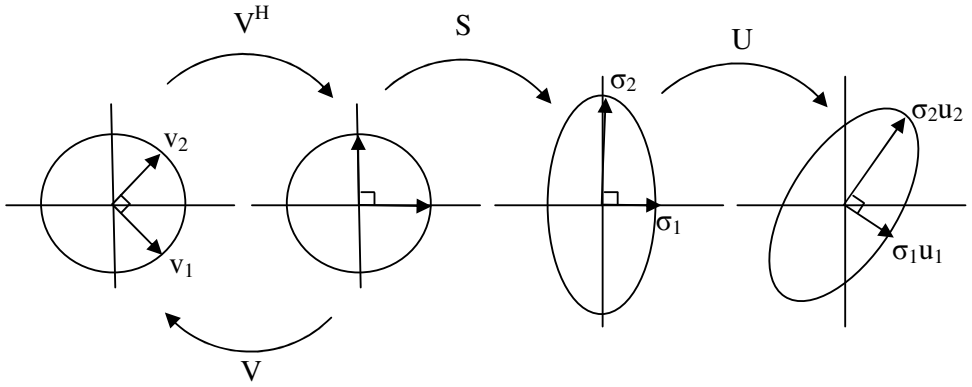

Figure 3.2 : **U** and V are rotations and reflections. S is a stretching matrix. [7]

3.3 Matlab Determination of Singular Values and Vectors

There are two MATLAB commands relating to the singular values of A_{mxn}. First, svd(A) returns a vector whose entries are the singular values of A. (MATLAB takes the position that zero eigenvalues of A^HA are singular values of A; hence, svd(A) returns all the eigenvalues of $(A^HA)^{1/2}$.) [6]

Second, [U,S,V] = svd(A) returns an orthonormal matrix of left singular vectors U, an orthonormal matrix of right singular vectors V, and S, an m x n matrix whose diagonal comprises the eigenvalues of $(A^HA)^{1/2}$. [6]. If we give an example,

```
>>A = [1 0 -1; 1 1 1]
```
(3.39)

```
A =

    1    0   -1

    1    1    1
```
(3.40)

```
>> [U,S,V]=svd(A)
```

U =

$$\begin{matrix} 0.0000 & -1.0000 \\ 1.0000 & 0.0000 \end{matrix} \quad \textbf{(3.41)}$$

S =

$$\begin{matrix} 1.7321 & 0 & 0 \\ 0 & 1.4142 & 0 \end{matrix} \quad \textbf{(3.42)}$$

V =

$$\begin{matrix} 0.5774 & -0.7071 & 0.4082 \\ 0.5774 & 0 & -0.8165 \\ 0.5774 & 0.7071 & 0.4082 \end{matrix} \quad \textbf{(3.43)}$$

Comparing these values with those example in section 3.1, we can see that, in some instances, the singular vectors using MATLAB are the negatives of those computed by hand.

Matlab computes rank(A) by counting the (positive) singular values of A. There are other important uses for svd(A). MATLAB uses the singular values to define a special norm for A (the largest singular value is norm(A)) the pseudo inverse and the condition number of A. The condition number is a measure of "the sensitivity of the solution of linear equations to errors in the data." Cond(A) returns the ratio of the largest singular value to the smallest. [6]. As an example,

>> Cond(A)

ans =

1.2247 (Largest singular value / smallest singular value (1.7321/1.4142=1.2248)

>> norm(A)

ans =

1.7321 (Largest singular value ($\sigma_1 = 1.7321$))

3.4 Relationship Between Singular Values and Resonance Frequencies

A useful tool in the dynamic analysis of structures is the frequency response function, or frf. The frequency response of a system is defined by the relationship between a sinusoidal input and the corresponding sinusoidal output for the system over a range of input frequencies. At resonant frequencies, amplitudes have a sharp peak at amplitude versus frequency plot.

When the singular value versus frequency plot of a system is examined, it is seen that, singular values get the maximum values and have sharp peaks at resonance frequencies. This interesting response shows that singular value decomposition method gives us information about the resonance frequency of a dynamical system. Mathematical proof of this condition can be seen below,

The euclidean unit sphere in C^n is a compact set and the function $f(x) = \|Ax\|_2$ is a continuous real valued function, so the weierstrauss theorem (a continuous function on a closed and bounded set will have a maximum and a minimum) guarantees that there is some unit vector $w \in C^n$ such that $\|Aw\|_2 = \max\{\|Ax\|_2 : x \in C^n, \|x\|_2 = 1\}$. [8]. Then,

$\sigma_1(A) = \max\{\|Ax\|_2 : x \in C^n, \|x\|_2 = 1\}$, so $\sigma_1 = \|Aw_1\|_2$ for some unit vector $w_1 \in C^n$

$\sigma_2(A) = \max\{\|Ax\|_2 : x \in C^n, \|x\|_2 = 1, x \perp w_1\}$, so $\sigma_2 = \|Aw_2\|_2$ for some unit vector $w_2 \in C^n$ such that $w_2 \perp w_1$

$\vdots$

$\sigma_k(A) = \max\{\|Ax\|_2 : x \in C^n, \|x\|_2 = 1, x \perp w_1, \ldots, w_{k-1}\}$, so $\sigma_k = \|Aw_k\|_2$ for some unit vector $w_k \in C^n$ such that $w_k \perp w_1, \ldots, w_{k-1}$

$\vdots$

If we take the A as a function of w,

$$\sigma_1(A(\omega)) = \sigma_1(\omega) = \max\{\|A(\omega)x\|_2 : x \in C^n, \|x\|_2 = 1\} \quad \textbf{(3.44a)}$$

$$\max_{\omega} \sigma_1(A(\omega)) = \max_{\omega} \max\{\|A(\omega)x\|_2 : x \in C^n, \|x\|_2 = 1\} \quad \textbf{(3.44b)}$$

$$\max_{\omega} \sigma_1(A(\omega)) = \max\left\{\max_{\omega} \|A(\omega)x\|_2 : x \in C^n, \|x\|_2 = 1\right\} \quad \textbf{(3.44c)}$$

$\max_{\omega} \|A(\omega)x\|_2$ shows that $\|A(\omega)x\|_2$ becomes max. at resonance frequencies. So,

$\sigma_1(A(\omega))$ also becomes max. at resonance frequencies.

As an example, frequency versus amplitude and frequency versus singular values graphs of a system are seen figures below. Resonance frequencies of the system are 1 rad/sec and 1.049 rad/sec. It is seen that both amplitudes and singular values have sharp peak values at resonance frequencies.

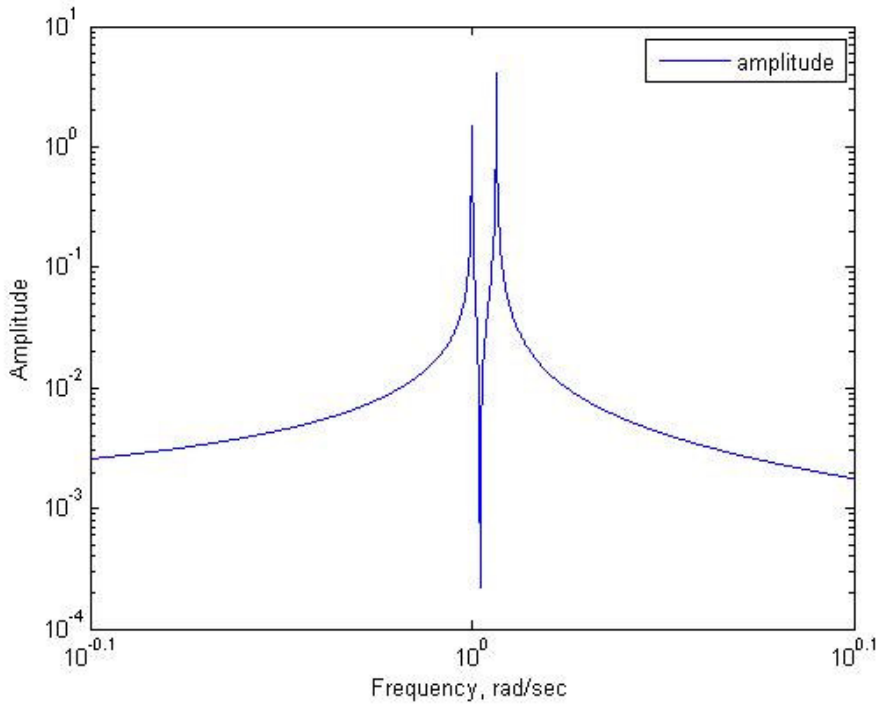

Figure 3.3 : Frequency versus amplitude plot. Peaks at resonance frequencies (1 rad/sec and 1.049 rad/sec)

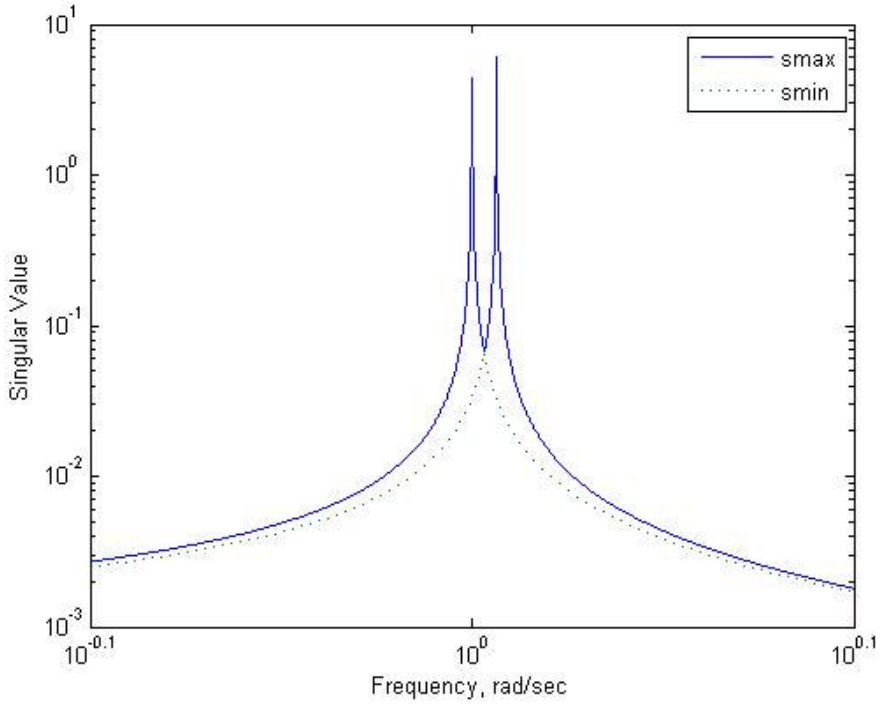

Figure 3.4 : Singular values versus amplitude plot. Peaks at resonance frequencies (1 rad/sec and 1.049 rad/sec)

3.5 Relationship Between Singular Vectors and Directional Properties

Consider the following time-independent linear equation system:

$$Kd = f \tag{3.45}$$

where in general, $K \in C^{nxn}, d \in C^n and\ f \in C^n$. Then, $d = K^{-1} f$. Suppose that K^{-1} has the SVD of $K^{-1} = USV^H$, where $U \in C^{nxn}, S \in \Re^{nxn}\ and\ V \in C^{nxn}$. In order to show that the system has different gains for different input directions, the SVD of K^{-1} is written in the following dyadic form [4].:

$$K^{-1} = \sum_{i=1}^{n} \sigma_i u_i v_i^H \tag{3.46}$$

Beforehand assume that the singular values are distinct which is the case for physical systems considered here. If the force vector f is in the direction of the kth right singular vector $f = v_k$, then one has [4]

$$d = \sum_{i=1}^{n} \sigma_i u_i v_i^H v_k \tag{3.47}$$

Since v_i are orthonormal, $v_i^H v_k = \delta_{ik}$ where δ_{ik} is Kronecker delta function, we get

$$d = \sigma_k u_k \tag{3.48}$$

and

$$\|d\|_2 = \sigma_k \tag{3.49}$$

Note that equation (3.48) shows that if f is in the direction of v_k, the output d is in the direction of u_k, and equation (3.49) shows that the system's gain is equal to σ_k. In brief, each right singular vector tells us how we would place an input into the system to produce a gain equal to the associated singular value, and the corresponding left singular vector tells us how the response to this input is distributed among the different degrees of freedom. [4]

For the application of the SVD to semidiscrete equation systems, consider the following matrix aquation of structural dynamics [4]

$$M\ddot{d} + C\dot{d} + K = f \tag{3.50}$$

where $M \in \Re^{nxn}$ is the mass matrix, $C \in \Re^{nxn}$ the viscous damping matrix, $K \in \Re^{nxn}$ the stiffness matrix, $f \in \Re^n$ the vector of applied forces, and $d \in \Re^n, \dot{d}\ and\ \ddot{d}$ are, respectively, the displacement, velocity and acceleration vectors. By taking the Laplace transform of equation (3.49) , one get [4]

D(s)=G(s)F(s), **(3.51)**

where the matrix transfer function G(s) is defined by

$$G(s) = \left(Ms^2 + Cs + K\right)^{-1} \tag{3.52}$$

Then, the steady state output $D(j\omega)$ of this system in response to the sinusoidal input of frequency ω, i.e., $f(t) = \tilde{f}\sin(\omega t)$, is given by [4]

$$D(j\omega) = G(j\omega)\tilde{f} \tag{3.53}$$

where $\tilde{f}$ is the input magnitude vector. In equation (3.53), the magnitude of $D_i(j\omega)$ is the magnitude of the ith component of the output vector d, while the phase of $D_i(j\omega)$ is the phase angle between the ith component of the output vector d and the input f. Similar to the time-independent case, if $\tilde{f}$ is in the direction of v_k, the response $D(j\omega)$ will be in the direction of u_k having the gain of σ_k. Note that the singular values and vectors are to be the function of the excitation frequency ω and we adopt the ordering, [4]

$$\sigma_1 \geq \sigma_2 \geq \ldots \geq \sigma_n \geq 0. \tag{3.54}$$

4. INPUT OUTPUT DIRECTIONAL PROPERTIES OF A TURBINE

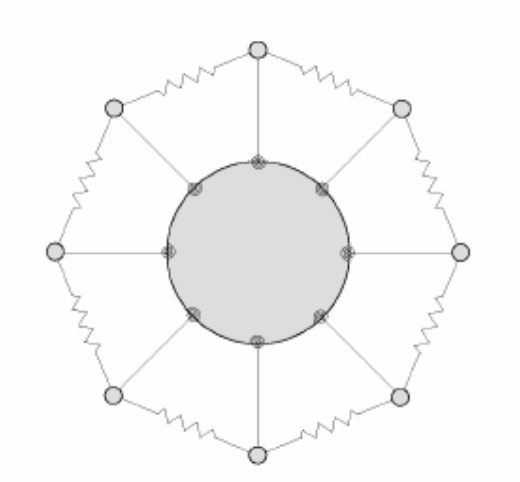

Figure 4.1 : A simple model of the bladed-disk system.

Bladed disks belong to a class of structure known as rotationally periodic structures (RPS). A simple model of the bladed-disk system is shown in Figure 4.1. Cyclic symmetry is a convenient assumption when analyzing an RPS, since they consist of spatially repetitive substructures; thus all substructures are geometrically and dynamically similar. For a turbine disk, this implies that: the blades are identical, they are uniformly spaced, and the hub is symmetric. If these conditions are met, then the system is said to be tuned [9].

An important feature of a tuned RPS is that in a given mode, all of the substructures have the same vibration amplitude and differ only in phase. These vibration modes, known as global or extended modes, allow the equations of motion to be decoupled [9]..

Unfortunately, real blades have material and manufacturing imperfections. The system is said to be mistuned when these defects cause mass, stiffness, and damping variances. Mistuning breaks down the rotationally periodic nature of the compressor disk, changing global modes into local modes. In a tuned system, the vibration energy is spread equally amongst all the blades. Mode localization, however, concentrates the energy in several blades, or even a single blade. This results in some blades having a higher steady state amplitude than in a perfectly tuned system. More importantly,

mode localization is amplified by weak or variable inter-blade coupling, be it aerodynamic or structural. A variation in blade natural frequency of less than 2% can cause amplitude increases of over 100%. Consequently, the high cycle fatigue (HCF) problem in bladed-disk assemblies is severely aggravated by mistuning effects [9]..

4.1 Equation of Motion

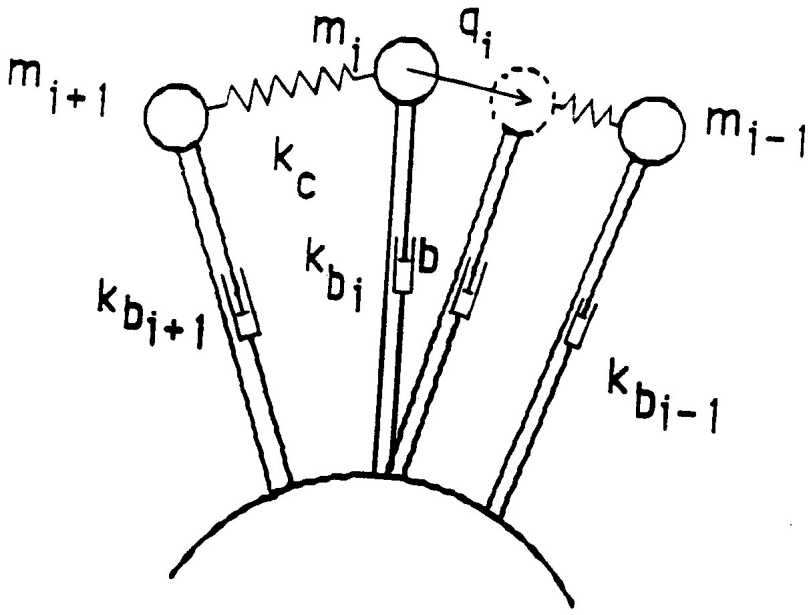

Figure 4.2 : Geometry of nearly periodic structure with cyclic symmetry [10]

The nearly cyclic assembly of N coupled component systems (blades) shown in Figure 4.2 is studied. Each component system, consisting of a single DOF oscillator with viscous damping, is coupled to the adjacent component systems through linear springs. This system is used as a simple model of continuously shrouded bladed disk assemblies to study localized free and forced vibrations in mistuned assemblies. For simlicity, mistuning is assumed to originate from discrepancies among the component systems' stiffnesses. The equation of motion are given by [10],

$$\ddot{\underline{q}} + 2\zeta\omega_b \dot{\underline{q}} + \omega_b^2 [A]\underline{q} = \frac{1}{m}\underline{F} \qquad \textbf{(4.1)}$$

where

$$[A]=\begin{bmatrix} 1+2R^2+\Delta f_1 & -R^2 & 0 & \cdots & 0 & -R^2 \\ -R^2 & 1+2R^2+\Delta f_2 & -R^2 & 0 & \cdots & 0 \\ 0 & \ddots & \ddots & \ddots & \ddots & \vdots \\ \vdots & \ddots & \ddots & \ddots & \ddots & 0 \\ 0 & \ddots & \ddots & \ddots & \ddots & -R^2 \\ -R^2 & 0 & \cdots & 0 & -R^2 & 1+2R^2+\Delta f_N \end{bmatrix} \quad \textbf{(4.2)}$$

is a nearly cyclic matrix, and

$$\underline{F} = Fe^{j\omega t}\left\{1, e^{j\phi_2}, \cdots, e^{j\phi_i}, \cdots, e^{j\phi_N}\right\}^T \quad \textbf{(4.3)}$$

$$\phi_i = \frac{2\pi n(i-1)}{N} \quad \textbf{(4.4)}$$

$$\zeta = \frac{b}{2\sqrt{k_b m}} \quad \textbf{(4.5)}$$

$$\omega_b = \sqrt{k_b/m} \quad \textbf{(4.6)}$$

$$\omega_c = \sqrt{k_c/m} \quad \textbf{(4.7)}$$

$$\Delta f_i = \left(\omega_{bi}^2 - \omega_b^2\right)/\omega_b^2 \quad \textbf{(4.8)}$$

$$R = \omega_c^2/\omega_b^2 \quad \textbf{(4.9)}$$

The external force adopted here is a travelling wave excitation which has been widely used for bladed disk assemblies in the literature. Two key dimensionless parameters in equation (4.2) are R^2 and Δf_i: R^2 is the dimensionless coupling between component systems and Δf_i represents the dimensionless mistuning strength for the ith component system. In the subsequent developments Δf_i is considered a random variable whose statistical properties can be obtained from the survey of a large population of manufactured blades [10].

If the equation of motion is modified,

$$m\underline{\ddot{q}} + 2m\zeta\omega_b\underline{\dot{q}} + m\omega_b^2[A]\underline{q} = \underline{F} \quad \textbf{(4.10)}$$

$$[M]\{\ddot{q}\}+2[M][\zeta][\omega_b]\{\dot{q}\}+[M][\omega_b]^2[A]\{q\}=\{F\} \quad \textbf{(4.11)}$$

$$[M]=[M] \quad \textbf{(4.12)}$$

$$[C]=2[M][\zeta][\omega_b] \quad \textbf{(4.13)}$$

$$[K]=[M][\omega_b]^2[A] \quad \textbf{(4.14)}$$

equation of motion is obtained as standart form,

$$[M]\{\ddot{q}\}+[C]\{\dot{q}\}+[K]\{q\}=\{F\} \quad \textbf{(4.15)}$$

If the Laplace transform is applied to this equation of motion,

$$\left([M]s^2+[C]s+[K]\right)q(s)=F(s) \quad \textbf{(4.16)}$$

and

$$q(s)=G(s)F(s)\Rightarrow \quad \textbf{(4.17)}$$

transfer function of equation of motion is obtained,

$$G(s)=\frac{F(s)}{q(s)}=\left([M]s^2+[C]s+[K]\right)^{-1} \quad \textbf{(4.18)}$$

$$s=j\omega\Rightarrow \quad \textbf{(4.19)}$$

The steady state output $D(j\omega)$ of this system in response to the sinusoidal input of frequency ω, i.e., $f(t)=\tilde{f}\sin(\omega t)$, is given by

$$D(j\omega)=G(j\omega)\tilde{f} \quad \textbf{(4.20)}$$

and

$$G(j\omega)=\left(-[M]\omega^2+\sqrt{-1}[C]\omega+[K]\right)^{-1} \quad \textbf{(4.21)}$$

The following parameter values are used in numerical studies;

Table 4.1: Parameter values for equation of motion.

	Weakly Coupled Blades	Strongly Coupled Blades
M	1	1
ζ	0	0
ω_b	1	1
R	0.1	1
Δf	0	0

When these parameters are replaced to three-bladed turbine's system matrices, we obtain,

$$M = \begin{bmatrix} 1 & 0 & 0 \\ 0 & 1 & 0 \\ 0 & 0 & 1 \end{bmatrix} \quad \textbf{(4.22)}$$

$$\varsigma = \begin{bmatrix} 0 & 0 & 0 \\ 0 & 0 & 0 \\ 0 & 0 & 0 \end{bmatrix} \quad \textbf{(4.23)}$$

$$\omega_b = \begin{bmatrix} 1 & 0 & 0 \\ 0 & 1 & 0 \\ 0 & 0 & 1 \end{bmatrix} \quad \textbf{(4.24)}$$

$$[A] = \begin{bmatrix} 1.002 & -0.01 & -0.01 \\ -0.01 & 1.002 & -0.01 \\ -0.01 & -0.01 & 1.002 \end{bmatrix} \text{ for weak coupled blades and,} \quad \textbf{(4.25)}$$

$$[A] = \begin{bmatrix} 3 & -1 & -1 \\ -1 & 3 & -1 \\ -1 & -1 & 3 \end{bmatrix} \text{ for strongly coupled blades.} \quad \textbf{(4.26)}$$

After these matrices obtained, system matrices M, C and K are determined by using equations 4.12, 4.13 and 4.14. These computations are done by using MATLAB software. After this, singular values, left singular vectors and right singular vectors of transfer function (equation 4.21) are determined for a frequency interval by using same MATLAB program. Program codes (first_matlabcode_for_SVD.m) can be seen in attached diskette that is in back cover of the thesis.

4.2 Repeated Eigenvalue Problem

The most common circumstances under which repeated eigenvalues or nearly equal eigenvalues occur in typical structural or mechanical systems are instances where system symmetry exists, such as structures with two or more planes of reflective or cyclic symmetry or in the limiting case of axisymmetric bodies or certain reasons [11].

Since the rotationally periodic structures or turbines have cyclic symmetry, repeated eigenvalue phenomena occurs in these systems.

When the matlab code for weakly coupled blades was run, repeated eigenvector phenomena was seen in the results. Max. and min. Singular value v.s. frequency is seen below in figure 4.3. When these graphics are examined, it is shown that max. singular value curve has only two peaks that show the natural frequencies of the system (section 3.4). Three bladed turbine model has three degree of freedom, so it should be three natural frequency. Because of this, one eigenvalue of the system is repeated. When the natural frequencies are calculated, they are found as,

$\omega_{b1} = 1.0000$ rad/s,

$\omega_{b2} = 1.0149$ rad/s,

$\omega_{b3} = 1.0149$ rad/s.

Max. singular value curve has peaks at these resonance frequencies, so there are only two peaks. It is also seen that smax and smin curves which are max. and min. singular values of system, are almost equal at frequency $\omega = 1.0075$ rad/s. Singular value veering phenomena occurs at this point (section 2). When max. and min. singular values loci approach each other, they either cross or do not cross. Often in

the latter case, even though the loci nearly intersect, in fact they do not but rather veer away from each other with high local curvature.

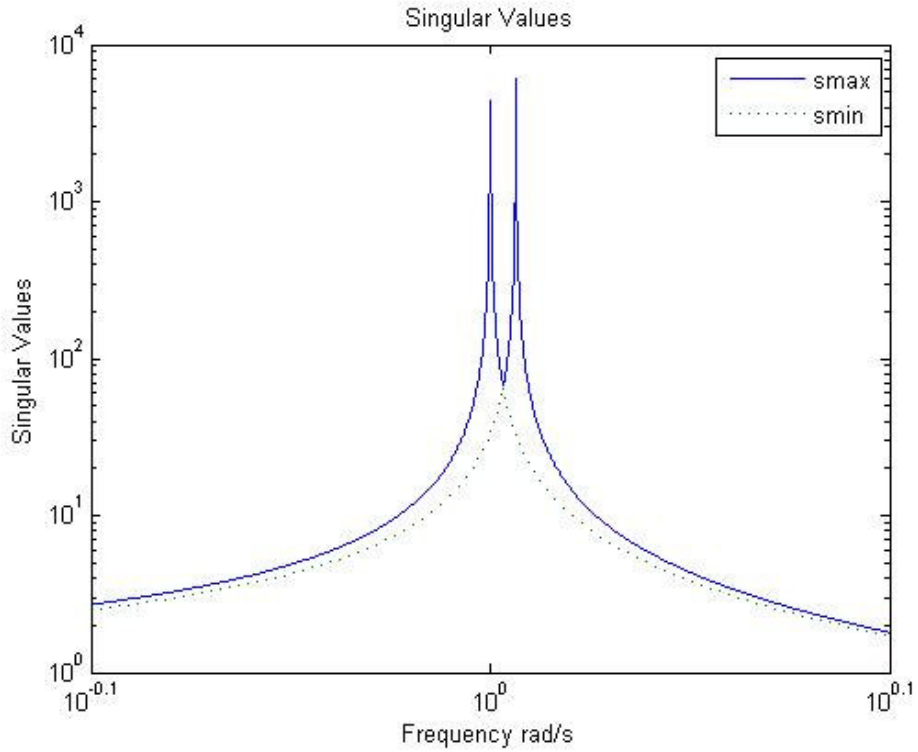

Figure 4.3 : Max. and min. singular values v.s. frequency.

When the left and right singular vectors of this system examined, it is seen that all components of singular vectors have oscilations. Figure 4.4 shows the U_{11} component of left singular vector U_1. It can be seen that, U_{11} value goes constant until veering point. After this point, it shows an unexpected behaviour and suddenly start to oscillate between 0 and 0.8. Other components of singular vectors also show similar behaviour. All plots of singular vectors can be seen Appendix-A.

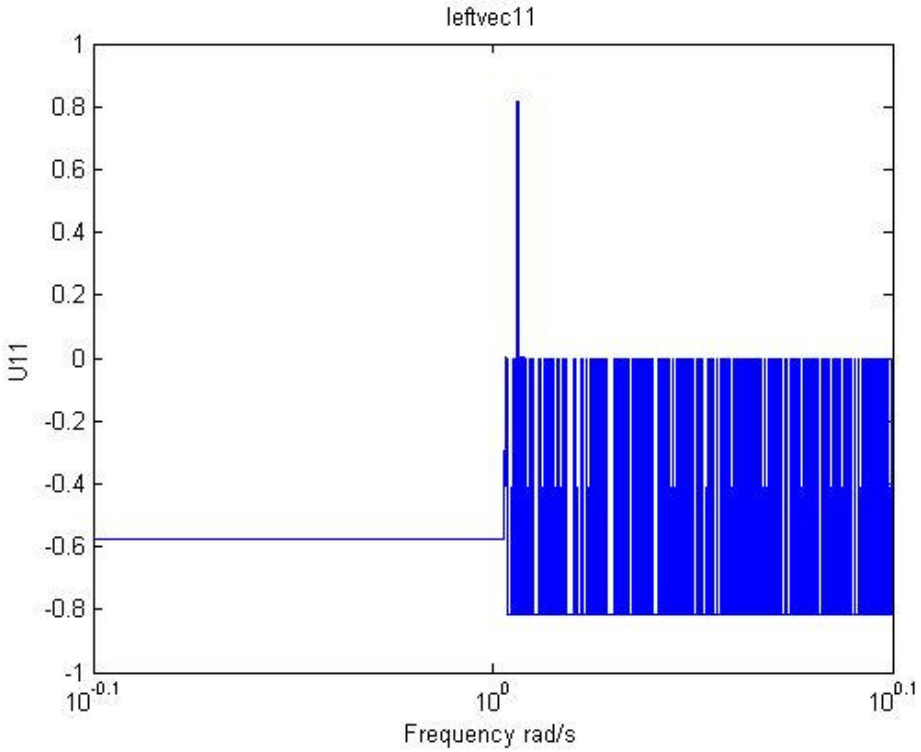

Figure 4.4 : U11 component of left singular vector U1.

Sensitivity analysis and several calculations by hand and mathematica code (can be seen in attached CD of the thesis (Mathematica_code_for_SVD.nb)) are done to determine if this is real behaviour of the system or program error. All calculations give the similar results with matlab calculations.

To understand this unexpected behaviour, another matlab code (can be seen in attached diskette that is in back cover of the thesis (repeated_singular value.m)) is prepeared to see the repeated singular values and repeated components of singular vectors. In this code, repeated singular values and their left and right singular vectors are listed for a frequency interval.

Table 4.2 shows repeated eigenvalues for each frequency. Is is seen that in the table 4.2, second and third singular values repeat each other until the curve veering point. When the frequency value reach the curve veering point, repeated singular value changes and first and second singular values start to repeat each other. As a result, curve veering phenomena effects the repeated singular values and change their order.

Table 4.2: Repeated singular values for each frequency.

No	Description	Frequency	Repeated SV	
1		0,794328235	2	3
2		0,794511248	2	3
3		0,794694304	2	3
⋮		⋮	⋮	⋮
999		0,999654499	2	3
1000		0,99988482	2	3
1001	ω_1	1,000115193	2	3
1002		1,00034562	2	3
1003		1,0005761	2	3
⋮		⋮	⋮	⋮
1031		1,007051141	2	3
1032		1,007283166	2	3
1033	Veering	1,007515244	1	2
1034		1,007747376	1	2
1035		1,007979561	1	2
⋮		⋮	⋮	⋮
1064		1,014502512	1	2
1065		1,014736253	1	2
1066	ω_2	1,014970049	1	2
1067		1,015203898	1	2
1068		1,015437801	1	2
⋮		⋮	⋮	⋮
1998		1,258345499	1	2
1999		1,258635422	1	2
2000		1,258925412	1	2

Table 4.3 shows the components of left singular vectors and table 4.4 shows the right singular vectors' components. When these tables examined it can be seen that, left and right singular vectors of repeated singular values change locations. For example, in the table 4.2, second and third singular values repeat each other until the curve veering point. When the frequency value reach the curve veering point, repeated singular value changes and first and second singular values start to repeat each other. So, 2nd and 3rd left and right singular vectors change locations until curve veering point, after this point 1st and 2nd left and right singular vectors start to change locations. This shifts causes singular vectors to oscilate.

Because of the cyclic symmetry, these shifts do not effect the systems gain. Shifting phenomena can be seen figure 4.5. So, singular values are not effected by these shifts. But, left and right singular vectors need to be arranged. This step is done by

hand. All the components of vectors were arranged and they were entered to MATLAB program by defining U_{11}, U_{21}, U_{31}, U_{12}, U_{22}, U_{32}, U_{13}, U_{23}, U_{33}, V_{11}, V_{21}, V_{31}, V_{12}, V_{22}, V_{32}, V_{13}, V_{23}, V_{33}.

Table 4.3: Components of left singular vectors for each frequency.

No	Desc.	Freq.	U11	U21	U31	U12	U22	U32	U13	U23	U33
1		0,794	-0,577	-0,577	-0,577	0,000	-0,707	0,707	0,816	-0,408	-0,408
2		0,795	-0,577	-0,577	-0,577	0,816	-0,408	-0,408	0,000	-0,707	0,707
3		0,795	-0,577	-0,577	-0,577	0,000	-0,707	0,707	0,816	-0,408	-0,408
⋮	⋮	⋮	⋮	⋮	⋮	⋮	⋮	⋮	⋮	⋮	⋮
999		1,000	-0,577	-0,577	-0,577	0,816	-0,408	-0,408	0,000	-0,707	0,707
1000		1,000	-0,577	-0,577	-0,577	0,000	-0,707	0,707	0,816	-0,408	-0,408
1001	ω_1	1,000	-0,577	-0,577	-0,577	0,000	-0,707	0,707	0,816	-0,408	-0,408
1002		1,000	-0,577	-0,577	-0,577	0,816	-0,408	-0,408	0,000	-0,707	0,707
1003		1,001	-0,577	-0,577	-0,577	0,816	-0,408	-0,408	0,000	-0,707	0,707
⋮	⋮	⋮	⋮	⋮	⋮	⋮	⋮	⋮	⋮	⋮	⋮
1031		1,007	-0,577	-0,577	-0,577	0,000	-0,707	0,707	0,816	-0,408	-0,408
1032		1,007	-0,577	-0,577	-0,577	0,816	-0,408	-0,408	0,000	-0,707	0,707
1033	Veering	1,008	0,000	-0,707	0,707	-0,816	0,408	0,408	-0,577	-0,577	-0,577
1034		1,008	0,000	-0,707	0,707	-0,816	0,408	0,408	-0,577	-0,577	-0,577
1035		1,008	-0,816	0,408	0,408	0,000	-0,707	0,707	-0,577	-0,577	-0,577
⋮	⋮	⋮	⋮	⋮	⋮	⋮	⋮	⋮	⋮	⋮	⋮
1063		1,015	0,000	-0,707	0,707	-0,816	0,408	0,408	-0,577	-0,577	-0,577
1064		1,015	-0,816	0,408	0,408	0,000	-0,707	0,707	-0,577	-0,577	-0,577
1065		1,015	-0,816	0,408	0,408	0,000	-0,707	0,707	-0,577	-0,577	-0,577
1066	ω_2	1,015	0,000	-0,707	0,707	-0,816	0,408	0,408	-0,577	-0,577	-0,577
1067		1,015	-0,816	0,408	0,408	0,000	-0,707	0,707	-0,577	-0,577	-0,577
⋮	⋮	⋮	⋮	⋮	⋮	⋮	⋮	⋮	⋮	⋮	⋮
1998		1,258	-0,816	0,408	0,408	0,000	-0,707	0,707	-0,577	-0,577	-0,577
1999		1,259	-0,816	0,408	0,408	0,000	-0,707	0,707	-0,577	-0,577	-0,577
2000		1,259	-0,816	0,408	0,408	0,000	-0,707	0,707	-0,577	-0,577	-0,577

Table 4.4: Components of right singular vectors for each frequency.

No	Desc.	Freq.	V11	V21	V31	V12	V22	V32	V13	V23	V33
1		0,794	-0,577	-0,577	-0,577	0,000	-0,707	0,707	0,816	-0,408	-0,408
2		0,795	-0,577	-0,577	-0,577	0,816	-0,408	-0,408	0,000	-0,707	0,707
3		0,795	-0,577	-0,577	-0,577	0,000	-0,707	0,707	0,816	-0,408	-0,408
⋮	⋮	⋮	⋮	⋮	⋮	⋮	⋮	⋮	⋮	⋮	⋮
999		1,000	-0,577	-0,577	-0,577	0,816	-0,408	-0,408	0,000	-0,707	0,707
1000		1,000	-0,577	-0,577	-0,577	0,000	-0,707	0,707	0,816	-0,408	-0,408
1001	ω_1	1,000	0,577	0,577	0,577	0,000	-0,707	0,707	0,816	-0,408	-0,408
1002		1,000	0,577	0,577	0,577	0,816	-0,408	-0,408	0,000	-0,707	0,707
1003		1,001	0,577	0,577	0,577	0,816	-0,408	-0,408	0,000	-0,707	0,707
⋮	⋮	⋮	⋮	⋮	⋮	⋮	⋮	⋮	⋮	⋮	⋮
1031		1,007	0,577	0,577	0,577	0,000	-0,707	0,707	0,816	-0,408	-0,408
1032		1,007	0,577	0,577	0,577	0,816	-0,408	-0,408	0,000	-0,707	0,707
1033	Veering	1,008	0,000	-0,707	0,707	-0,816	0,408	0,408	0,577	0,577	0,577
1034		1,008	0,000	-0,707	0,707	-0,816	0,408	0,408	0,577	0,577	0,577
1035		1,008	-0,816	0,408	0,408	0,000	-0,707	0,707	0,577	0,577	0,577
⋮	⋮	⋮	⋮	⋮	⋮	⋮	⋮	⋮	⋮	⋮	⋮
1063		1,015	0,000	-0,707	0,707	-0,816	0,408	0,408	0,577	0,577	0,577
1064		1,015	-0,816	0,408	0,408	0,000	-0,707	0,707	0,577	0,577	0,577
1065		1,015	-0,816	0,408	0,408	0,000	0,707	-0,707	0,577	0,577	0,577
1066	ω_2	1,015	0,000	0,707	-0,707	0,816	-0,408	-0,408	0,577	0,577	0,577
1067		1,015	0,816	-0,408	-0,408	0,000	0,707	-0,707	0,577	0,577	0,577
⋮	⋮	⋮	⋮	⋮	⋮	⋮	⋮	⋮	⋮	⋮	⋮
1998		1,258	0,816	-0,408	-0,408	0,000	0,707	-0,707	0,577	0,577	0,577
1999		1,259	0,816	-0,408	-0,408	0,000	0,707	-0,707	0,577	0,577	0,577
2000		1,259	0,816	-0,408	-0,408	0,000	0,707	-0,707	0,577	0,577	0,577

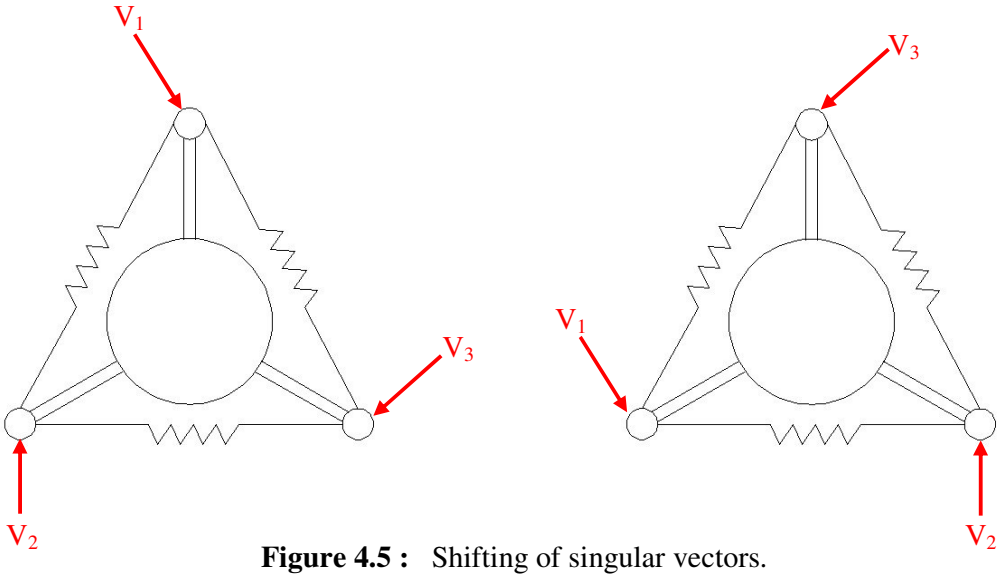

Figure 4.5 : Shifting of singular vectors.

4.2.1 Generalized Eigenvectors and Calculation of Repeated Eigenvectors

After all components of left and right singular vectors are entered the MATLAB software, repeated singular vectors are need to be calculated according to generalized eigenvector formulation. Because, MATLAB software does not calculate repeated singular vectors correctly.

It is well known that in case of a repeated eigenvalue of multiplicity m, there may not exist a full sub-basis of m linearly independent eigenvectors. These systems are generally termed ‘‘defective.’’ the matrix [12].

Suppose A is 3 x 3 matrix with eigenvalues $\lambda_1, \lambda_2, \lambda_2$. Let A_ε, be a perturbation of A, say, $A_\varepsilon = A + \varepsilon B, |\varepsilon| << 1$, B = arbitrary, such that A_ε has distict eigenvalues $\lambda_1, \lambda_2, \lambda_2 = \lambda_2 + \delta, |\delta| << 1$, and corresponding eigenvectors $\{p_1, p_2\}$ and $p_3 = p_2 + \delta z$. When $\varepsilon \to 0$ [13],

$$(A - \lambda_i I) p_i = 0, i = 1,2 \qquad \textbf{(4.27)}$$

$$(A - \lambda_2 I) z = p_2 \qquad \textbf{(4.28)}$$

$\{p_1, p_2, z\}$ are linearly independent and the vector z is called a generalized eigenvector of A [13].

According to this definition, all components of repeated singular values were calculated by using another matlab code. (can be seen in attached diskette that is in back cover of the thesis (repeated_singular_vectors_and_graphs.m)). Finally, effects of mode localization and curve veering on input-output properties of a three bladed turbine for weakly coupled and strongly coupled conditions were studied by using the matlab codes in diskette. (repeated_singular_value.m and repeated_singular_vectors_and_graphs.m).

4.3 Tuned Turbine Model

In this section, input-output properties of tuned assembly of turbine model is examined. For tuned systems, it is assumed that, blades are uniformly spaced, and the hub is symmetric. Hence, all terms of equation of motion (equation 4.21) are similar and Δf_i term (equation 4.2) that represents the dimensionless mistuning strength for the ith component system is zero for the tuned system. Choosen parameter values are seen in table 4.5.

Table 4.5: Choosen parameter values for tuned assembly of turbine model.

	Weakly Coupled Blades	Strongly Coupled Blades
M	1	1
ζ	0	0
ω_b	1	1
R	0.1	1
Δf	0	0

Another important parameter for equation of motion is R^2 which is the dimensionless coupling between component systems. This parameter is choosen 0.1 for weakly coupled assembly of turbine blades and 1 for strongly coupled assembly of turbine blades. After these parameters are choosen, SVD based analysis of mode localization and curve veering on input-output properties of turbine is performed.

One interested case for a mechanical system is the worst possible loading case. If we consider an equation of motion as [4],

$$q(s) = G(s)F(s) \tag{4.29}$$

we look for the displacement vector d in response to the worst loading f; that is [4],

Find

$$\max \|q\|_2 \qquad s.t. \qquad \|f\|_2 = 1, \tag{4.30}$$

Where the forcing vector length is set to unity $\|f\|_2 = 1$ to quantify the input-output relationships uniquely. By definition of singular values, the above problem defined is equivalent to finding the largest singular value σ_1 of the transfer function matrix G between the input f and output q [4].

Instead of solving the original problem defined by equation (4.30), finding the largest singular value σ_1 is computationally cheaper, because it eliminates the need to find the worst possible load case which is cumbersome. As revisited in section 3, the right singular vector v_1 and left singular vector u_1 give the worst possible loading direction and the corresponding structural response respectively. Thus the original problem reduces to finding the maximum eigenvalue of GG^H which is computationally much cheaper to solve. For instance, in order to solve equation (4.25) for ten coupled pendulums with four external force terms, if a constrained optimization algorithm employing the Newton method in the International Mathematical Subroutines Library (IMSL) is used to compute the worst load case, it is found to be about 90 times slower than the SVD. If the proble size increases, the difference between the CPU times of the SVD-based analysis and conventional methods even deepens. Note that there is no need to compute all the singular values, because only the first singular value and associated singular vectors are needed that can be computed very efficiently by using selective algorithms, e.g., see references [14-16]. [4].

So, maximum singular value σ_1 and related singular vectors u_1 and v_1 are analysed continuous parts of this study.

4.3.1 Weakly Coupled Assembly of Tuned Turbine Blades

The following parameter values are used in numerical study of tuned weakly coupled assembly of turbine blades.

Table 4.6: Parameter values for tuned weakly coupled assembly of blades.

Parameters	i=1	i=2	i=3
m_i	1	1	1
ζ_i	0	0	0
ω_{bi}	1	1	1
R	0.1	0.1	0.1
Δf_i	0	0	0

Figure 4.6 shows the max. (σ_1) and min. (σ_3) singular values' respond to excitation frequency. It is seen that, σ_1 has only two peaks. These peaks occur at resonance frequencies of system ω_1=1 rad/s and ω_2=1.0149 rad/s. Because of the repeated eigenvalue phenomena there are only two resonance frequencies. Third frequency ω_3 is repeated for this system.

It is also seen that, singular value veering phenomena occurs at ω_v=0.0075 rad/s, where max. (σ_1) and min. (σ_3) singular values approach each other, and suddenly they move away from each other. In contrast to early studies about curve veering phenomena of tuned systems' eigenvalues [1,2,3,5,10], singular value veering phenomena of tuned systems occurs. This property causes singular vectors to change direction. It is also seen that, singular values change smoothly that means input-output transfer function relationships and power-energy transmission ratios are smooth.

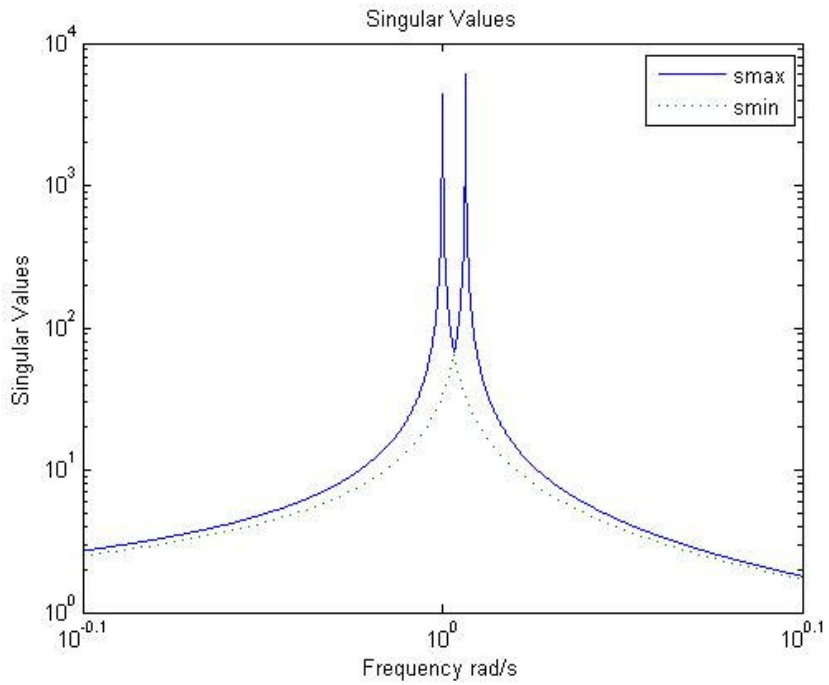

Figure 4.6 : Max. (σ_1) and min. (σ_3) singular values of tuned weakly coupled blades, where R=0.1.

It is showed that left (U) and right (V) singular vectors' component's responds from figure 4.7 to 4.12.

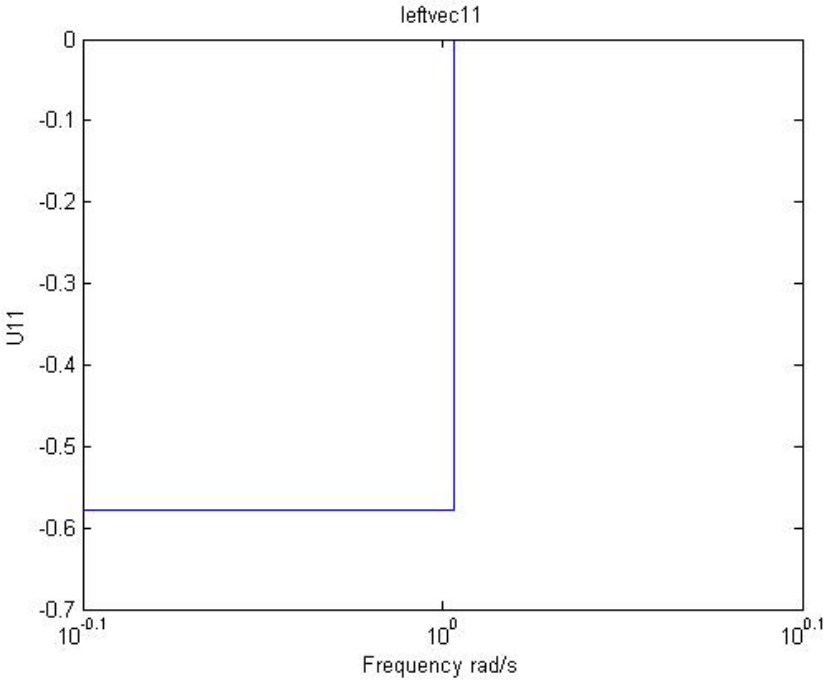

Figure 4.7 : The left singular vector component u11, where R = 0.1.

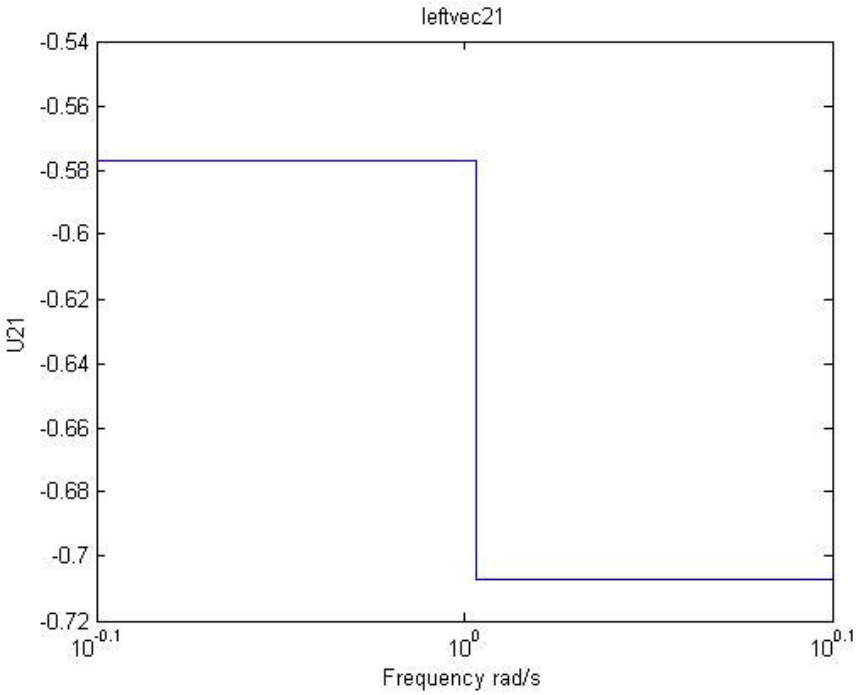

Figure 4.8 : The left singular vector component u21, where R = 0.1.

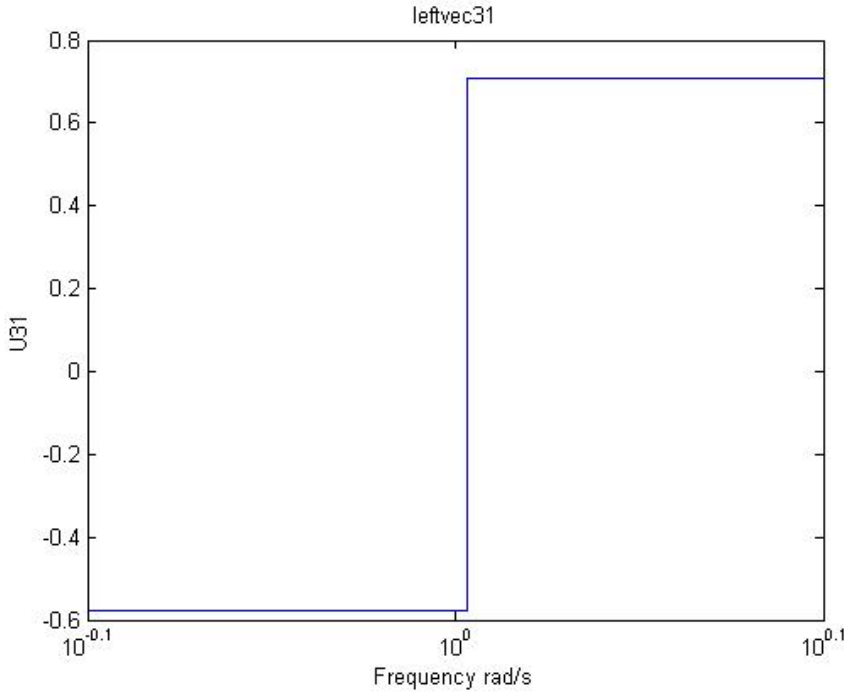

Figure 4.9 : The left singular vector component u31, where R = 0.1.

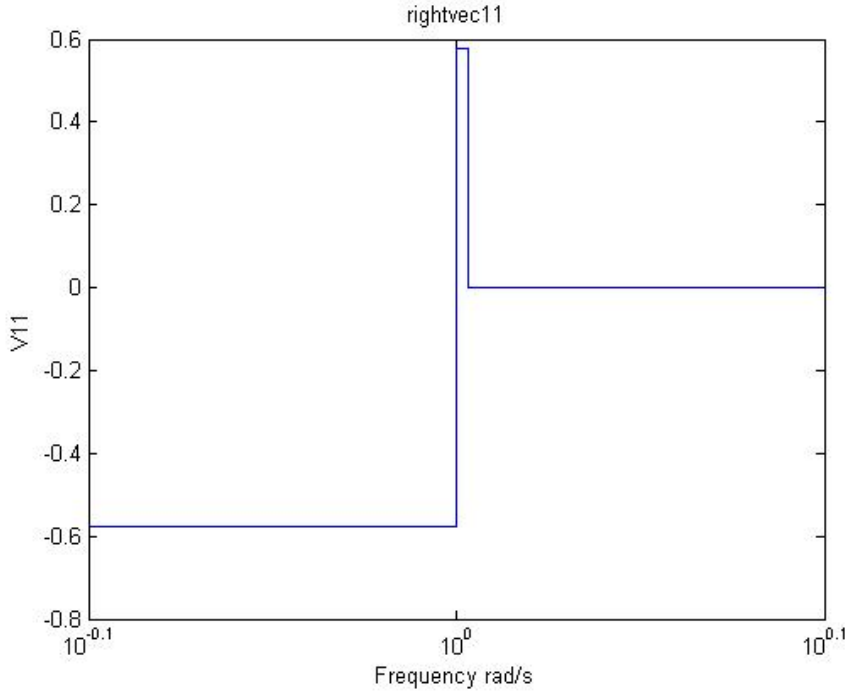

Figure 4.10 : The right singular vector component v11, where R = 0.1.

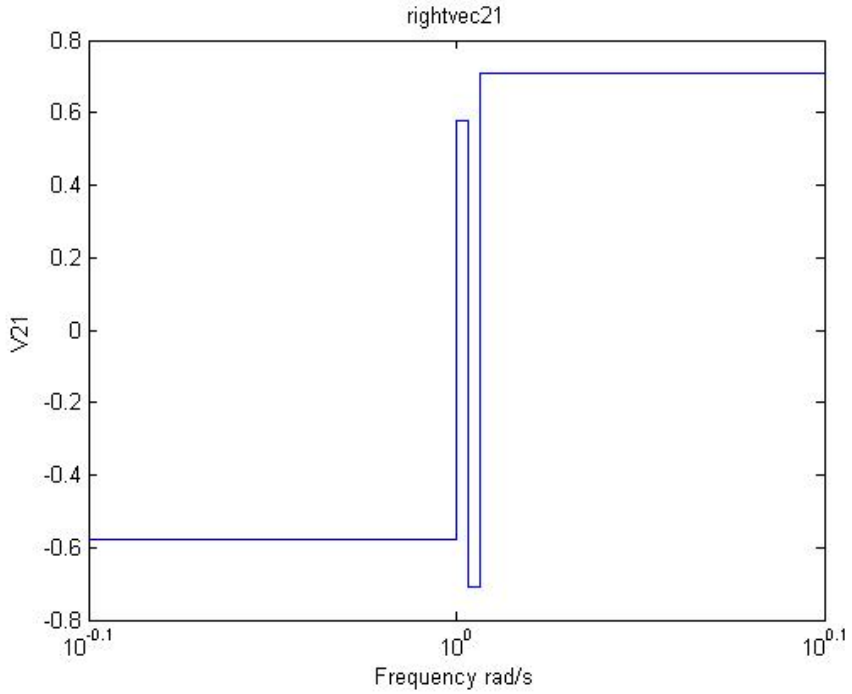

Figure 4.11 : The right singular vector component v21, where R = 0.1.

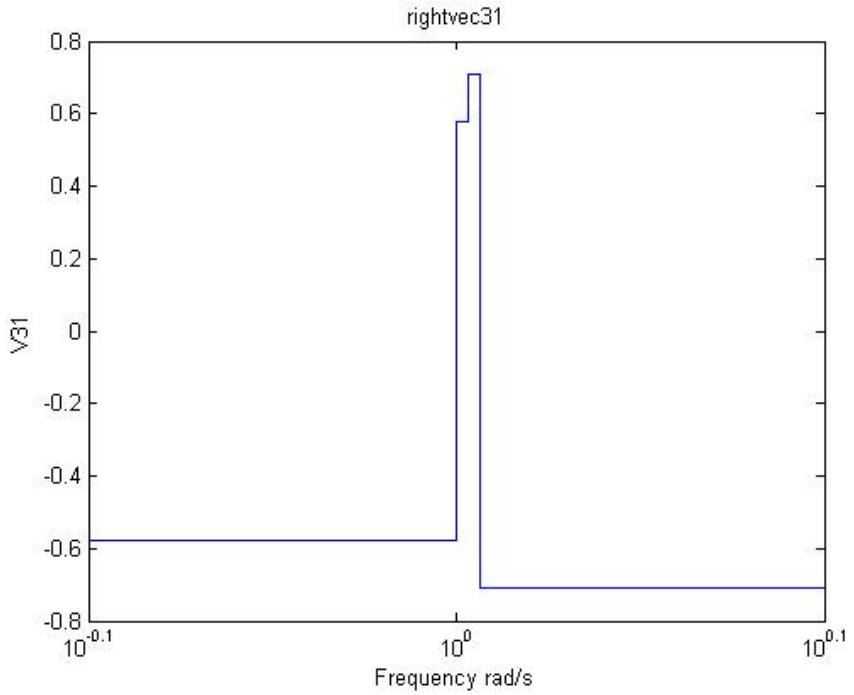

Figure 4.12 : The right singular vector component v31, where R = 0.1.

It is seen that components of first left singular vector (u_{11}, u_{21} and u_{31}) change abrubtly when singular value loci veering occurs at ω_v=1.58 rad/s. When the components of first right singular vector (v_{11}, v_{21} and v_{31}) are examined, v_{11} shows abrubt changes on first resonance frequency (ω_1=1 rad/s) and veering frequency (ω_v=1.58 rad/s). v_{21} and v_{31} shows abrubt changes on resonance frequencies (ω_1=1 rad/s and ω_2=1.99 rad/s) and veering frequency (ω_v=1.58 rad/s).

As a result of singular vector localization, input directions change drastically at resonance frequencies and veering frequency to obtain the gain equal to singular values and the distribution of system's energy among different degrees of freedom also changes drastically. All figures of singular values and singular vectors can be seen in Appendix-C.

4.3.2 Strongly Coupled Assembly of Tuned Turbine Blades

The following parameter values are used in numerical study of tuned strongly coupled assembly of turbine blades.

Table 4.7: Parameter values for tuned strongly coupled assembly of blades.

Parameters	i=1	i=2	i=3
m_i	1	1	1
ζ_i	0	0	0
ω_{bi}	1	1	1
R	1	1	1
Δf_i	0	0	0

Figure 4.13 shows the max. (σ_1) and min. (σ_3) singular values' respond to excitation frequency. Repeated singular value phonemena also occurs in strongly coupled assembly of tuned turbine blades. It is seen that, σ_1 has two peaks. These peaks occur at resonance frequencies of system ω_1=1 rad/s and ω_2=1.99 rad/s. Because of the repeated eigenvalue phenomena there are only two resonance frequencies. Third frequency ω_3 is repeated for this system. The gap between the peaks of σ_1 is wider for strongly coupled system than the gaps between the peaks of σ_1 for weak coupled system. This is caused because of the higher coupling stifness (k_c).

It is also seen that, singular value veering phenomena occurs at ω_v=1,58 rad/s, where max. (σ_1) and min. (σ_3) singular values approach each other, and suddenly they move away from each other. In contrast to early studies about curve veering phenomena of tuned systems' eigenvalues [1,2,3,5,10], singular value veering phenomena of tuned systems occurs. This property causes singular vectors to change direction. It is also seen that, singular values change smoothly that means input-output transfer function relationships and power-energy transmission ratios are smooth.

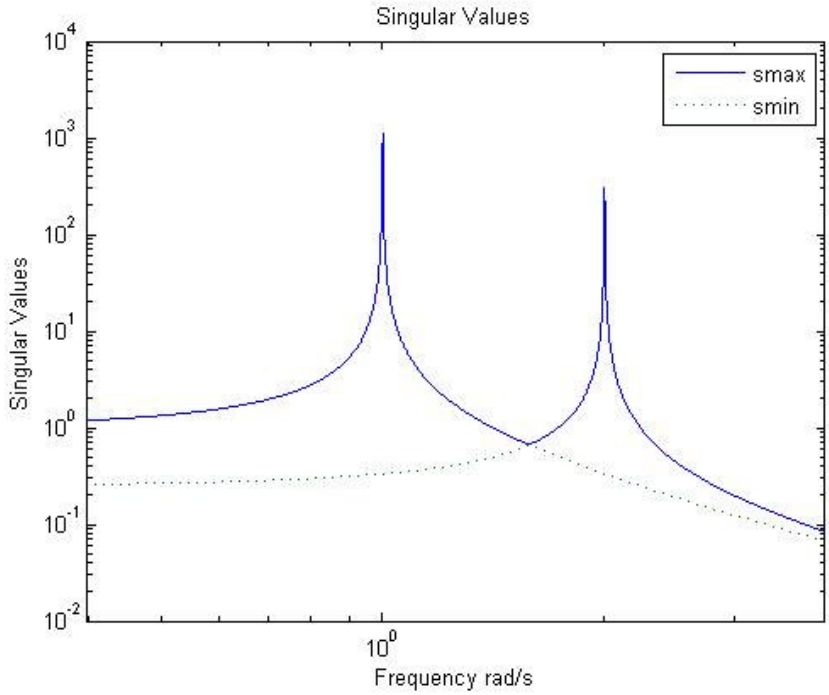

Figure 4.13 : Max. (σ_1) and min. (σ_3) singular values of tuned strongly coupled blades, where R=1.

It is showed that left (U) and right (V) singular vectors' component's responds from figure 4.14 to 4.19.

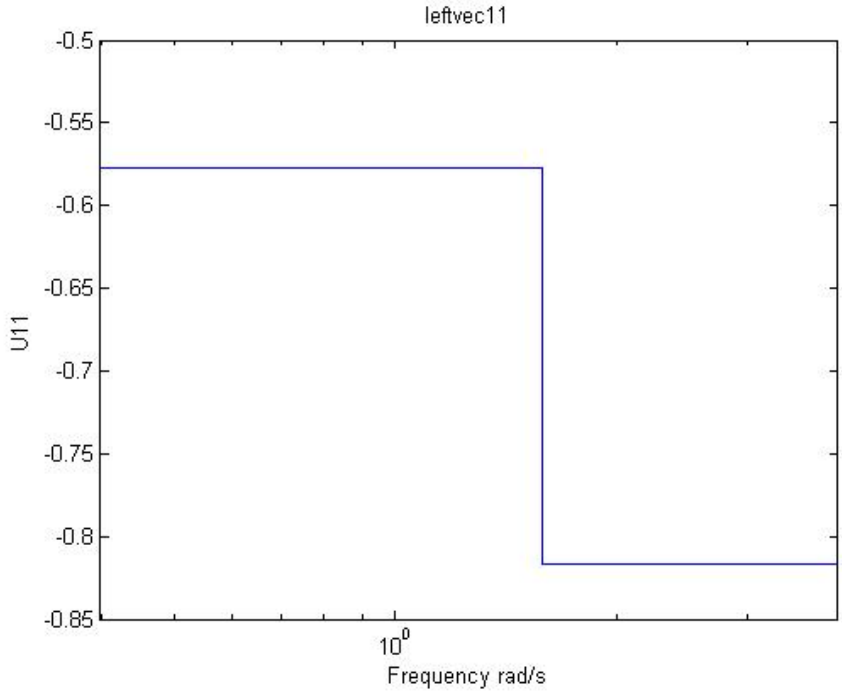

Figure 4.14 : The left singular vector component u11, where R = 1.

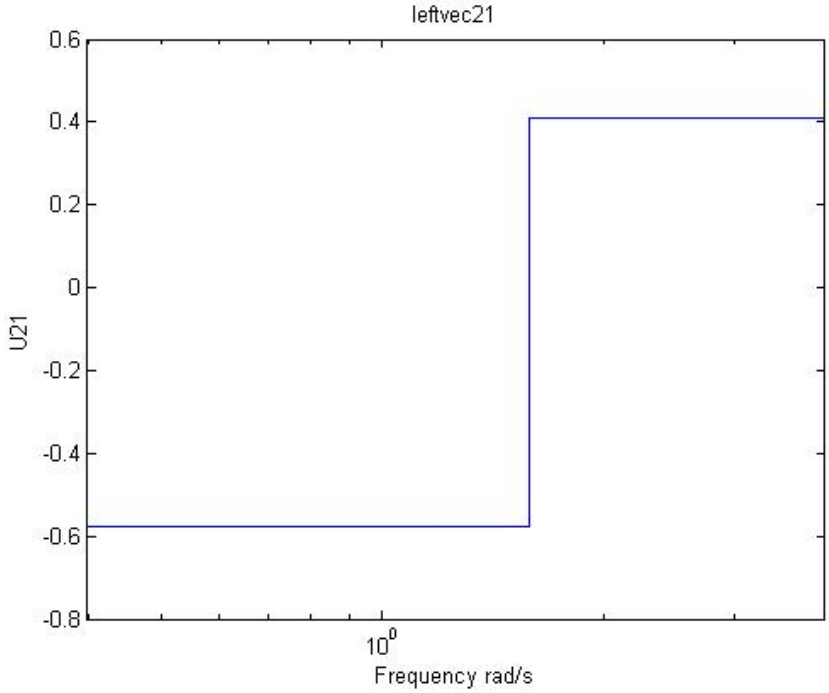

Figure 4.15 : The left singular vector component u21, where R = 1.

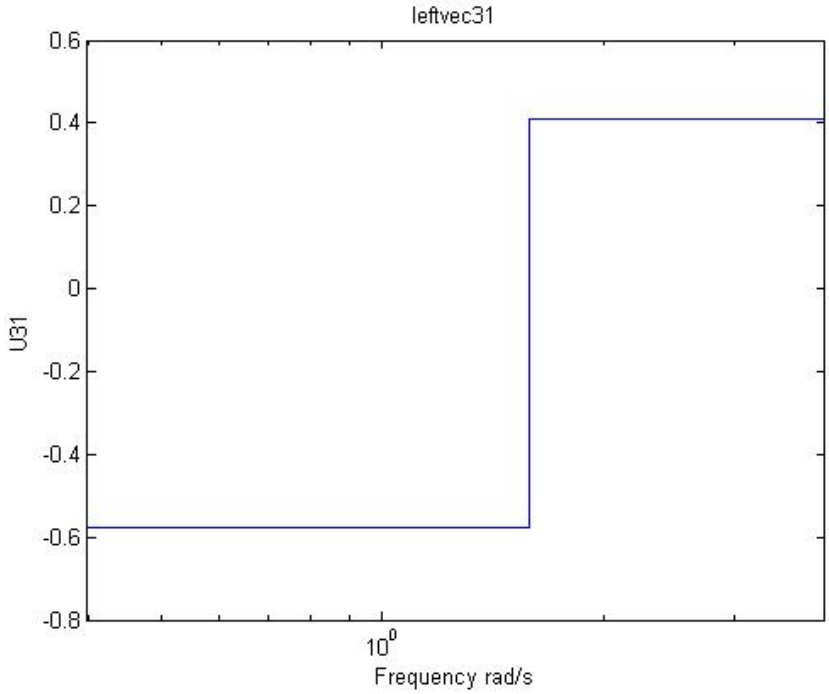

Figure 4.16 : The left singular vector component u31, where R = 1.

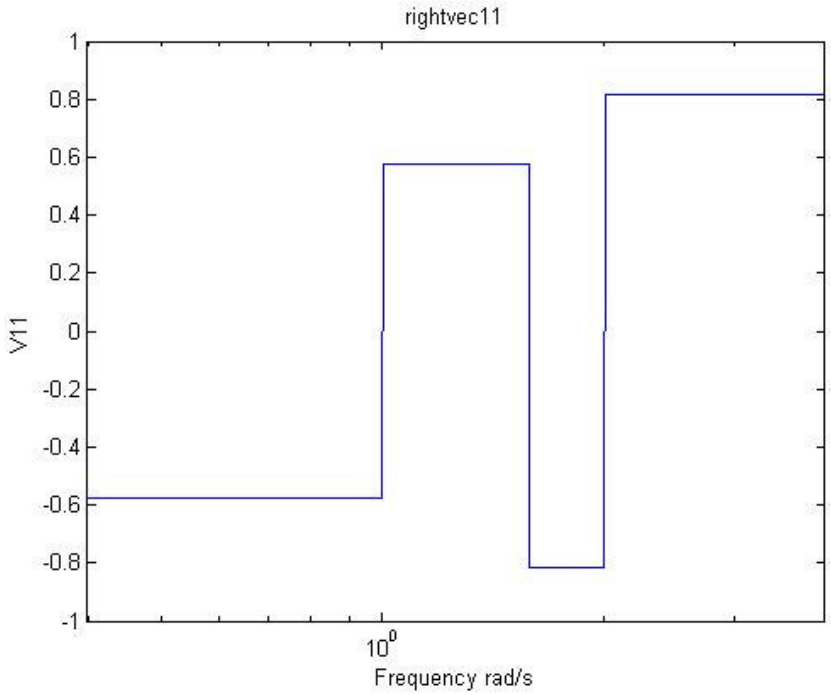

Figure 4.17 : The left singular vector component v11, where R = 1.

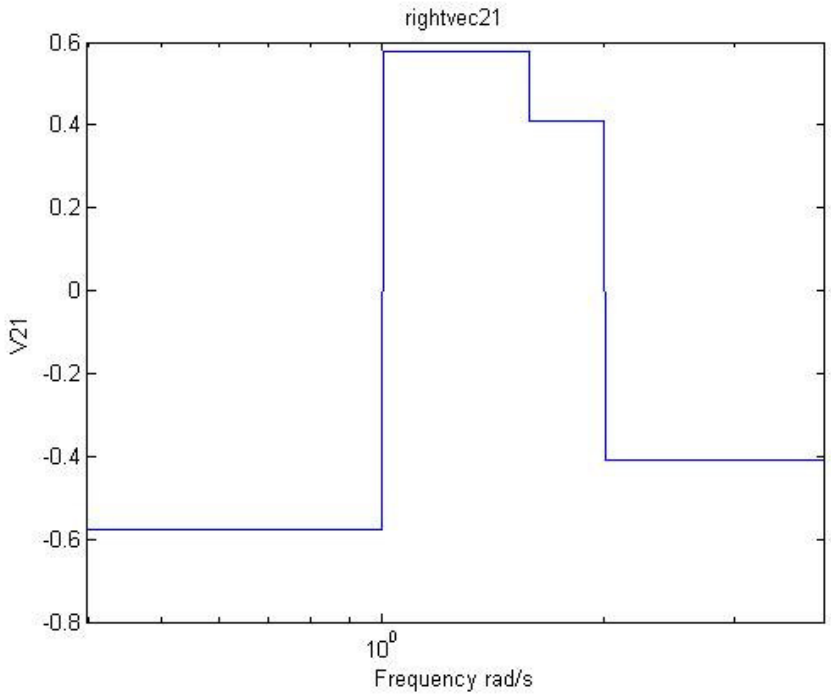

Figure 4.18 : The left singular vector component v21, where R = 1.

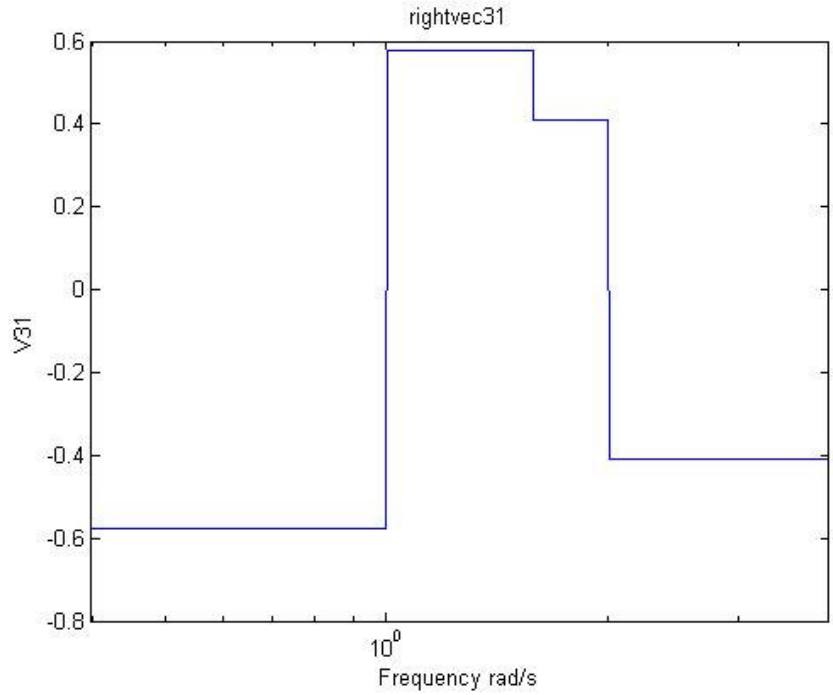

Figure 4.19 : The left singular vector component v31, where R = 1.

It is seen that components of first left singular vector (u_{11}, u_{21} and u_{31}) change abrubtly when singular value loci veering occurs at ω_v=0.0075 rad/s. When the components of first right singular vector (v_{11}, v_{21} and v_{31}) are examined, v_{11} shows abrubt changes on first resonance frequency (ω_1=1 rad/s) and veering frequency (ω_v=0.0075 rad/s). v_{21} and v_{31} shows abrubt changes on resonance frequencies (ω_1=1 rad/s and ω_2=1.0149 rad/s) and veering frequency (ω_v=0.0075 rad/s).

As a result of singular vector localization, input directions change drastically at resonance frequencies and veering frequency to obtain the gain equal to singular values and the distribution of system's energy among different degrees of freedom also changes drastically. All figures of singular values and singular vectors can be seen in Appendix-C.

4.4 Mistuned Turbine Model

In this section, input-output properties of mistuned assembly of turbine model is examined. For mistuned systems, it is assumed that, blades are uniformly spaced, and the hub is symmetric but blades' resonance frequencies are different. Hence, all

terms of equation of motion (equation 4.21) are similar and Δf_i term (equation 4.2) that represents the dimensionless mistuning strength for the ith component system changes between -0.36 and 0.44 for the mistuned system. Choosen parameter values are seen in table 4.8. Program codes can be seen in the CD. For strongly coupled blades strongly_disorder_blades.m and for weakly coupled blades weakly_disorder_blades.m codes are written.

Table 4.8: Choosen parameter values for mistuned assembly of turbine model.

	Weakly Coupled Blades	Strongly Coupled Blades
M	1	1
ζ	0	0
ω_b	1	1
R	0.1	1
Δf	-0.36, ..., 0.44	-0.36, ..., 0.44

Another important parameter for equation of motion is R^2 which is the dimensionless coupling between component systems. This parameter is choosen 0.1 for weakly coupled assembly of turbine blades and 1 for strongly coupled assembly of turbine blades. After these parameters are choosen, SVD based analysis of mode localization and curve veering on input-output properties of turbine is performed.

Because of the one interested case for a mechanical system is the worst possible loading case, maximum singular value σ_1 and related singular vectors u_1 and v_1 are analysed continuous parts of this study.

4.4.1 Weakly Coupled Assembly of Mistuned Turbine Blades

The following parameter values are used in numerical study of mistuned weakly coupled assembly of turbine blades. When this study is performed to examine the disorder effects, it is assumed that resonance frequency of the first blade of the turbine change between 0.8 Hz and 1.2 Hz. According to equation 4.8,

$$\Delta f_i = \left(\omega_{bi}^2 - \omega_b^2\right)/\omega_b^2 \quad \textbf{(4.31)}$$

$$\omega_{bi} = [0.8 \quad \cdots \quad 1.2] \quad \textbf{(4.32)}$$

$$\Delta f_1 = [-0.36 \quad \cdots \quad 0.44] \quad \textbf{(4.33)}$$

Δf_1 changes between -0.36 and 0.44. When the $\omega_{bi} = 1Hz$, system is tuned because of the disorder parameter Δf =0. Because the equation of motion is linear, transposition principle can be applied to examine different blade configuration. So disorder is given only one blade in this study.

Table 4.9: Parameter values for mistuned weakly coupled assembly of blades.

Parameters	i=1	i=2	i=3
m_i	1	1	1
ζ_i	0	0	0
ω_{bi}	1	1	1
R	0.1	0.1	0.1
Δf_i	-0.36, ..., 0.44	0	0

Figure 4.20 and 4.21 show the max. (σ_1) singular value's respond to excitation frequency. It is seen that, there are three peaks on figures 4.20 and 4.21. This shows that there is no repeated singular value phenomena occurs, when the system has disorder. When the disorder approaches to 1, resonance frequencies approach each other and suddenly change directions. 3D singular value Veering phenomena occurs when the blades are weakly coupled. Red line shows the change of ω_1, orange line shows the change of ω_2 and green line shows the change of ω_3. These peaks occur at resonance frequencies of system and resonance frequencies change as related to disorder, because the stiffness matrix of the system changes for every disorder value.

This condition shows that, 1st resonance frequency is effected a lot from disorder. 2nd and 3rd resonance frequencies change smoothly until the point where disorder is 1. That means, while the input-output transfer function relationships and power-

energy transmission ratios are smooth for 2nd and 3rd resonance frequencies, they are not smooth for 1st resonance frequency.

When the disorder is greater than 1, 1st and 2nd resonance frequencies change smoothly but 3rd resonance frequency shows abrupt changes. That means, while the input-output transfer function relationships and power-energy transmission ratios are smooth for 1st and 2nd resonance frequencies, they are not smooth for 3rd resonance frequency.

Since the 1st singular value represents the worst loading conditions, it is seen that system's gain is effected a lot with the disorder.

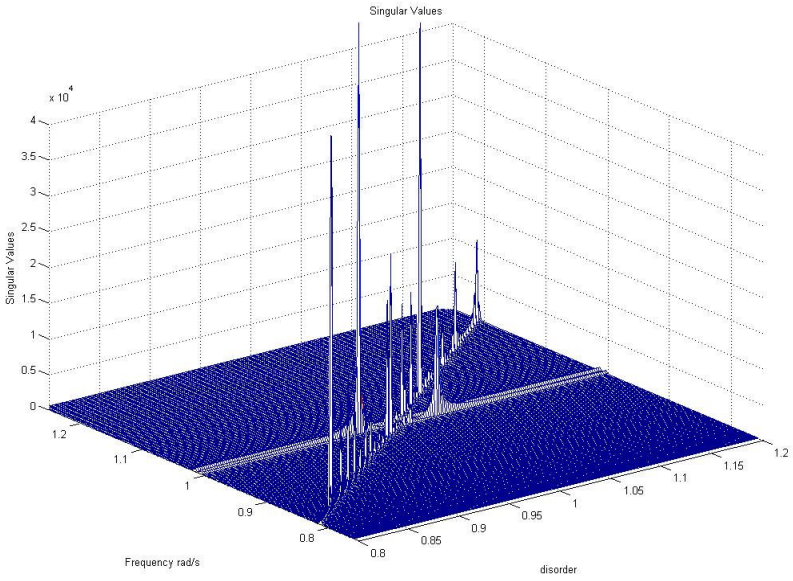

Figure 4.20 : Effects of Disorder on Max. (σ_1) singular value of tuned weakly coupled blades, where R=0.1.

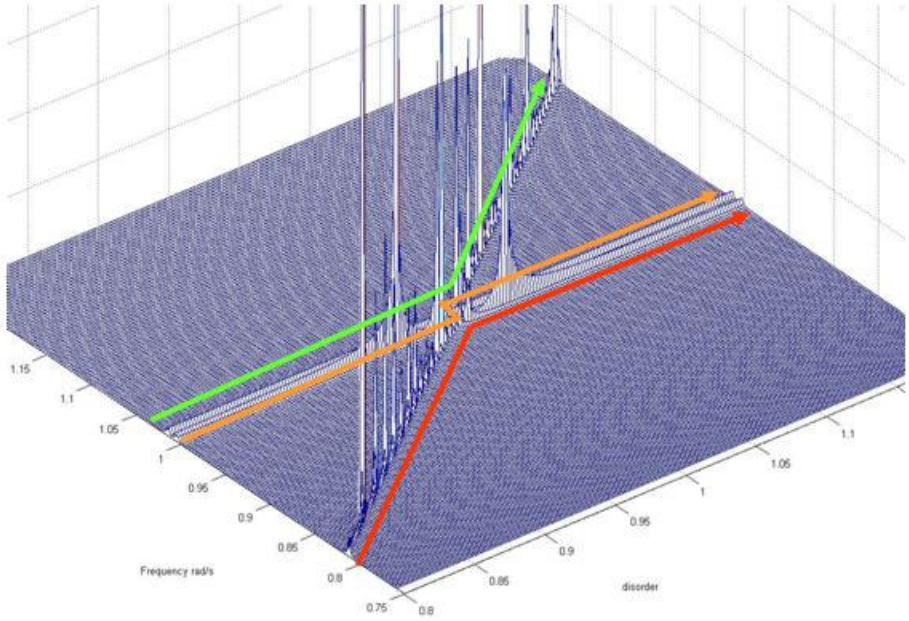

Figure 4.21 : Effects of Disorder on Max. (σ_1) singular value of tuned weakly coupled blades, where R=0.1.

It is showed that left (U) and right (V) singular vectors' component's responds of 1st singular value from figure 4.22 to 4.33.

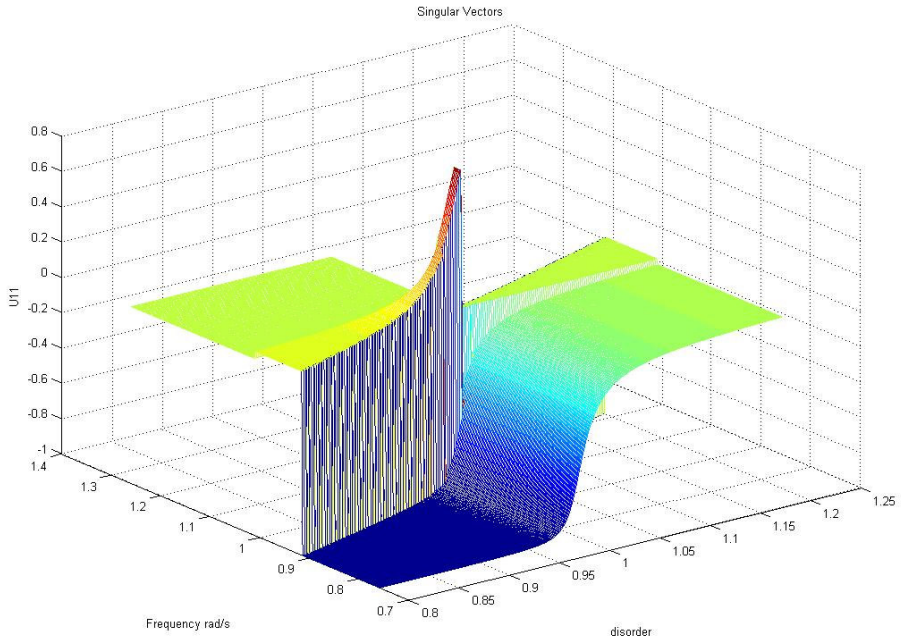

Figure 4.22: Effects of disorder on the left singular vector component u11, where R= 0.1.

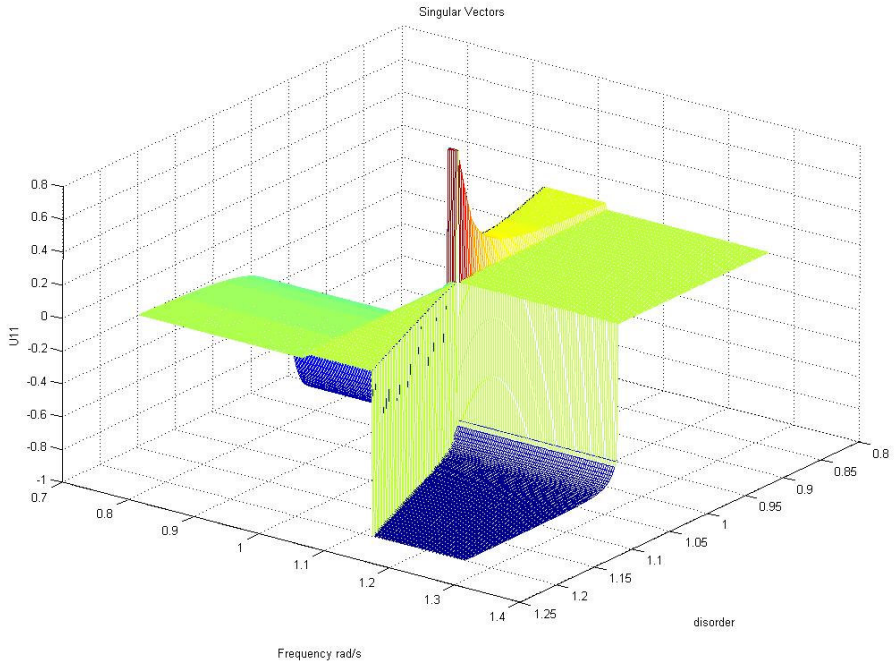

Figure 4.23: Effects of disorder on the left singular vector component u11, where R= 0.1.

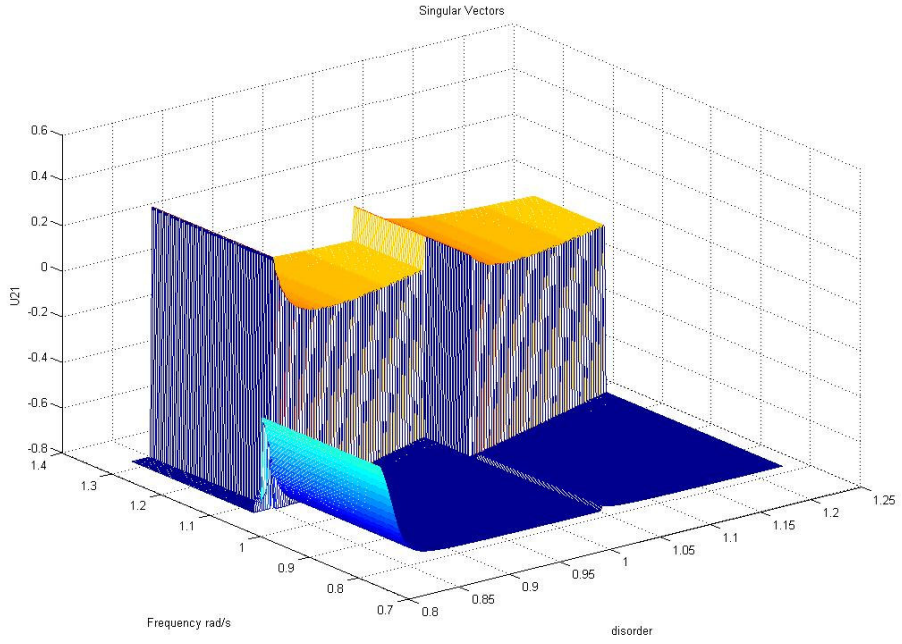

Figure 4.24: Effects of disorder on the left singular vector component u21, where R= 0.1.

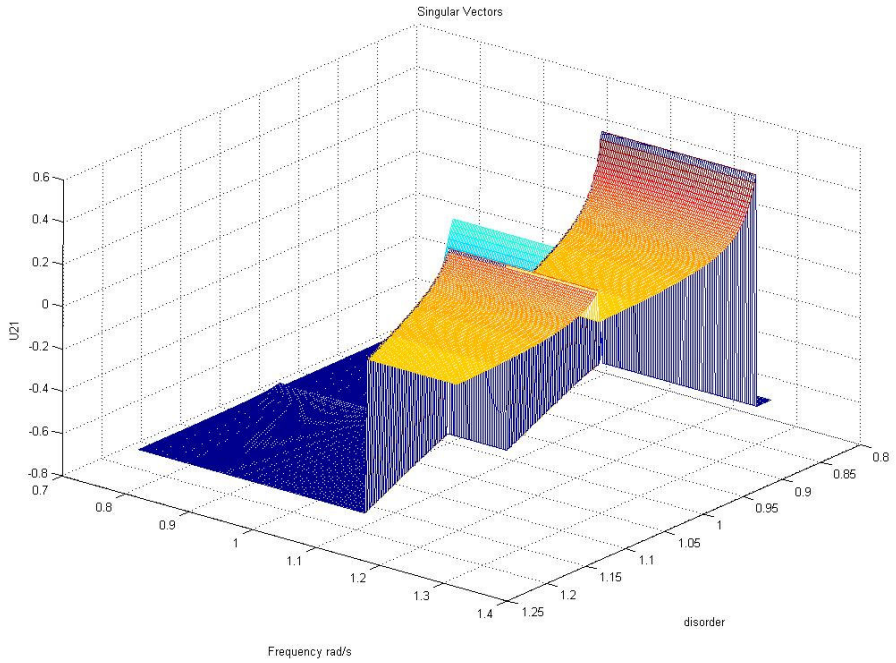

Figure 4.25: Effects of disorder on the left singular vector component u21, where R= 0.1.

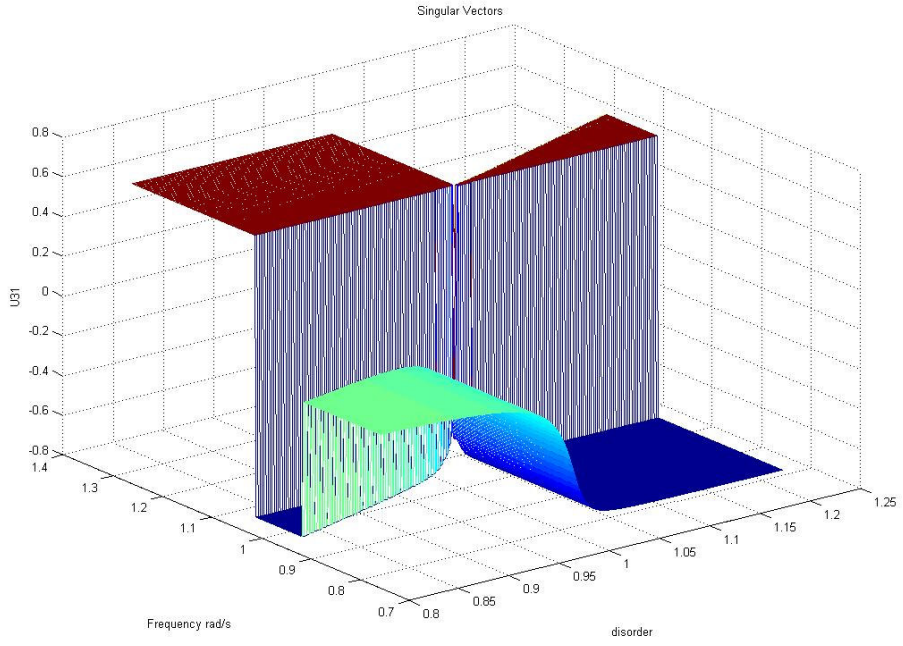

Figure 4.26: Effects of disorder on the left singular vector component u31, where R= 0.1.

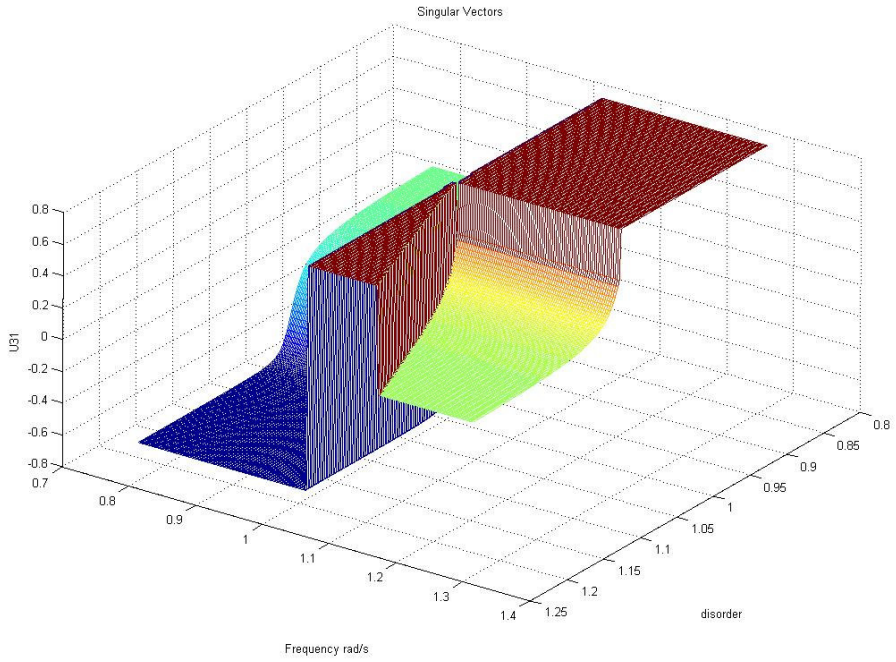

Figure 4.27: Effects of disorder on the left singular vector component u31, where R= 0.1.

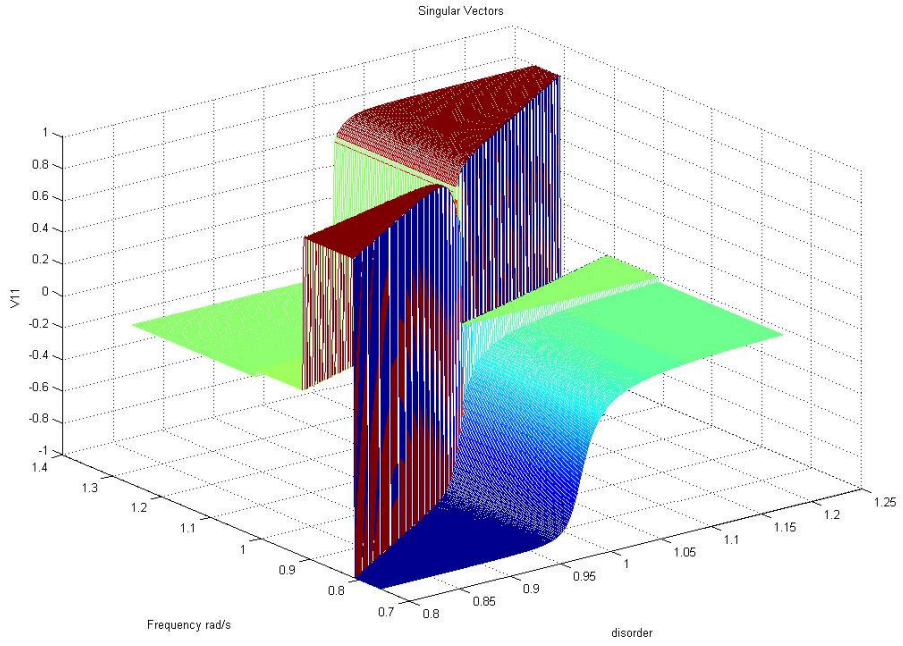

Figure 4.28: Effects of disorder on the right singular vector component v11, where R= 0.1.

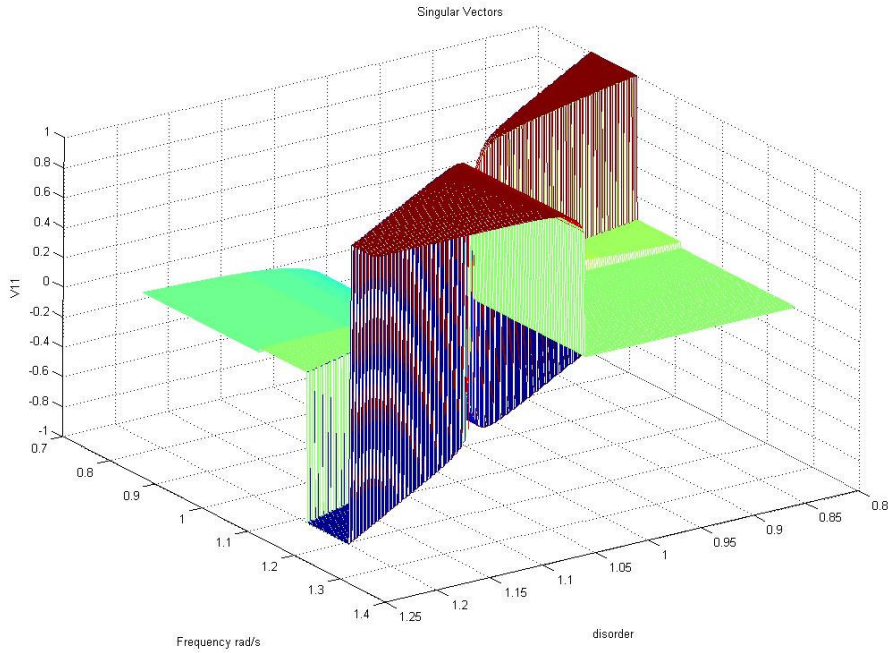

Figure 4.29: Effects of disorder on the right singular vector component v11, where R= 0.1.

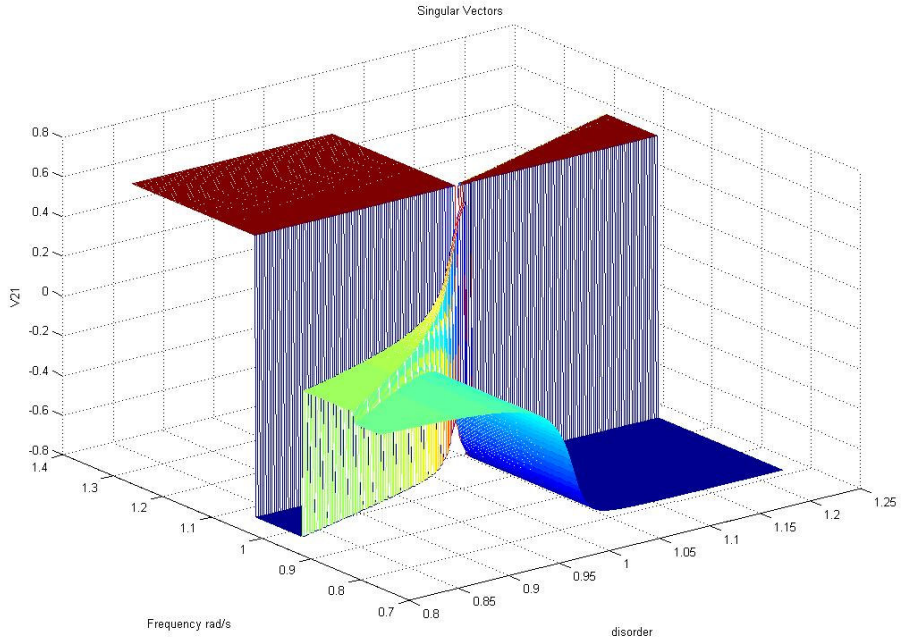

Figure 4.30: Effects of disorder on the right singular vector component v21, where R= 0.1.

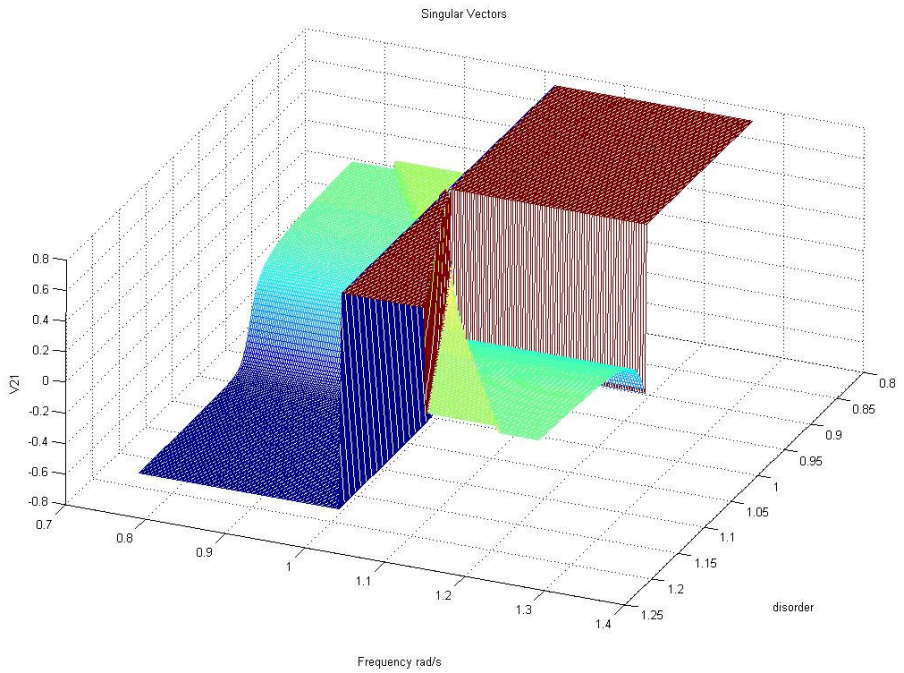

Figure 4.31: Effects of disorder on the right singular vector component v21, where R= 0.1.

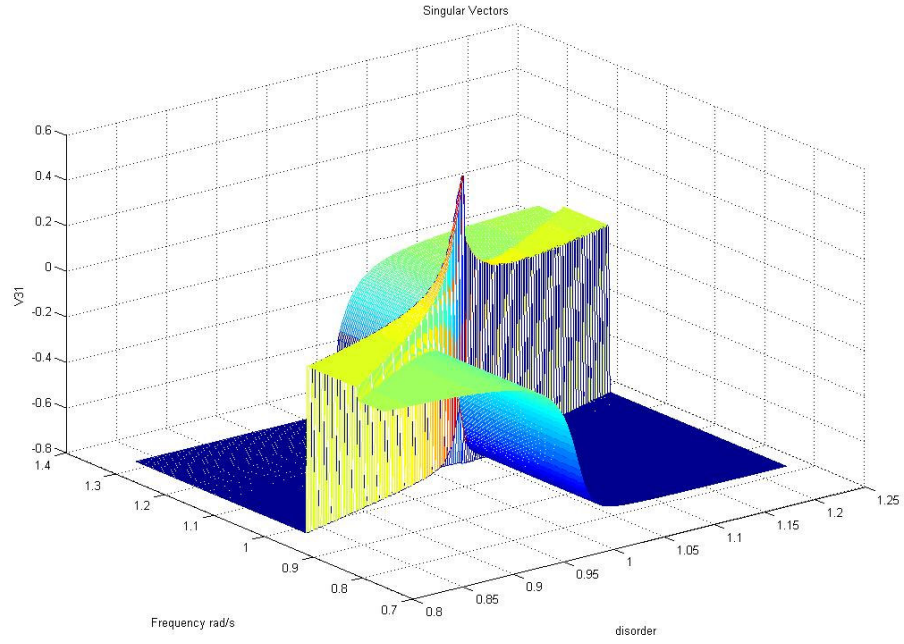

Figure 4.32: Effects of disorder on the right singular vector component v31, where R= 0.1.

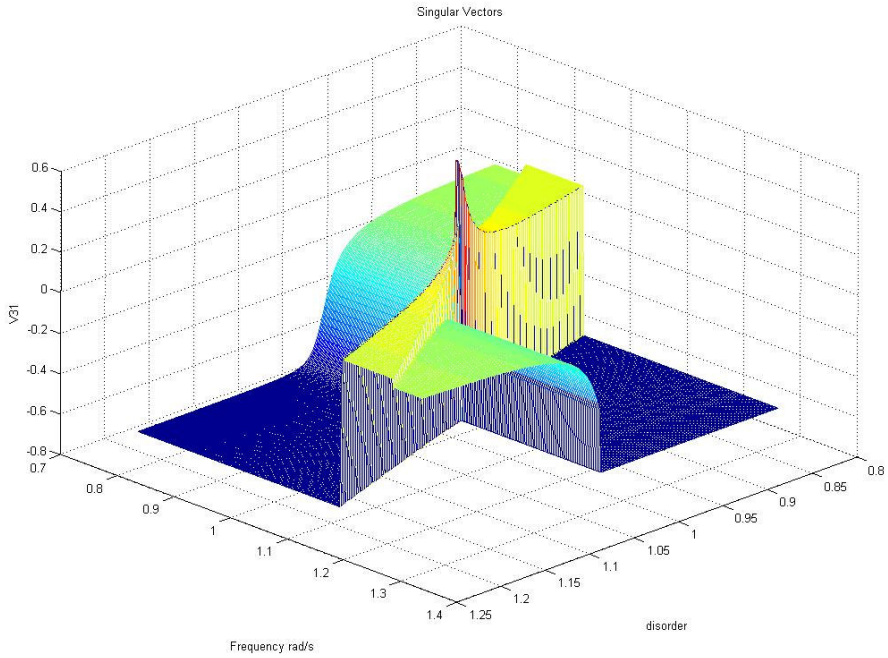

Figure 4.33: Effects of disorder on the right singular vector component v31, where R= 0.1.

It is seen that components of first left singular vector (u_{11}, u_{21} and u_{31}) change abruptly when the exication frequency approaches to first and second resonance frequencies. Also when the disorder approaches to 1 which is tuned condition of the blade assembly, components of first left singular vector (u_{11}, u_{21} and u_{31}) change smoothly and they gets max. values around this point. This point is also 3D Curve veering point.

It is seen that first and second components of first right singular vector (v_{11} and v_{21}) change abruptly when the exication frequency approaches to first, second and third resonance frequencies. Third component of the first singular vector is effected only first and second resonance frequencies. Also when the disorder approaches to 1 which is tuned condition of the blade assembly, components of first left singular vector (u_{11}, u_{21} and u_{31}) change smoothly and they gets max. values around this point. This point is also 3D Curve veering point.

As a result of singular vector localization, input directions change drastically at resonance frequencies and veering disorder to obtain the gain equal to singular values and the distribution of system's energy among different degrees of freedom also changes drastically. All figures of singular values and singular vectors can be seen in Appendix-D.

4.4.2 Strongly Coupled Assembly of Mistuned Turbine Blades

The following parameter values are used in numerical study of mistuned strongly coupled assembly of turbine blades. When this study is performed to examine the disorder effects, it is assumed that resonance frequency of the first blade of the turbine change between 0.8 Hz and 1.2 Hz. According to equation 4.8,

$$\Delta f_i = \left(\omega_{bi}^2 - \omega_b^2\right)/\omega_b^2 \quad \textbf{(4.34)}$$

$$\omega_{bi} = [0.8 \quad \cdots \quad 1.2] \quad \textbf{(4.35)}$$

$$\Delta f_1 = [-0.36 \quad \cdots \quad 0.44] \quad \textbf{(4.36)}$$

Δf_1 changes between -0.36 and 0.44. When the $\omega_{bi} = 1Hz$, system is tuned because of the disorder parameter Δf =0. Because the equation of motion is linear, transposition principle can be applied to examine different blade configuration. So disorder is given only one blade in this study.

Table 4.10: Parameter values for mistuned strongly coupled assembly of blades.

Parameters	i=1	i=2	i=3
m_i	1	1	1
ζ_i	0	0	0
ω_{bi}	1	1	1
R	1	1	1
Δf_i	-0.36, ..., 0.44	0	0

Figure 4.34 and 4.35 show the max. (σ_1) singular value's respond to excitation frequency. It is seen that, there are three peaks on figures 4.34 and 4.35. This shows that there is no repeated singular value phenomena occurs, when the system has disorder. When the disorder approaches to 1, second and third resonance frequencies approach each other and suddenly change directions. 2D singular value Veering phenomena occurs when the blades are strongly coupled. Red line shows the change of ω_1, orange line shows the change of ω_2 and green line shows the change of ω_3.

These peaks occur at resonance frequencies of system and resonance frequencies change as related to disorder, because the stiffness matrix of the system changes for every disorder value.

This condition shows that, resonance frequencies of strongly coupled system are not effected as much as weakly coupled system's frequencies. 2nd and 3rd resonance frequencies change smoothly until the point where disorder is 1. After this point small change is observed in their directions. That means, while the input-output transfer function relationships and power-energy transmission ratios are smooth for 2nd and 3rd resonance frequencies.

When the the first frequency is examined, it is seen that it changes smoothly according to disorder and it is not effected from the tuned system disorder. That means, while the input-output transfer function relationships and power-energy transmission ratios are smooth for 1st resonance frequency.

Since the 1st singular value represents the worst loading conditions, it is seen that system's gain is effected few with the disorder.

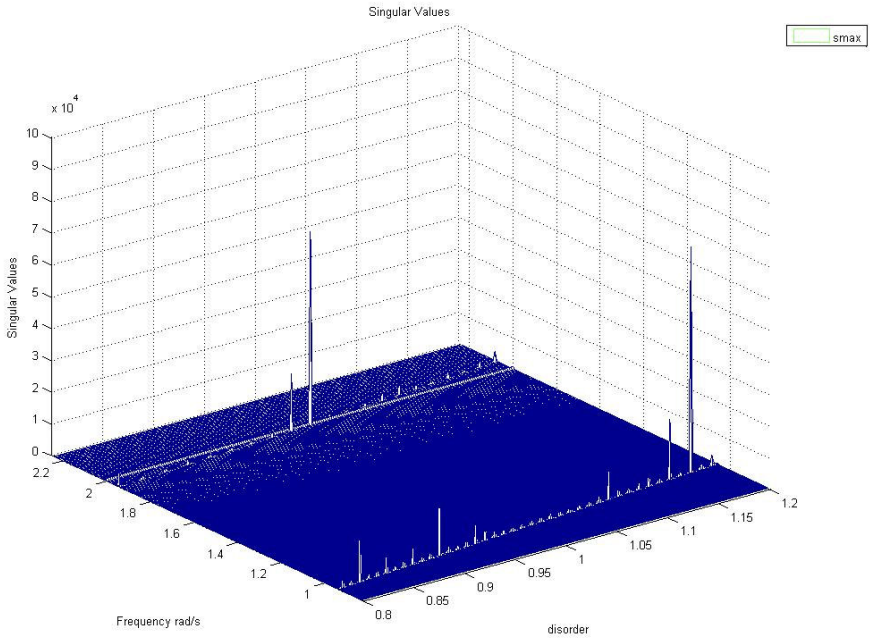

Figure 4.34 : Effects of Disorder on Max. (σ_1) singular value of mistuned weakly coupled blades, where R=0.1.

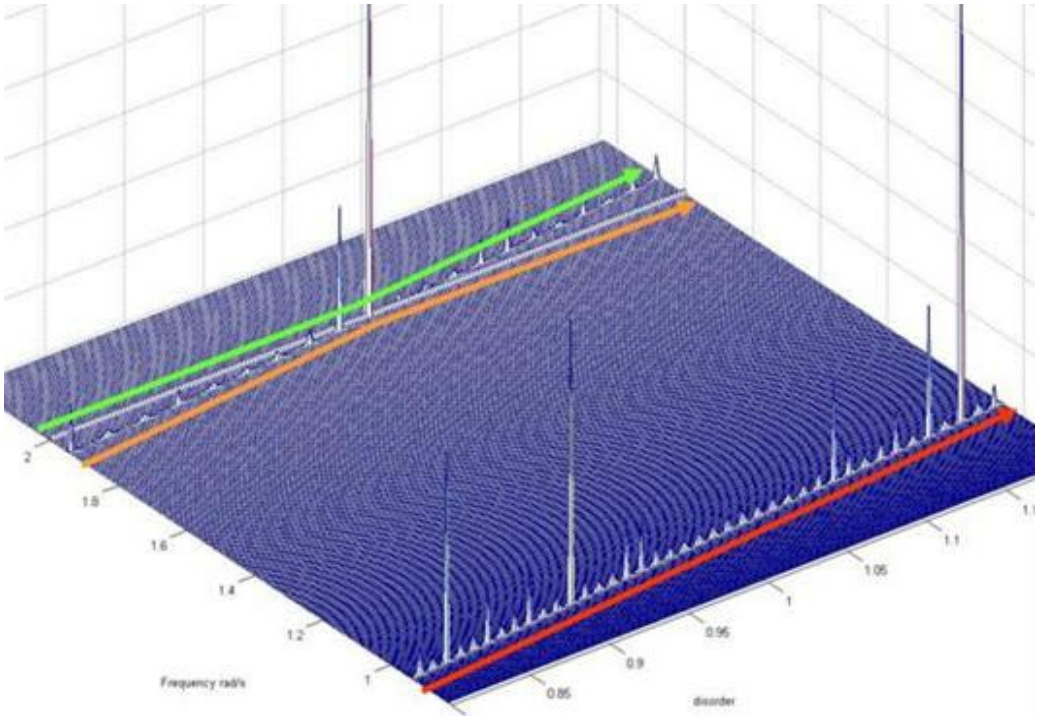

Figure 4.35 : Effects of Disorder on Max. (σ_1) singular value of mistuned weakly coupled blades, where R=0.1.

It is showed that left (U) and right (V) singular vectors' component's responds of 1st singular value from figure 4.36 to 4.48.

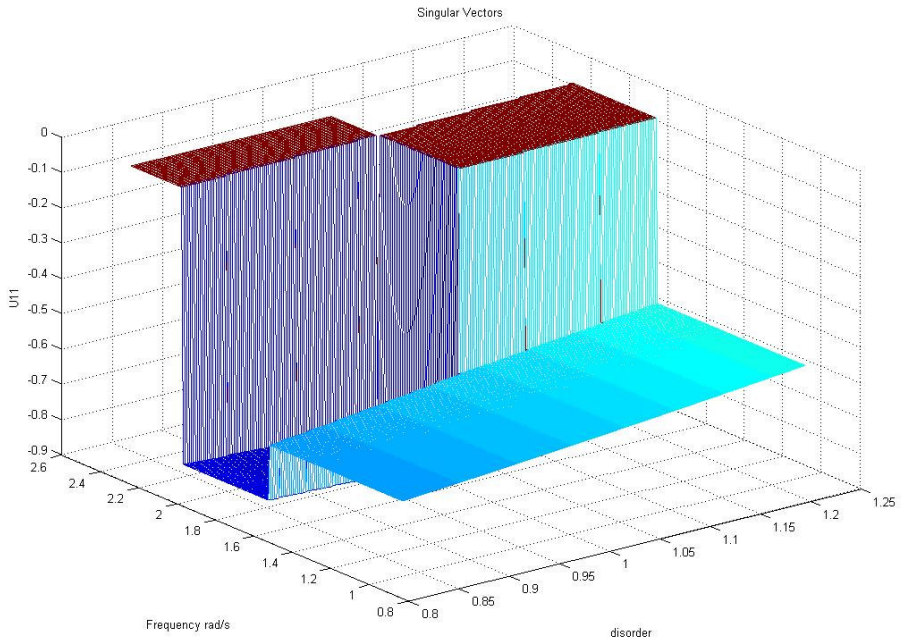

Figure 4.36: Effects of disorder on the left singular vector component u11, where R= 1.

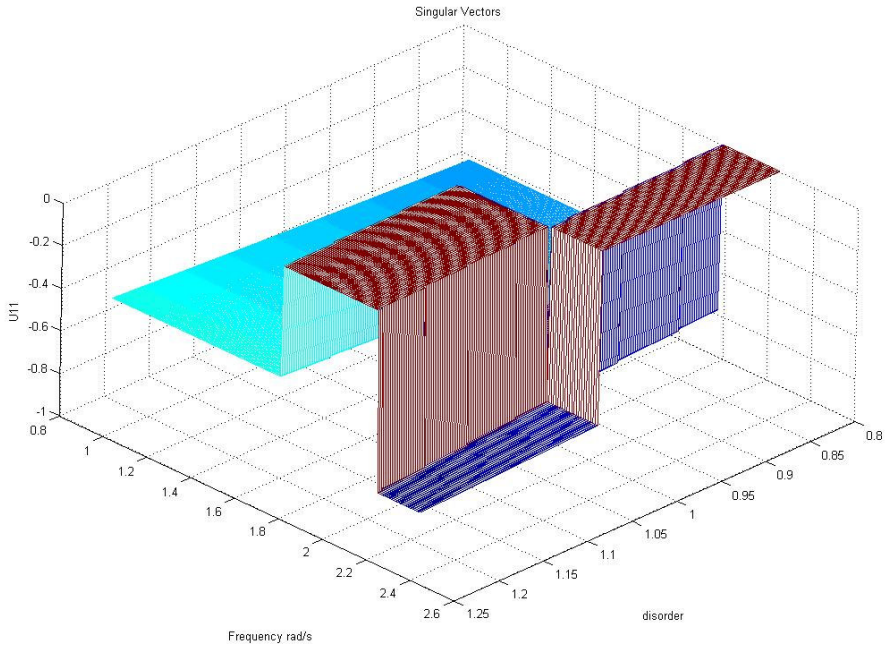

Figure 4.37: Effects of disorder on the left singular vector component u11, where R= 1.

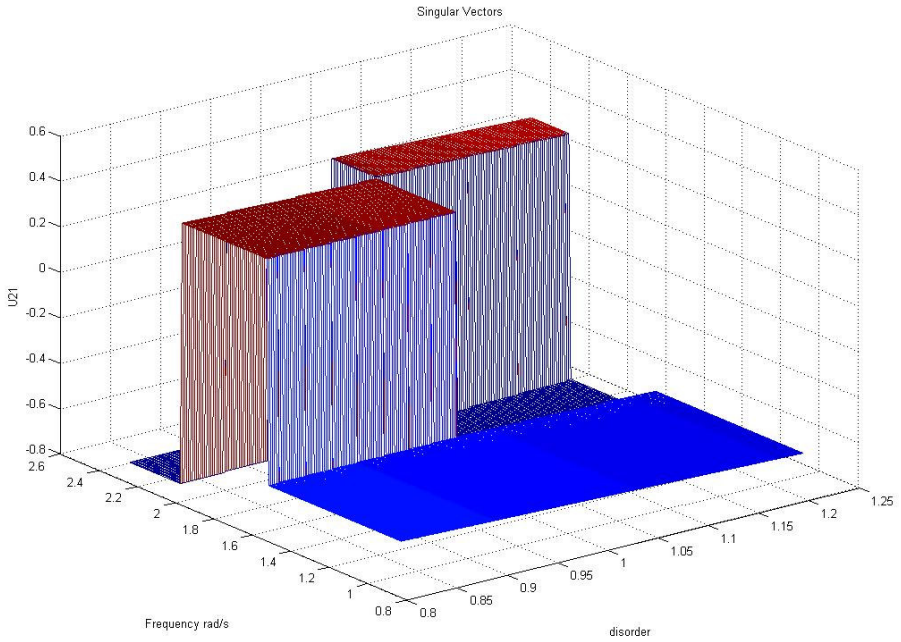

Figure 4.38: Effects of disorder on the left singular vector component u21, where R= 1.

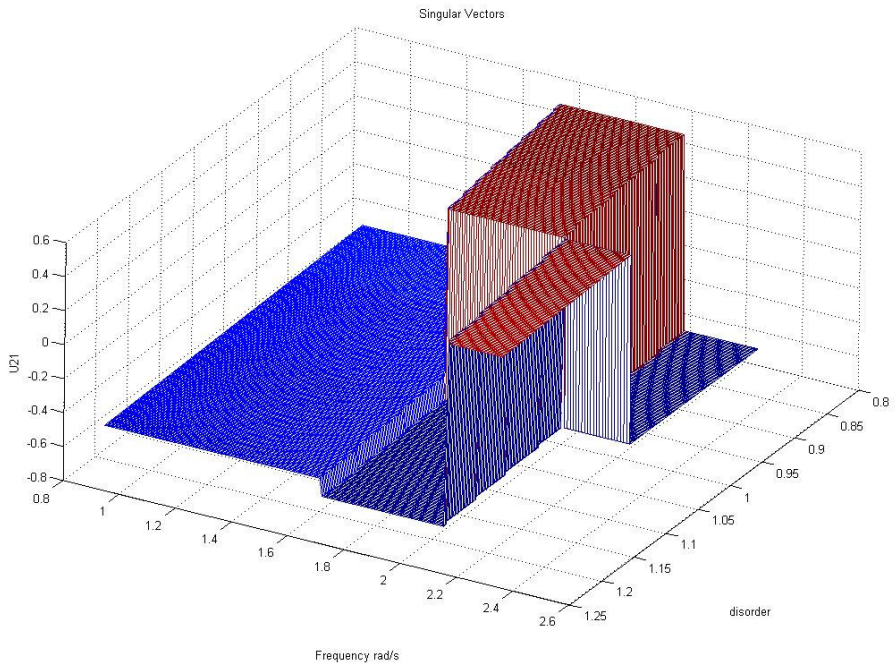

Figure 4.39: Effects of disorder on the left singular vector component u21, where R= 1.

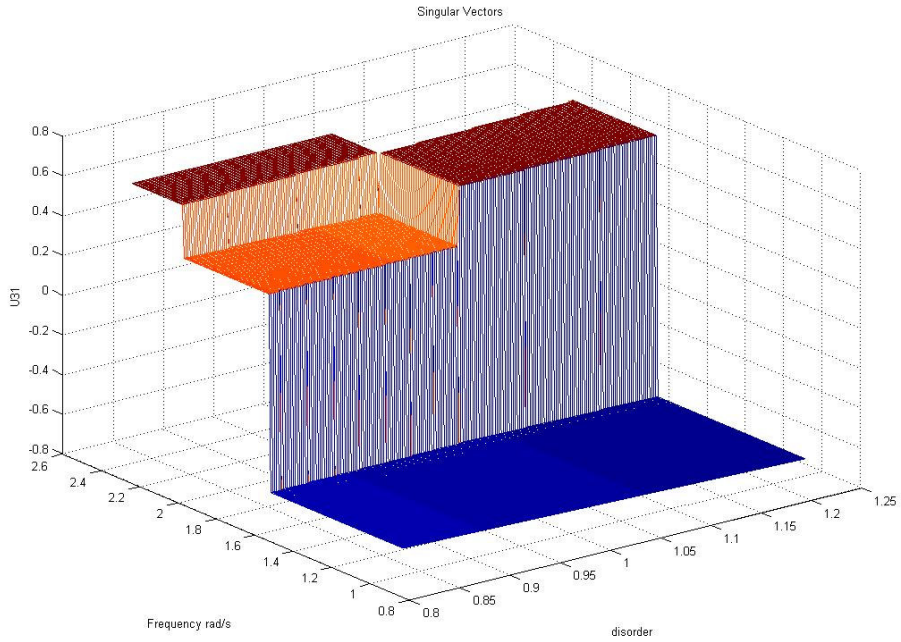

Figure 4.40: Effects of disorder on the left singular vector component u31, where R= 1.

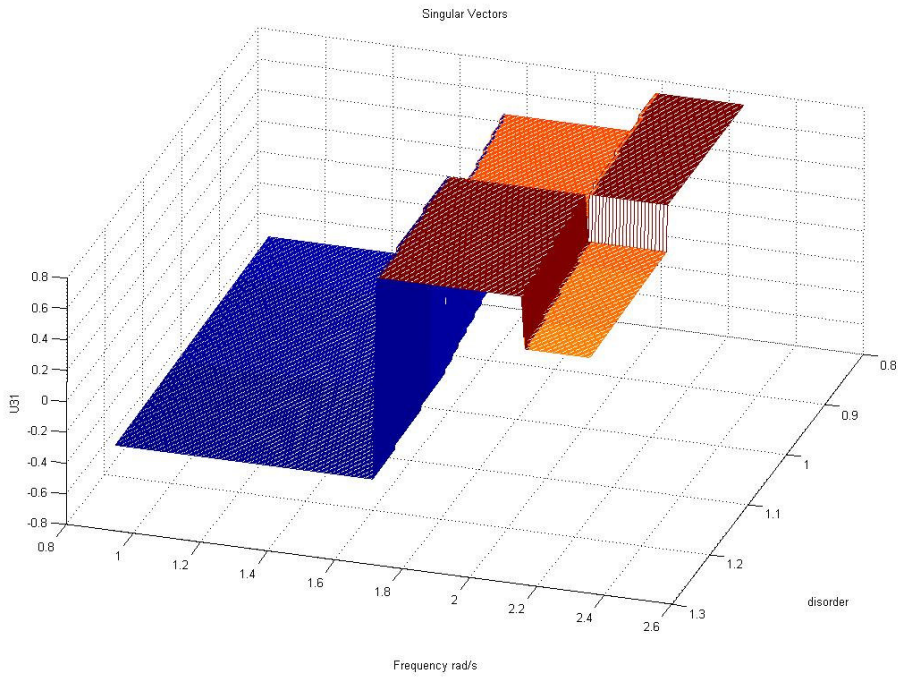

Figure 4.41: Effects of disorder on the left singular vector component u31, where R= 1.

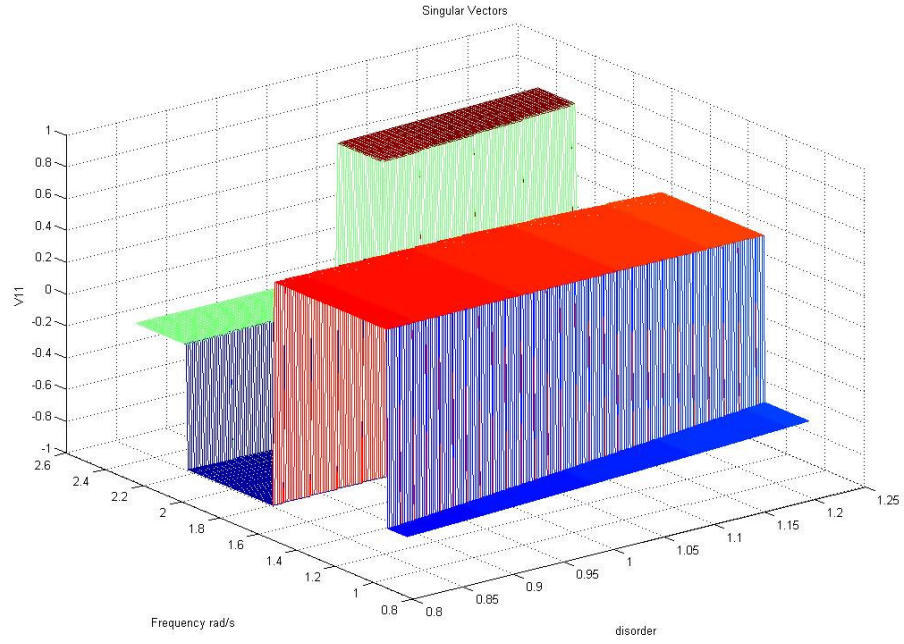

Figure 4.42: Effects of disorder on the right singular vector component v11, where R= 1.

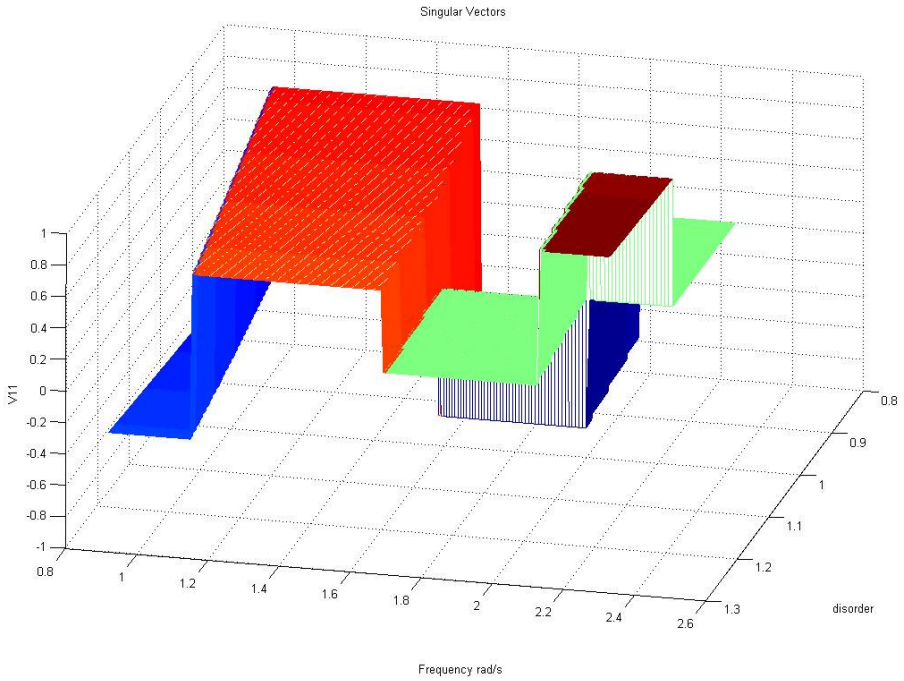

Figure 4.43: Effects of disorder on the right singular vector component v11, where R= 1.

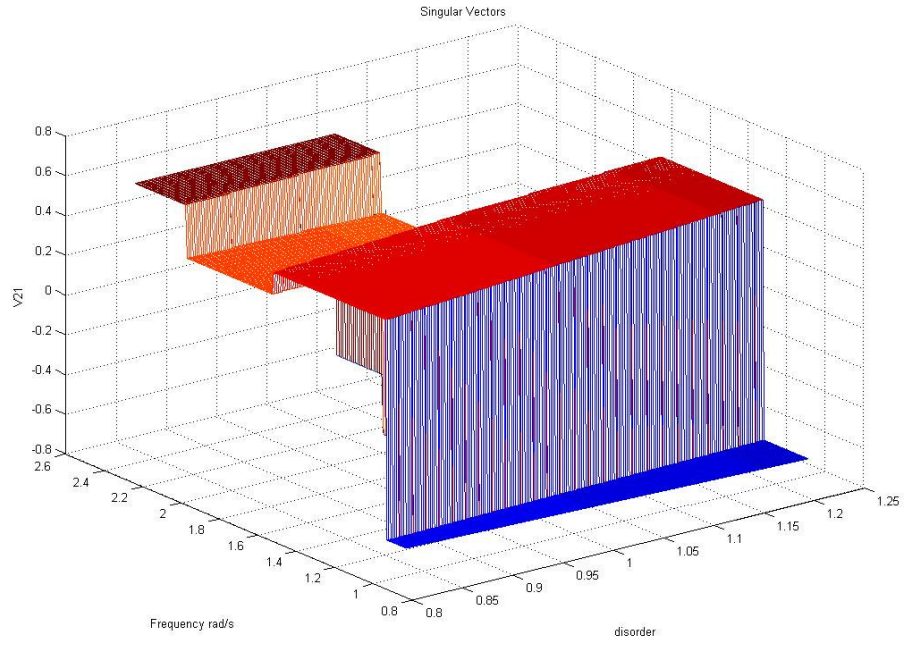

Figure 4.44: Effects of disorder on the right singular vector component v21, where R= 1.

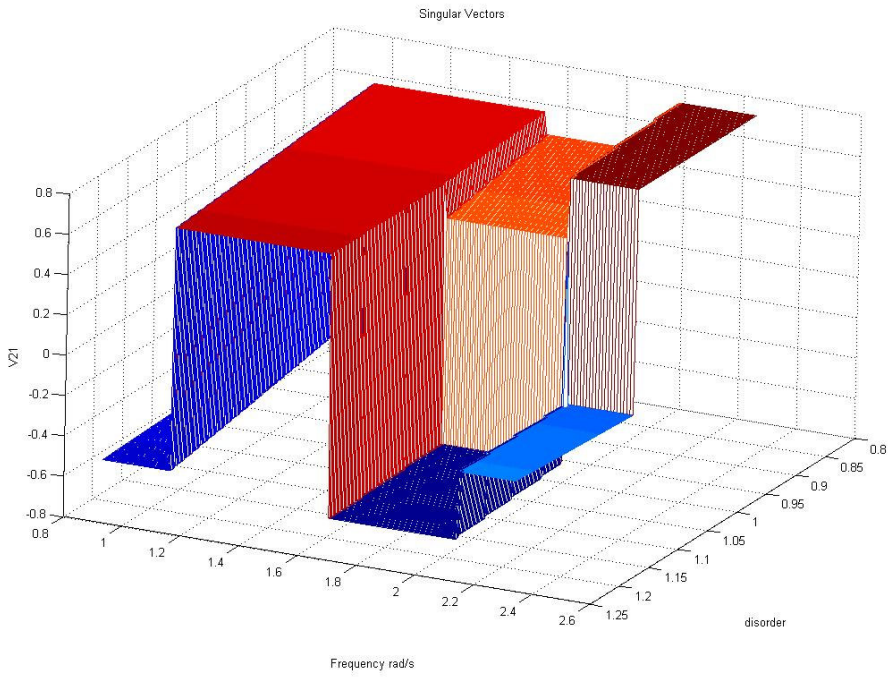

Figure 4.45: Effects of disorder on the right singular vector component v21, where R= 1.

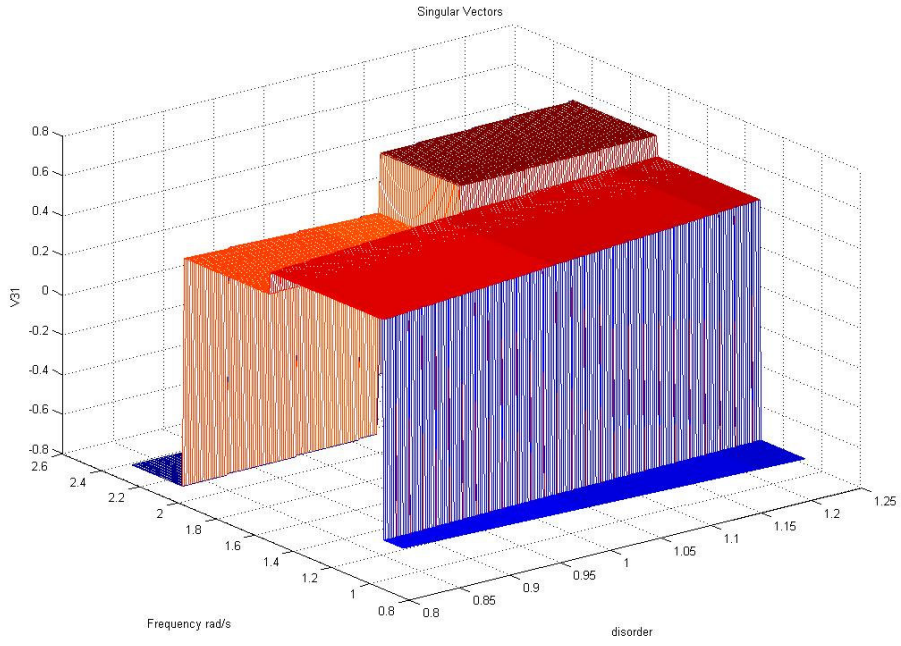

Figure 4.46: Effects of disorder on the right singular vector component v31, where R= 1.

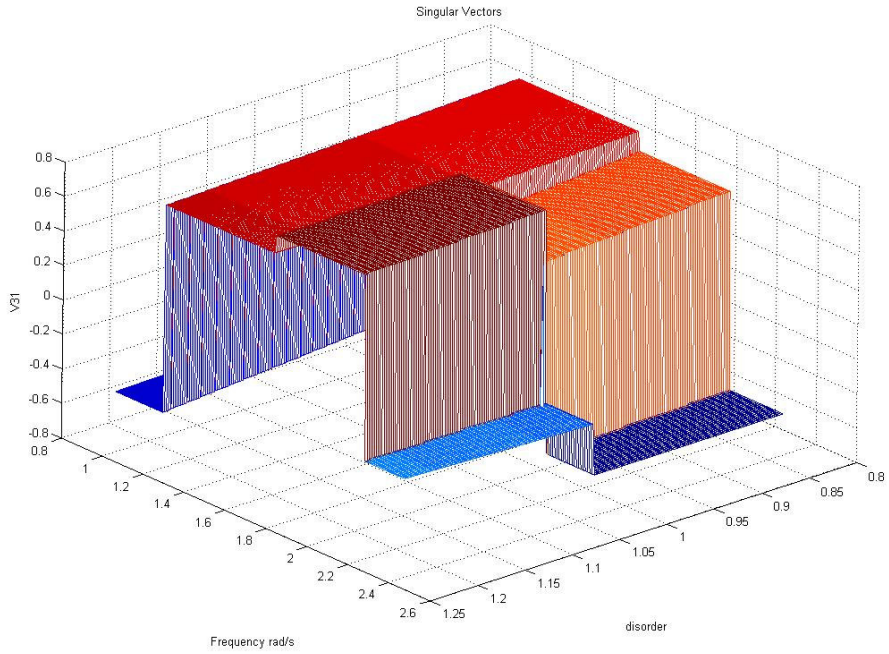

Figure 4.47: Effects of disorder on the right singular vector component v31, where R= 1.

It is seen that components of first left singular vector (u_{11}, u_{21} and u_{31}) change abruptly when the exication frequency approaches to first and second resonance frequencies. Also when the disorder approaches to 1 which is tuned condition of the blade assembly, components of first left singular vector (u_{11}, u_{21} and u_{31}) change abrubtly between the second and third resonance frequencies. This point is also 2D Curve veering point.

It is seen that components of first right singular (v_{11}, v_{21} and v_{31}) change abruptly when the exication frequency approaches to first, second and third resonance frequencies. Also when the disorder approaches to 1 which is tuned condition of the blade assembly, components of first left singular vector (v_{11}, v_{21} and v_{31}) change abrubtly between the second and third resonance frequencies. This point is also 2D Curve veering point.

As a result of singular vector localization, input directions change drastically at resonance frequencies and veering disorder to obtain the gain equal to singular values and the distribution of system's energy among different degrees of freedom also changes drastically. All figures of singular values and singular vectors can be seen in Appendix-E.

5. CONCLUSIONS

In this thesis, input-output directional properties of rotationally periodic structures are studied by using SVD method. SVD based analysis is well suited to study the directional properties of inputs and outputs. If an input is distributed in the direction of a right singular vector v_i, the system's response will be distributed to the system degrees of freedom in the direction of associated left singular vector u_i with a gain that is equal to the corresponding singular value σ_i.

It is shown that when the SVD method is applied to rotationally periodic structure, repeated eigenvalue phenomena occurs at this system. This phenomena causes singular values to repeat. SVD method is applied to 3-bladed, 6-bladed, 7-bladed, 8-bladed and 30-bladed turbine models. Repeated singular value phenomena is observed for all models. If N is total number of blades,

$$(N-1)/2 \qquad \textbf{(5.1)}$$

formulation gives us the number of repeated singular values for odd numbers of blades and,

$$(N-2)/2 \qquad \textbf{(5.2)}$$

formulation gives us the number of repeated singular values for even numbers of blades. When the corresponding eigenvectors are calculated, oscillations are seen in the plots. This abnormal condition is caused by the repeated singular value phenomena. Components of singular vectors which are associated with repeated singular values change places with each other. So, singular vector values need to be organized to correct order and then repeated singular vector needs to be calculated again by using generalized eigenvalue formulation.

In extend to mode localization and eigenvalue loci veering phenomena of weakly coupled disordered systems, existence of singular vector localization and singular value loci veering phenomena (occuring at the so called isopower frequencies) are

shown in tuned weakly and strongly coupled systems. Occurence of strong mode localization causes abrupt changes in input-output relationships of systems. But the changes in singular values and input-output transfer function relationships are smooth. Thus, power and energy transmission ratios change smoothly. As a result of singular vector localization, the distribution of system's energy among different degrees of freedom changes drastically and abrupt changes in the outputs are observed.

When the effects of disorder on weakly coupled and strongly coupled turbine blades's singular values are examined, it is seen that both of them are effected with the disorder and resonance frequencies. Both of the weakly and strongly coupled blades show changes on resonance frequencies and near the tuned disorder point. While the 3D singular value veering occurs near the tuned disorder point for the weakly coupled turbine blades, 2D singular value veering occurs near the tuned disorder point for the strongly coupled turbine blades. Weakly coupled system is more sensitive to disorder than strongly coupled system. This result is the same with the early studies about disorder effects [1,2,3,5,10]. So, the singular values or resonance frequencies of weakly coupled blades are effected more than strongly coupled ones'. So, power and energy transmission ratios are more sensitive for weakly coupled blades.

When the effects of disorder on weakly coupled and strongly coupled turbine blades' singular vectors are examined, it is seen that both of them are effected with the disorder and resonance frequencies. Because the weakly coupled blades are more sensitive to disorder than strongly coupled blades, left and right singular vectors of them change more smoothly, and they get bigger values near the tuned disorder point than the strongly coupled blades's singular vectors. This shows that input output directional properties of weakly coupled blades are effected more with the given disorder.

Both of the weakly and strongly coupled blades show abrubt changes with the resonance frequencies and no repeated singular value phenomena occurs when the disorder is given. This is an expected result according to reference [13]. But strongly coupled blades are effected by the disorder, when the excitation frequency is between the second and thid resonance frequencies.

As a result of disorder and singular vector localization, input directions change drastically at resonance frequencies and veering disorder to obtain the gain equal to singular values and the distribution of system's energy among different degrees of freedom also changes drastically.

Since singular values are related to power and energy transmission ratios, they can be used to shape vibration absorbing or magnifying characteristics of a system. For example, if we design a system, our goal should be minimizing σ_1 to minimize displacements in all load cases. It is found in design trials on lumped parameter systems that using singular values in such tasks has computationally advantages over using frequency domain constraints.

If the worst forced vibration case of a structure is sought in the existence of multiple load cases, forced response for each load case should be investigated which is cumbersome; the use of singular values is computationally adventagous in this case. To this end, σ_1 has a special meaning since it is the largest system gain and corresponding right and left singular vectors v_1 and u_1 give the worst possible load case and the corresponding system response. While eigenvalue based analyses give information about the resonance frequencies and vibration modes of a structure, singular values of the structure are related to the forced response characteristics and give the dynamical behaviour in the frequency domain.

In this study all turbines are modeled as one dimensional. In future studies turbines can be modeled with elastic beams as two dimensional and also stiffness, mass data's can be taken from a finite element model to apply this method and FSI simulations can be done for new design parameters. Also bird strike effects on jet engines can be researched because SVD method gives information about input output properties of systems. As another study resonance frequencies of the turbines can be optimized.

REFERENCES

[1] **Xie, W.C. and Wang, X.,** 1997. Vibration Mode Localization in One Dimensional Systems, *AIAA Journal*, **Vol.35, No. 10**, 1645-1652.

[2] **Leissa A.W.,** 1974. On a Curve Veering Aberration, *Journal of Applied Mathematics and Physics (ZAMP),* **25,** 99-111.

[3] **Pierre C.,** 1988. Mode Localization and Eigenvalue Loci Veering Phenomena in Disordered Structures, *Journal of Sound and Vibration,* **126(3),** 485-502.

[4] **Muğan A.,** 2002. Effects of Mode Localization on Input-Output Directional Properties of Structures, *Journal of Sound and Vibration,* **258(1),** 45-63.

[5] **Baik S., Castainer M.P., Pierre C.,** 2004. Mistuning Sensitivity Prediction of Bladed Disks Using Eigenvalue Curve Veerings, *The 9th National Turbine Engine High Cycle Fatigue Conference,* Pinehurst, NC, Mar. 17.

[6] **Goldberg J.L.,** 1991. Matrix Theory with Applications, pp. 389-400. McGraw-Hill, Inc, International Series in Pure and Applied Mathematics.

[7] **Strang G.,**1998. Introduction to Linear Algebra, pp. 313-317. Wellesley-Cambridge Press.

[8] **Horn R.A. and Johnson C.R.,** 1994. Topix in Matrix Analysis, pp. 144-148. Cambridge University Press.

[9] **Keller M.J.,** 2001. Vibration Suspension of a Rotationally Periodic Structure Using an Adaptive/PPF Control Law, *Master Thesis,* Department of the Airforce Air University, Airforce Institute of Technology, Ohio.

[10] **Wei. S.T. and Pierre C.,** 1989. A Statistical Analysis of the Effects of Mistuning on the Forced Response of Cyclic Assemblies, *AIAA Journal,* **to appear.**

[11] **Choi K.M, Cho S.W., Ko M.G. and Lee I.W.,** 2003. Higher Order Eigensensitivity Analysis of Damped Systems with Repeated Eigenvalues, *Computers & Structures,* **82,** 63-69.

[12] **Friswell M.I.,** 2000. A Relationship Between Defective Systems and Unit Rank Modification of Classical Damping, *Journal of Vibration and Acoustics,* **Vol 122,** 180-187.

[13] **Kailath T.,** 1980. Linear Systems, pp. 665-666. Prentice Hall, Englewood Cliffs, New Jersey.

[14] **Press W.H., Teukolsky S.A., Vetterling W.T. and Flannery B.P.,** 1992. Numerical Recipes, Cambridge University Press, Cambridge, England.

[15] **Freudenberg J.S. and Looze D.P.,** 1988. Frequency Domain Properties of Scalar and Multivariable Feedback Systems, Springer-Verlag, Berlin.

[16] **Golub G.H. and Van Loan C.F.,** 1983. Matrix Computations, John Hopkins University Press, Baltimore.

APPENDICES

Appendix-A

REPEATED SINGULAR VALUES AND VECTORS

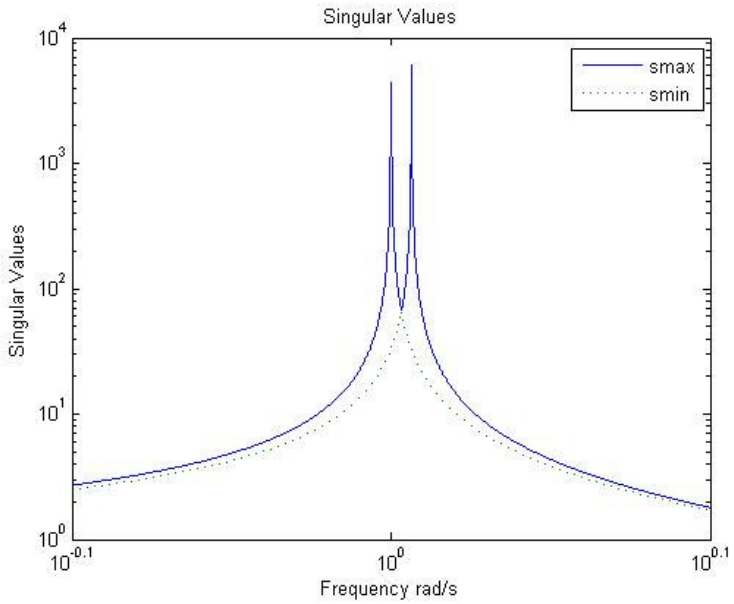

Figure A.1 : Singular Values

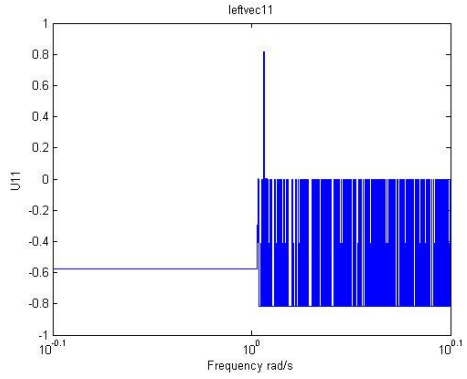

Figure A.2 : U11 component

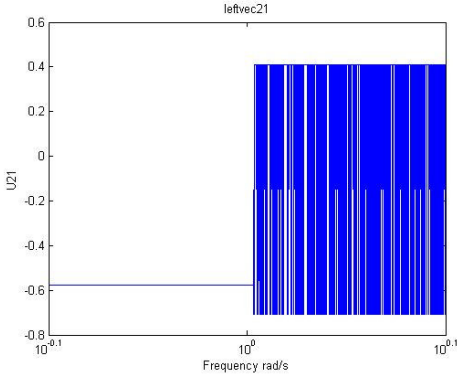

Figure A.3 : U21 component

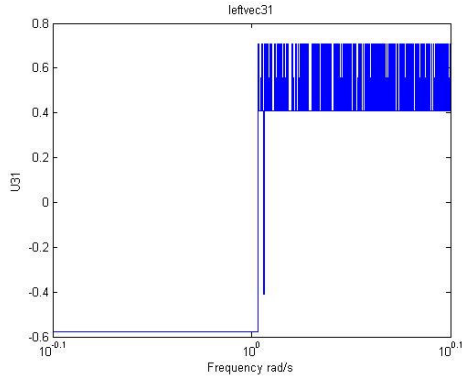

Figure A.4 : U31 component

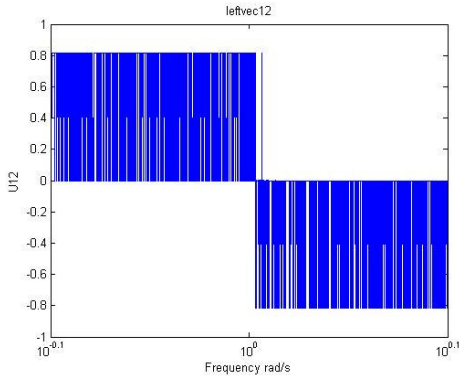

Figure A.5 : U12 component

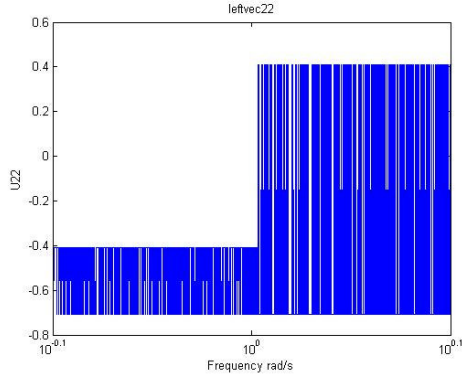

Figure A.6 : U22 component

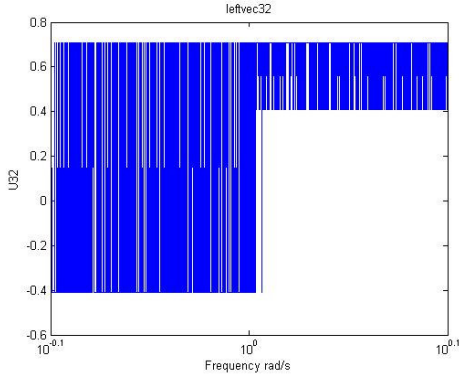

Figure A.7 : U32 component

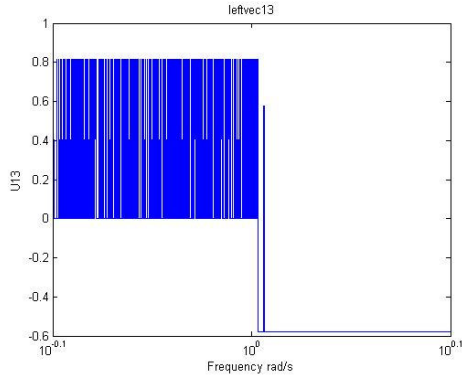

Figure A.8 : U13 component

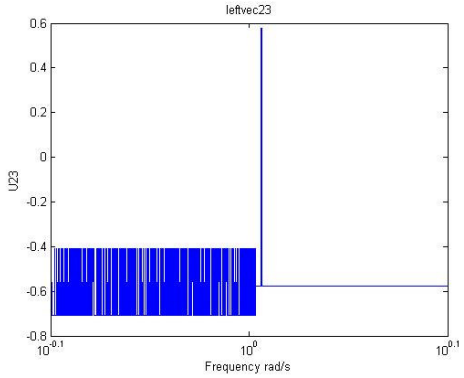

Figure A.9 : U23 component

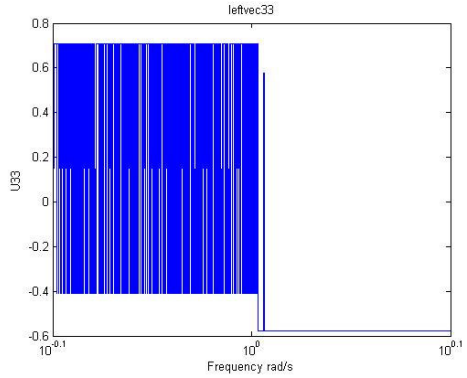

Figure A.10 : U33 component

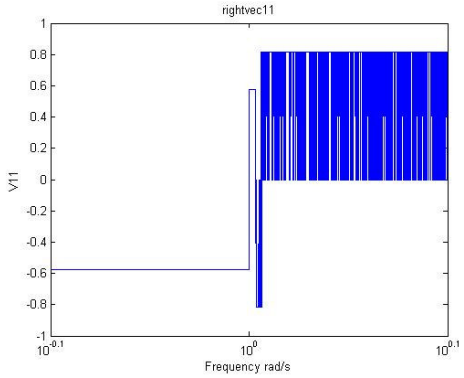

Figure A.11 : V11 component

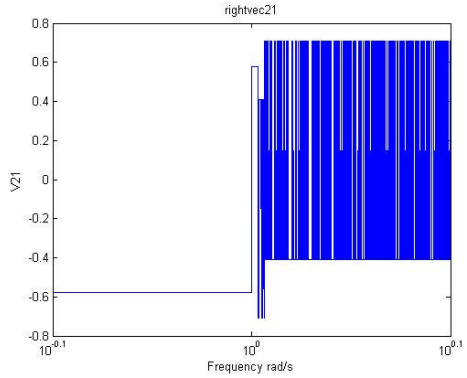

Figure A.12 : V21 component

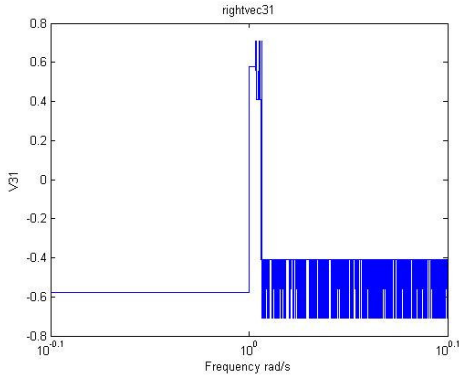

Figure A.13 : V31 component

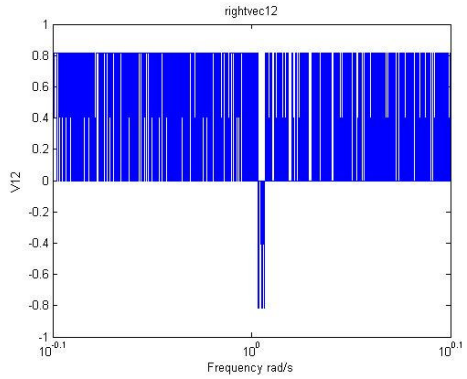

Figure A.14 : V12 component

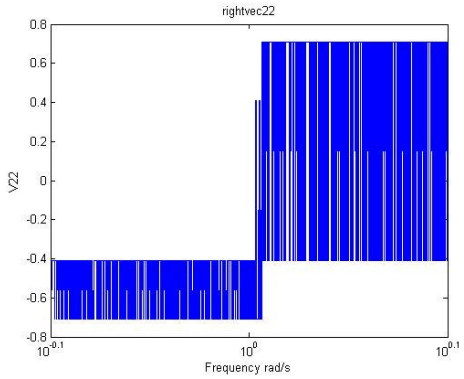

Figure A.15 : V22 component

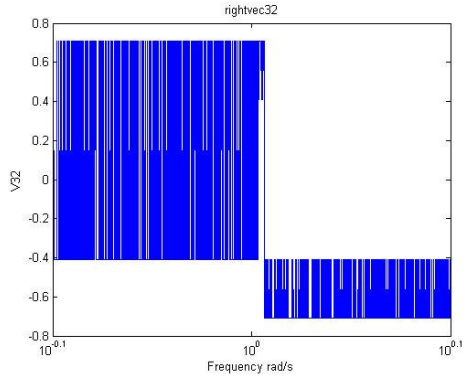

Figure A.16 : V32 component

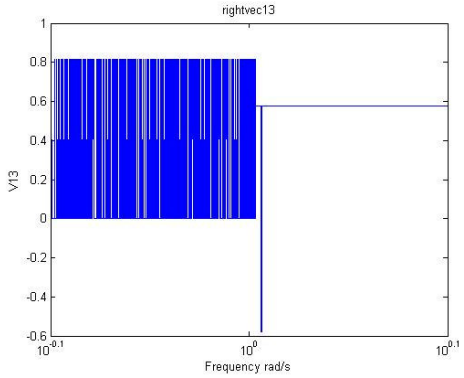

Figure A.17 : V13 component

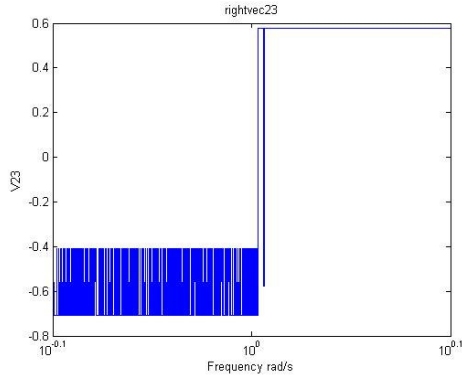

Figure A.18 : V23 component

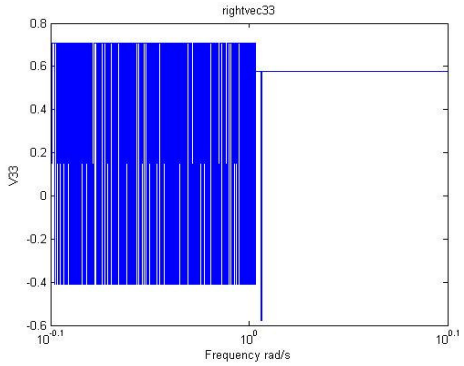

Figure A.19 : V33 component

Appendix-B

SINGULAR VALUES AND VECTORS OF WEAKLY COUPLED ASSEMBLY OF TURBINE BLADES, WHERE R=0.1

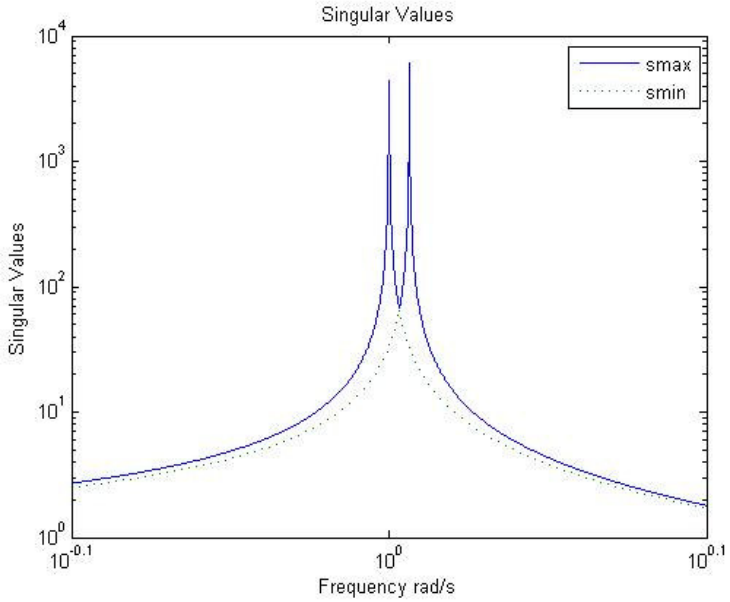

Figure B.1 : Singular Values

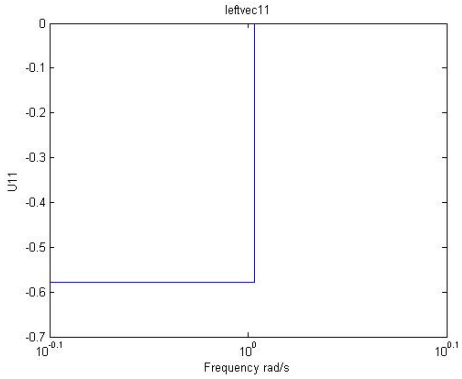

Figure B.2 : U11 component

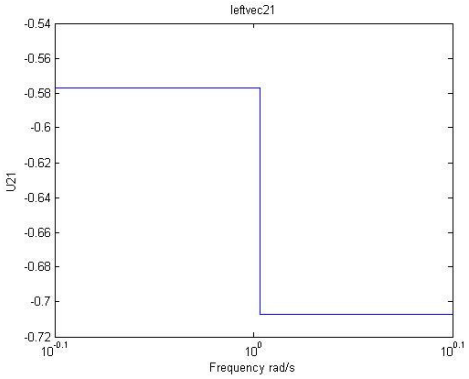

Figure B.3 : U21 component

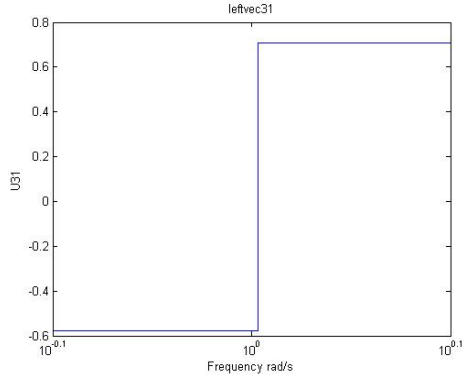

Figure B.4 : U31 component

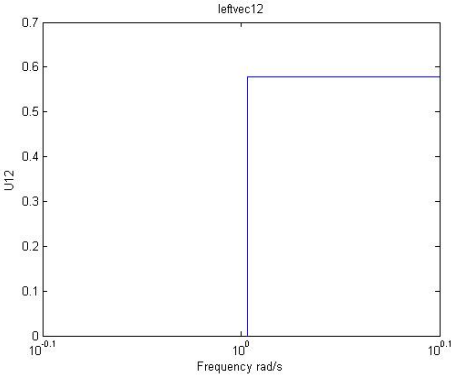

Figure B.5 : U12 component

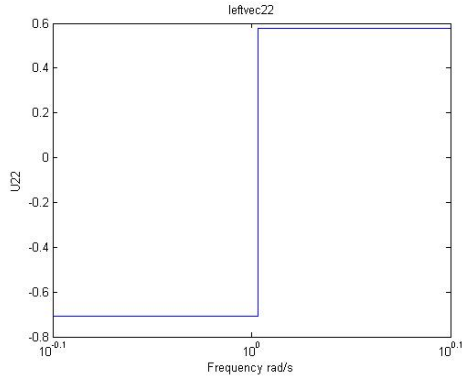

Figure B.6 : U22 component

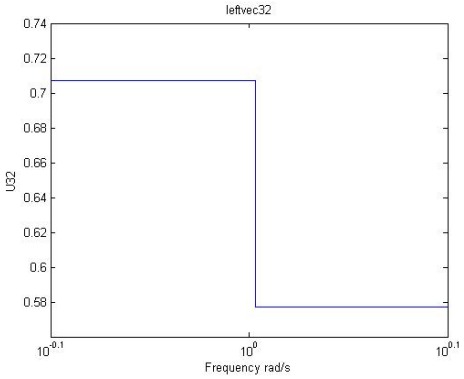

Figure B.7 : U32 component

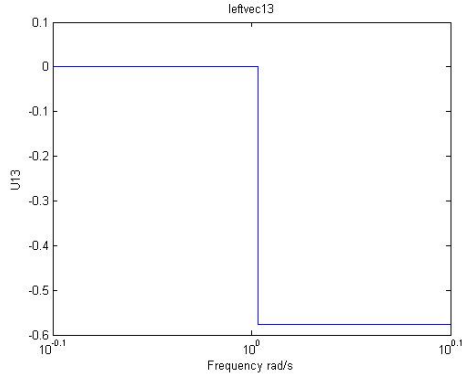

Figure B.8 : U13 component

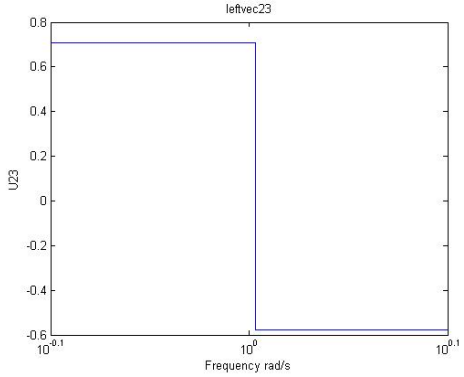

Figure B.9 : U23 component

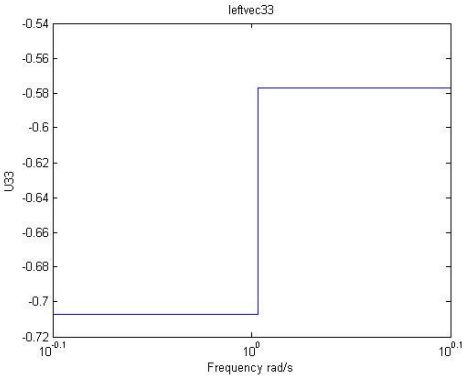

Figure B.10 : U33 component

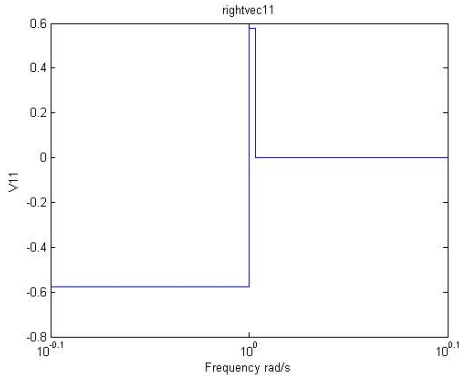

Figure B.11 : V11 component

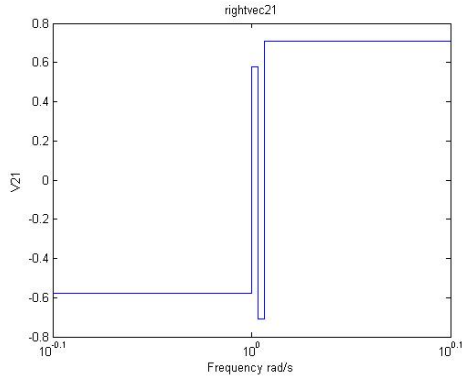

Figure B.12 : V21 component

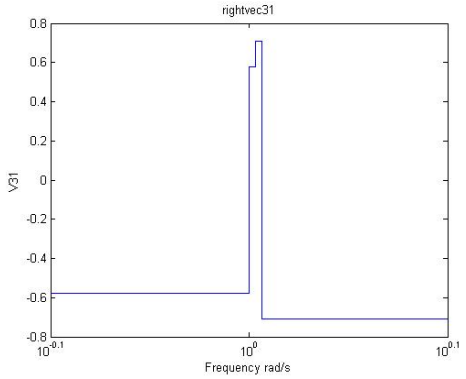

Figure B.13 : V31 component

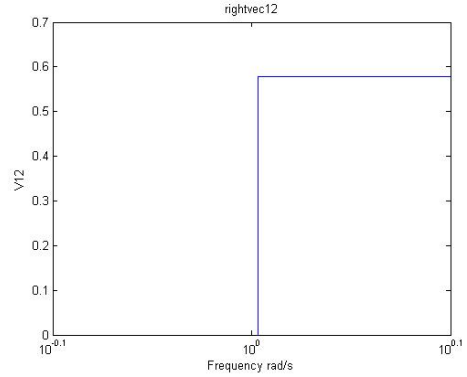

Figure B.14 : V12 component

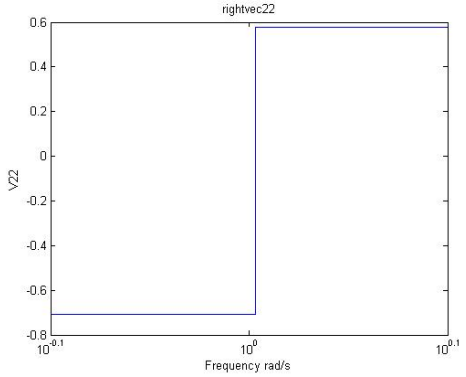

Figure B.15 : V22 component

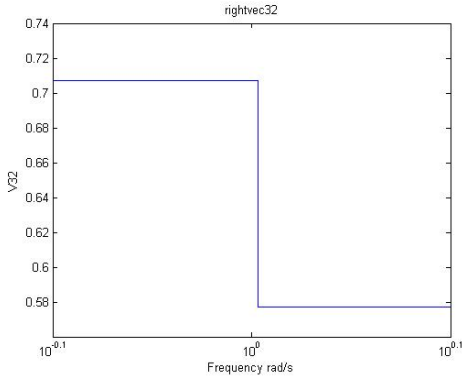

Figure B.16 : V32 component

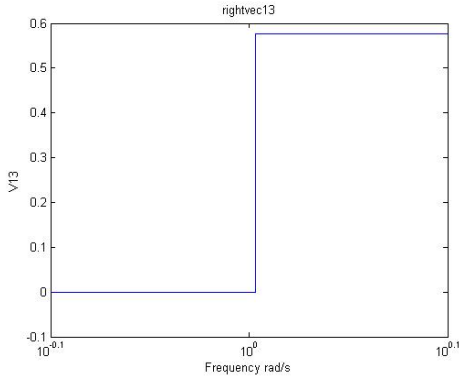

Figure B.17 : V13 component

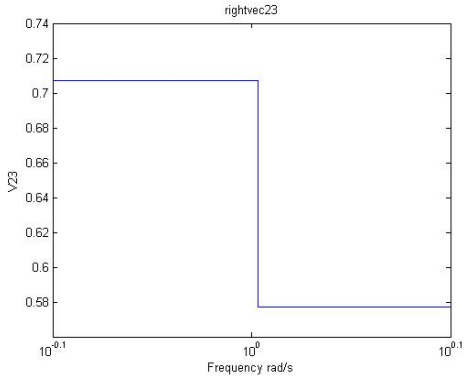

Figure B.18 : V23 component

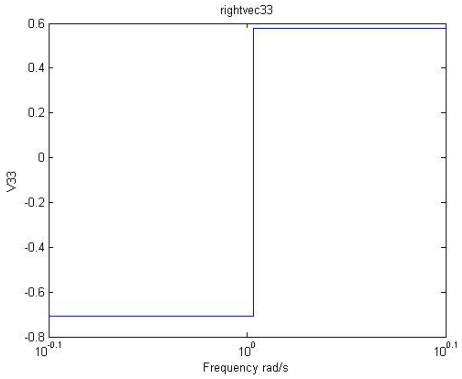

Figure B.19 : V33 component

Appendix-C

SINGULAR VALUES AND VECTORS OF STRONG COUPLED ASSEMBLY OF TURBINE BLADES, WHERE R=1

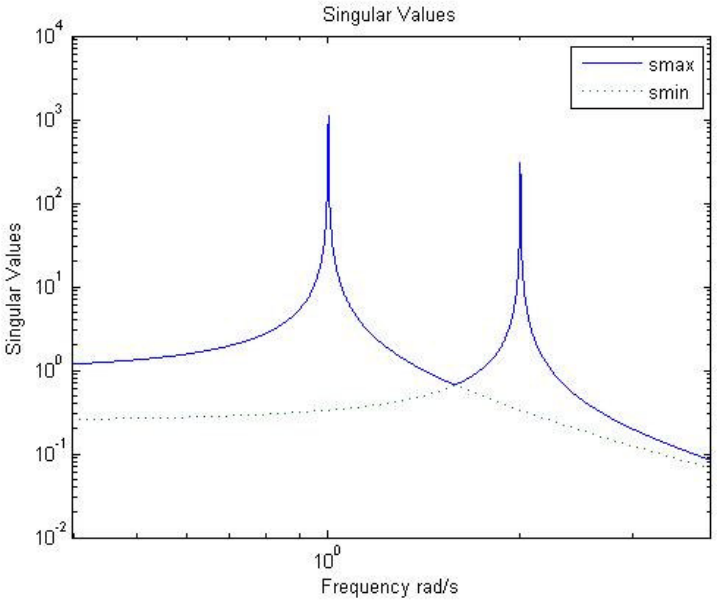

Figure C.1 : Singular Values

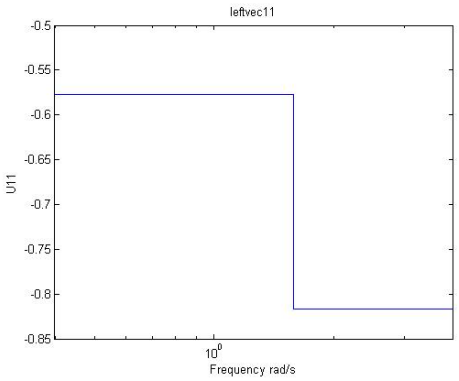

Figure C.2 : U11 component

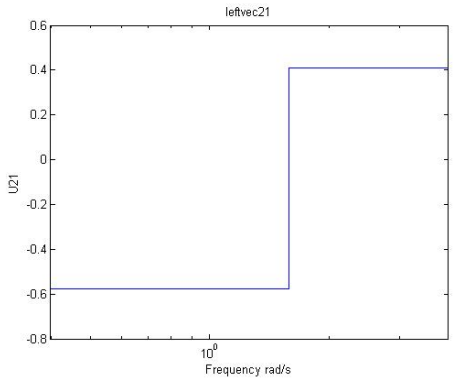

Figure C.3 : U21 component

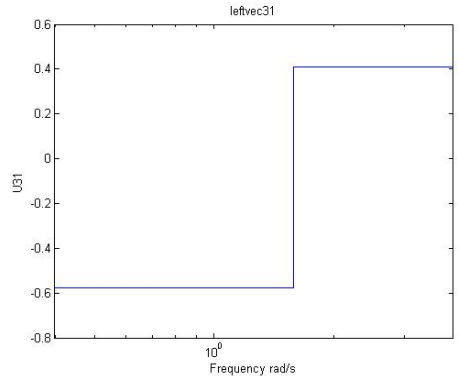

Figure C.4 : U31 component

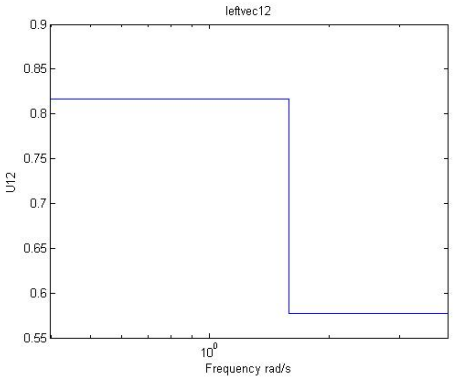

Figure C.5 : U12 component

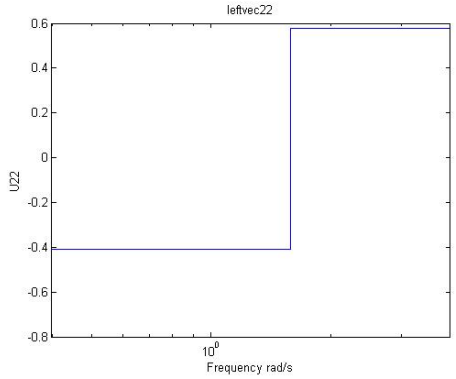

Figure C.6 : U22 component

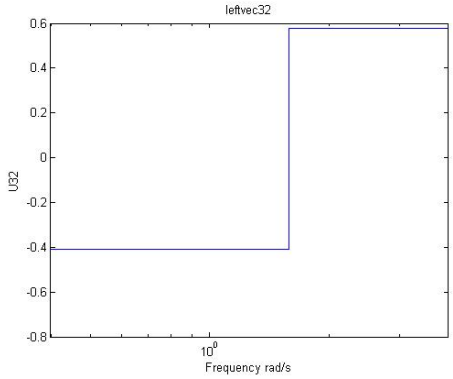

Figure C.7 : U32 component

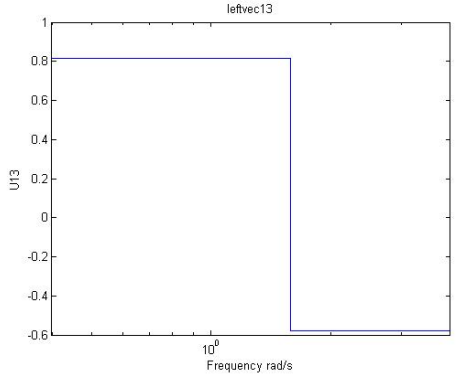

Figure C.8 : U13 component

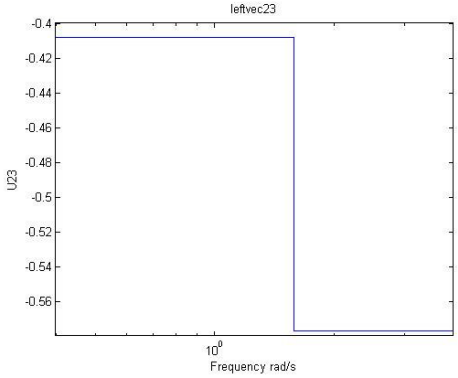

Figure C.9 : U23 component

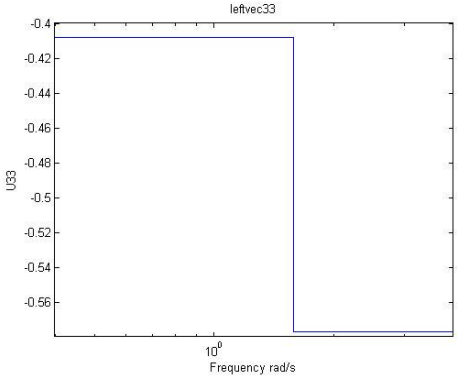

Figure C.10 : U33 component

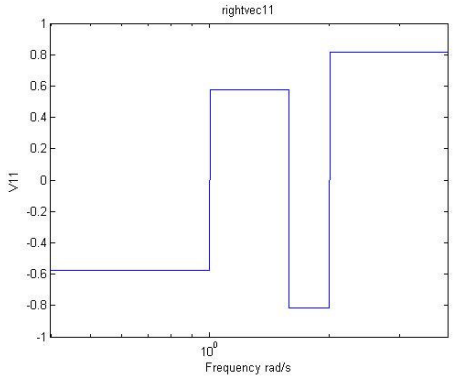

Figure C.11 : V11 component

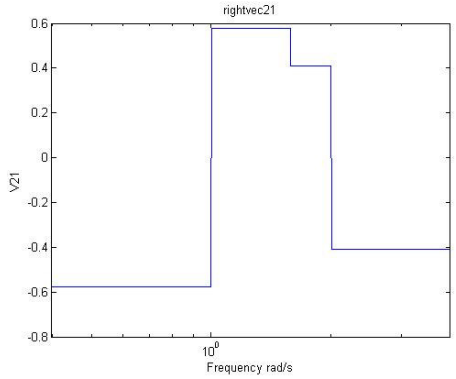

Figure C.12 : V21 component

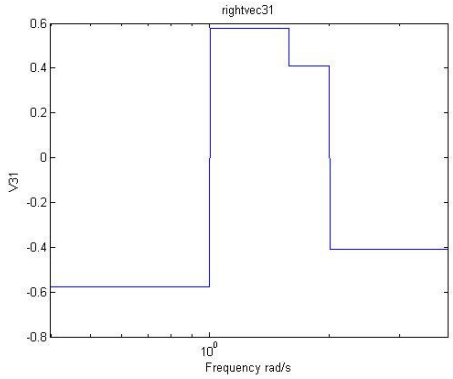

Figure C.13 : V31 component

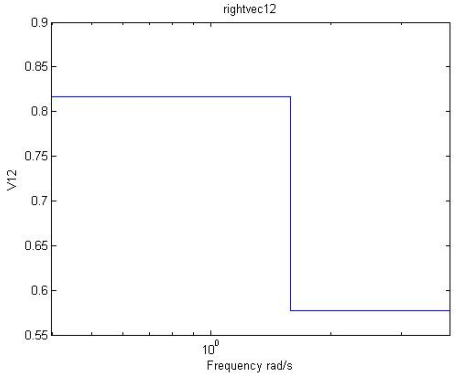

Figure C.14 : V12 component

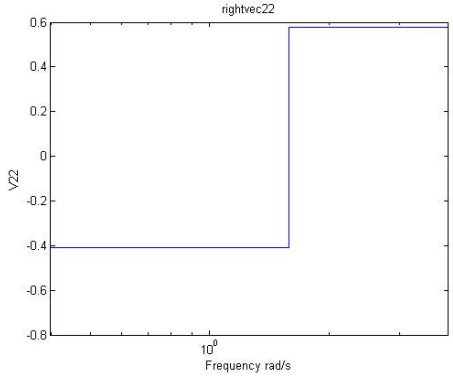

Figure C.15 : V22 component

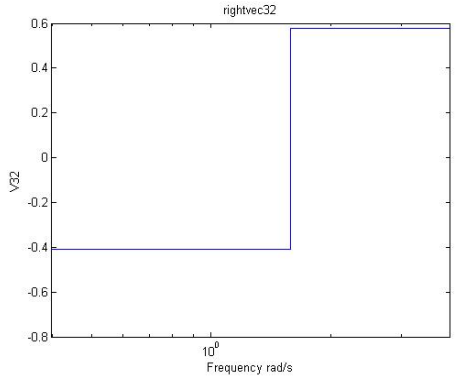

Figure C.16 : V32 component

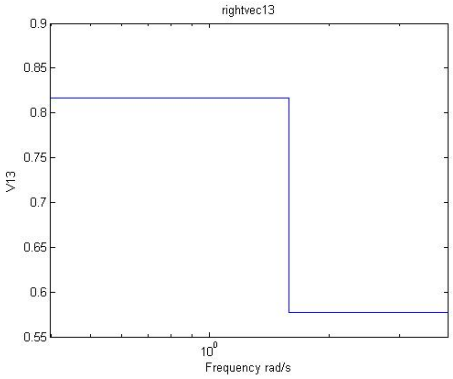

Figure C.17 : V13 component

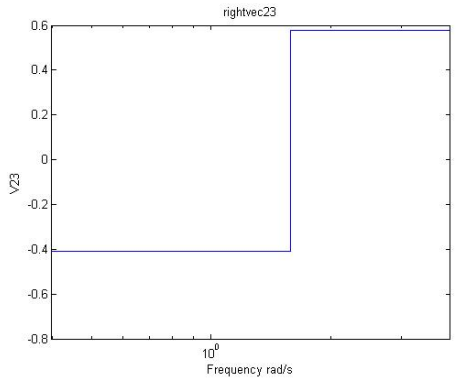

Figure C.18 : V23 component

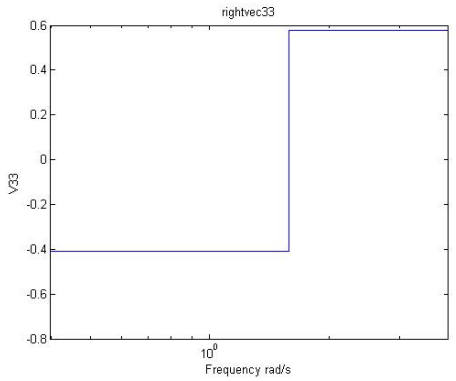

Figure C.19 : V33 component

Appendix-D

EFFECTS OF DISORDER ON SINGULAR VALUES AND VECTORS OF WEAKLY COUPLED ASSEMBLY OF TURBINE BLADES, WHERE R=0.1

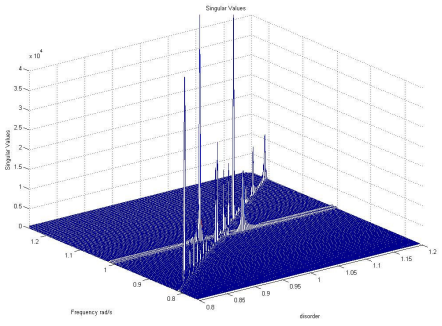

Figure D.1 : Max.Singular Values

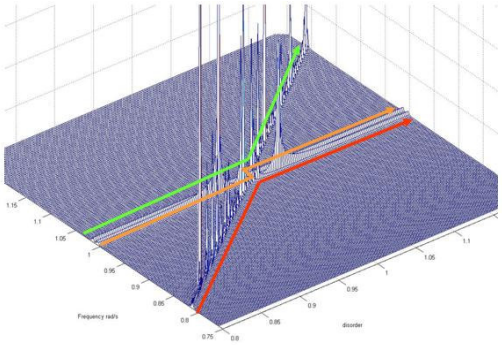

Figure D.2 : Max.Singular Values

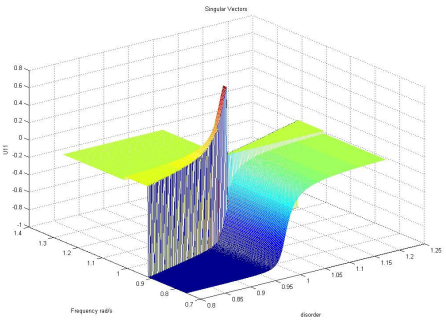

Figure D.3 : U11 component

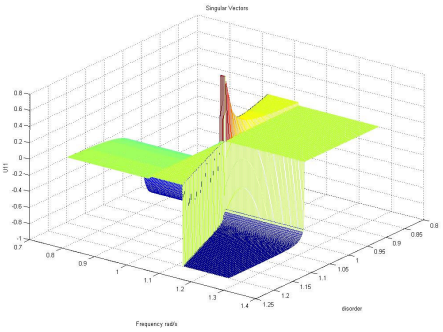

Figure D.4 : U11 component

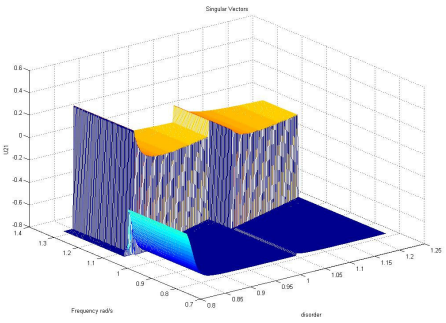

Figure D.5 : U21 component

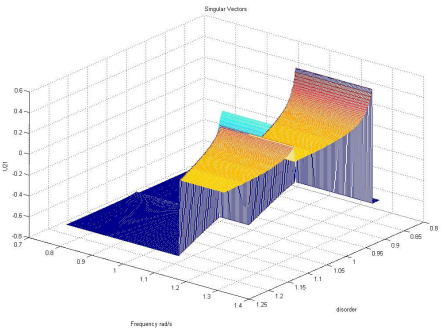

Figure D.6 : U21 component

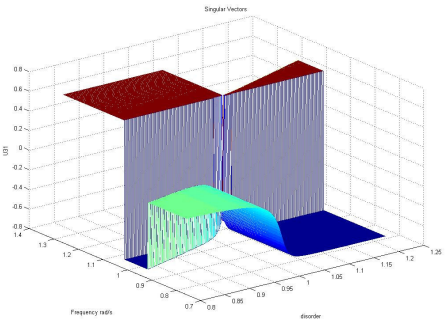

Figure D.7 : U31 component

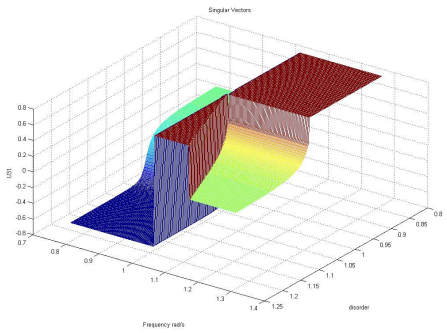

Figure D.8 : U31 component

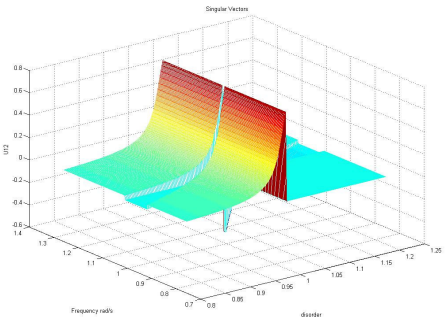

Figure D.9 : U12 component

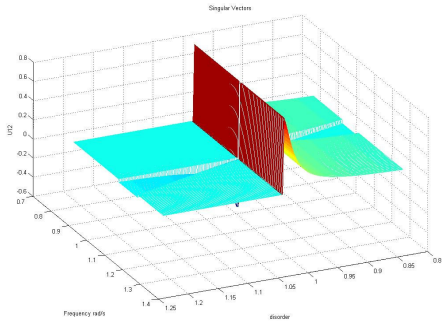

Figure D.10 : U12 component

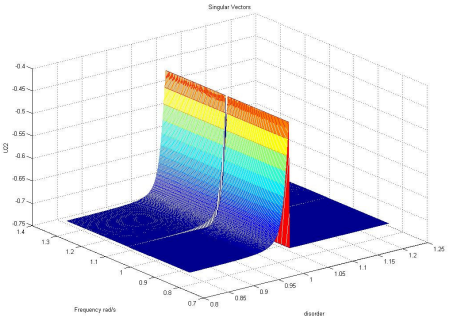

Figure D.11 : U22 component

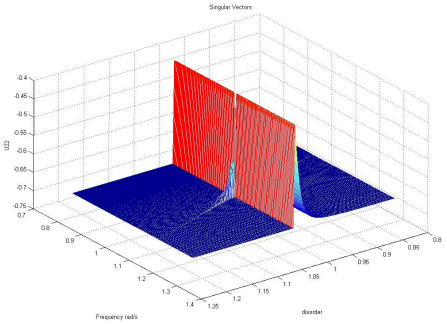

Figure D.12 : U22 component

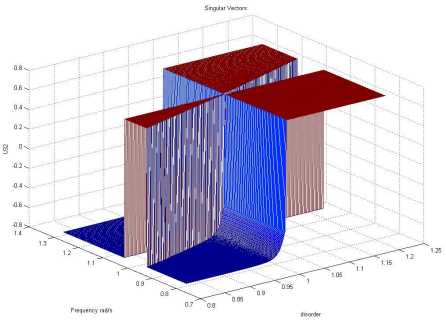

Figure D.13 : U32 component

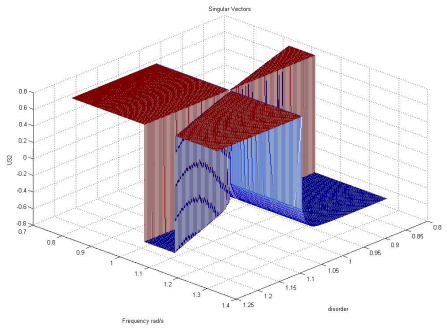

Figure D.14 : U32 component

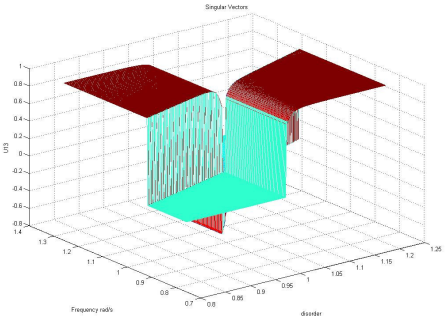

Figure D.15 : U13 component

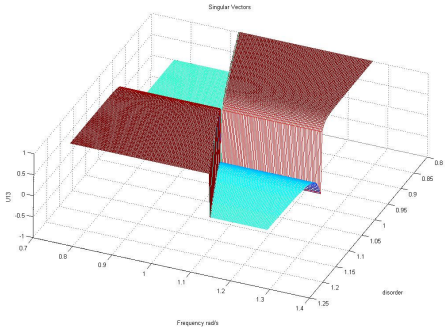

Figure D.16 : U13 component

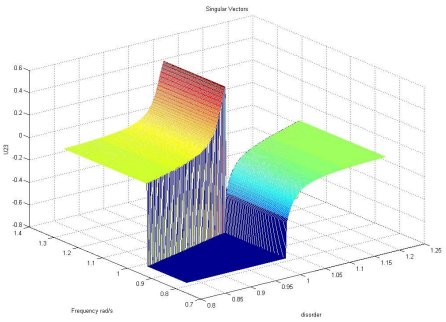

Figure D.17 : U23 component

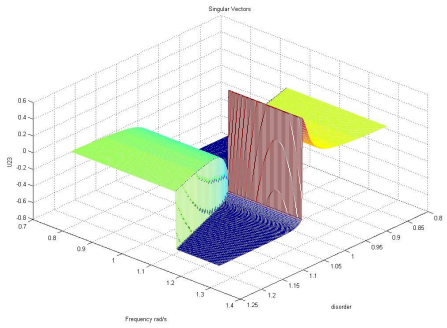

Figure D.18 : U23 component

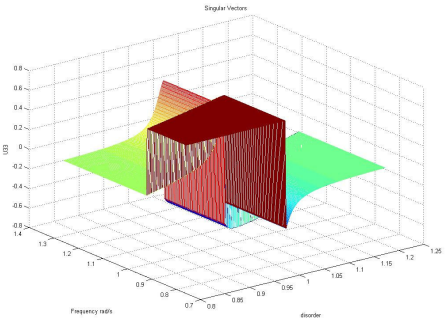

Figure D.19 : U33 component

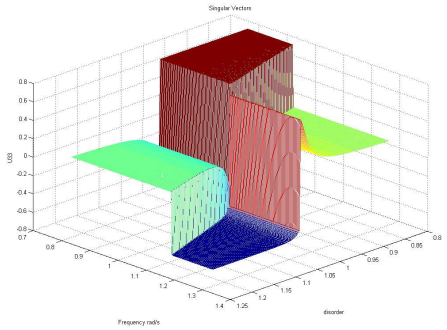

Figure D.20 : U33 component

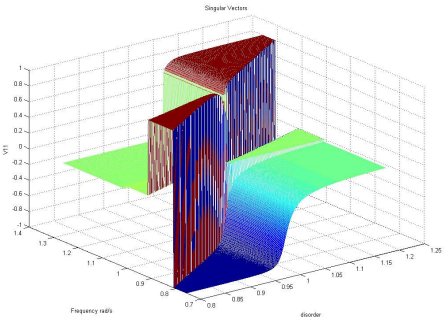

Figure D.21 : V11 component

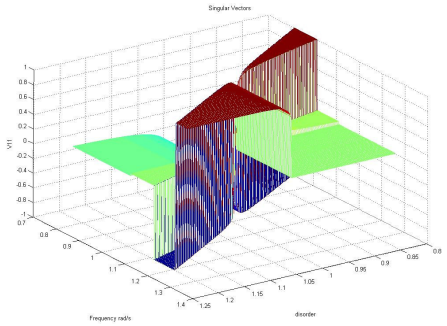

Figure D.22 : V11 component

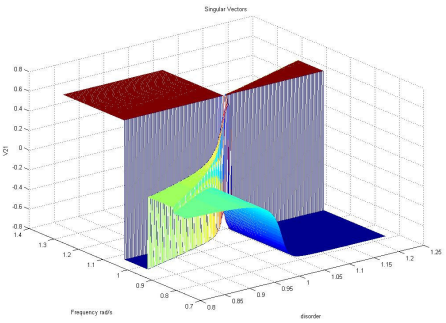

Figure D.23 : V21 component

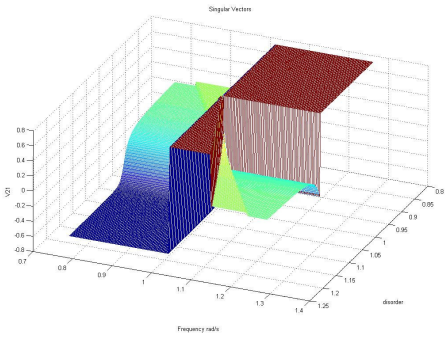

Figure D.24 : V21 component

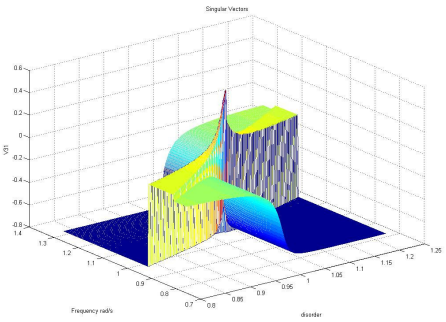

Figure D.25 : V31 component

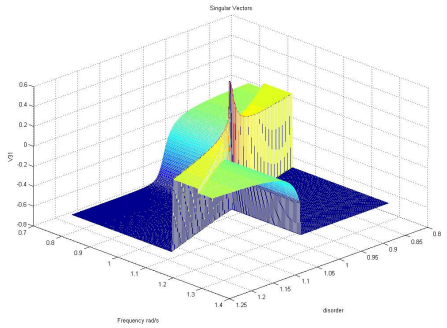

Figure D.26 : V31 component

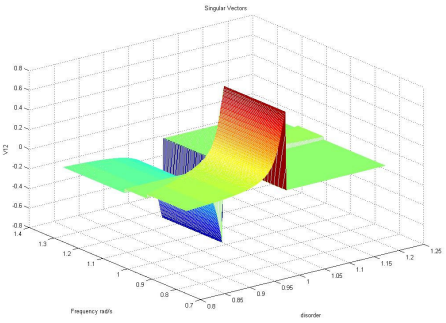

Figure D.27 : V12 component

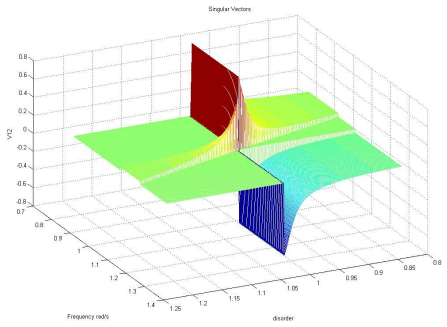

Figure D.28 : V12 component

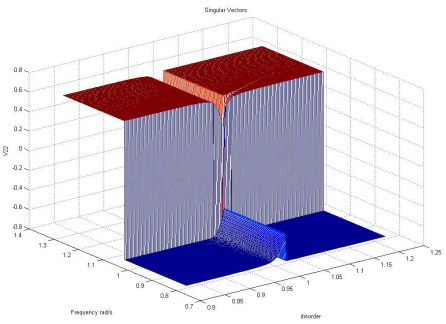

Figure D.29 : V22 component

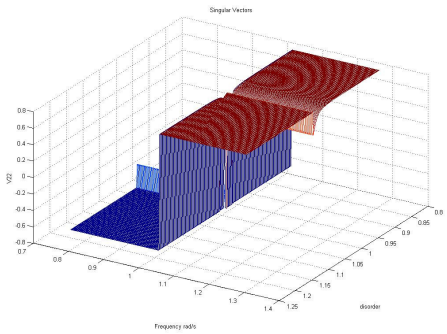

Figure D.30 : V22 component

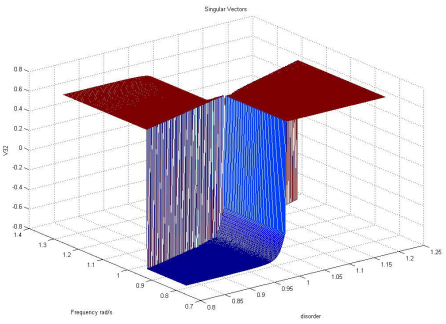

Figure D.31 : V32 component

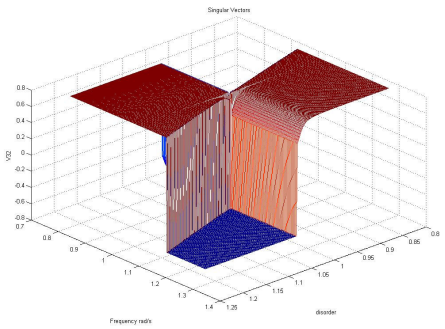

Figure D.32 : V32 component

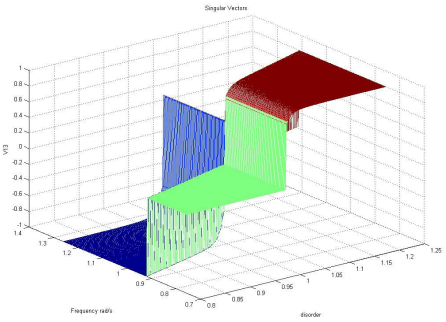

Figure D.33 : V13 component

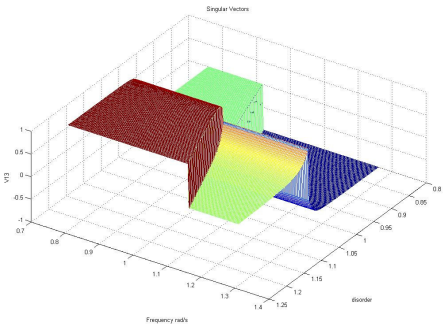

Figure D.34 : V13 component

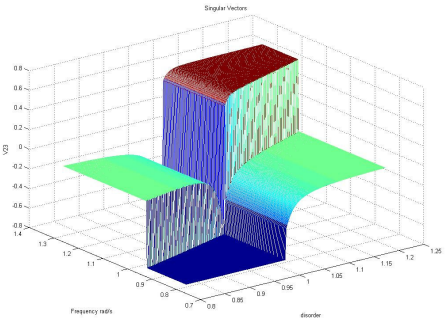

Figure D.35 : V23 component

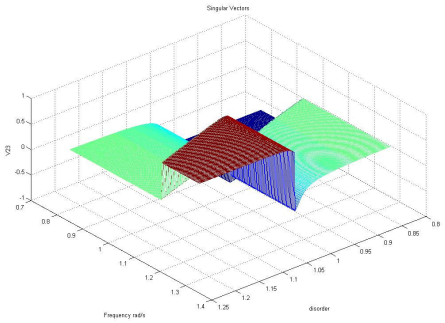

Figure D.36 : V23 component

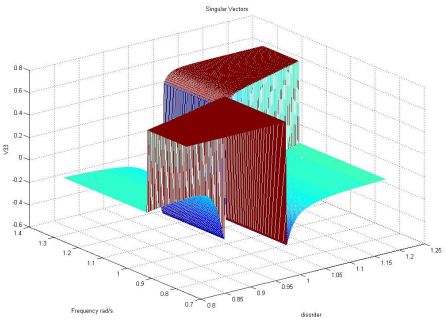

Figure D.37 : V33 component

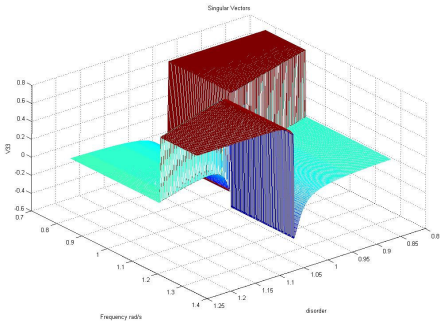

Figure D.38 : V33 component

Appendix-E

EFFECTS OF DISORDER ON SINGULAR VALUES AND VECTORS OF STRONGLY COUPLED ASSEMBLY OF TURBINE BLADES, WHERE R=1

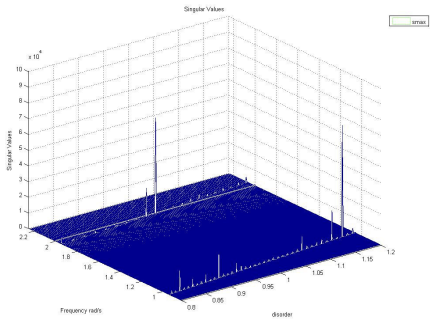

Figure E.1 : Max.Singular Values

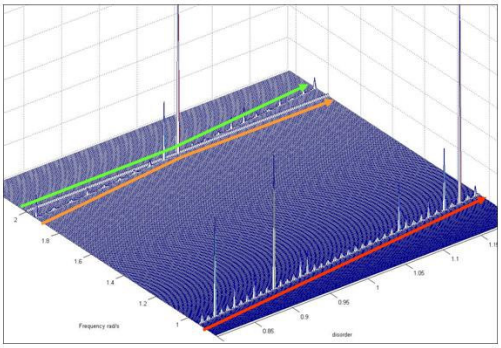

Figure E.2 : Max.Singular Values

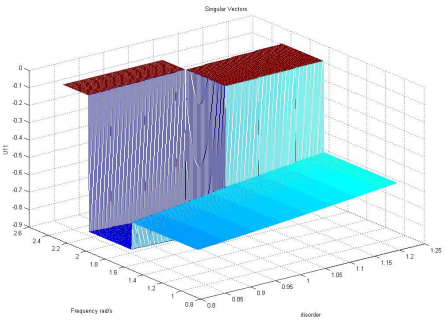

Figure E.3 : U11 component

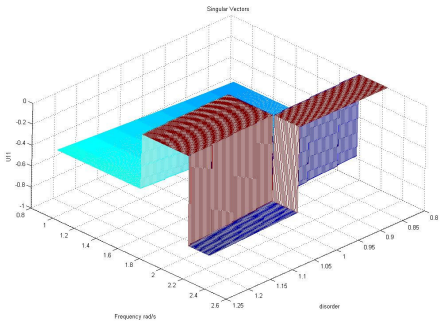

Figure E.4 : U11 component

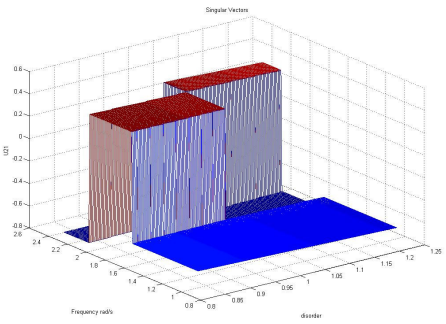

Figure E.5 : U21 component

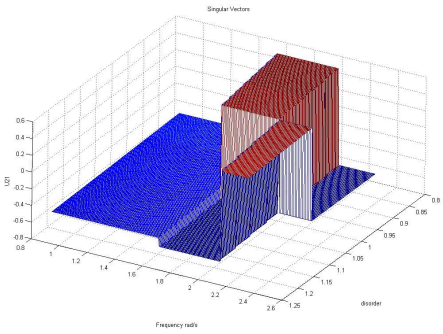

Figure E.6 : U21 component

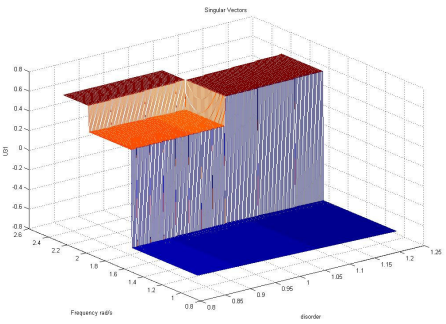

Figure E.7 : U31 component

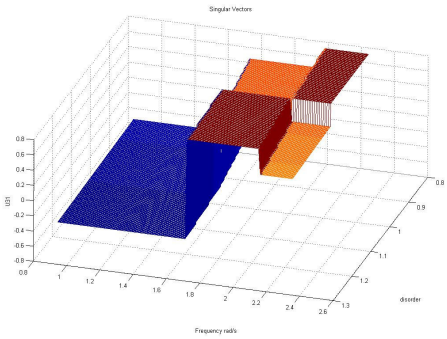

Figure E.8 : U31 component

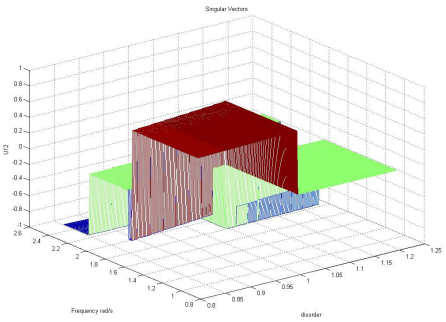

Figure E.9 : U12 component

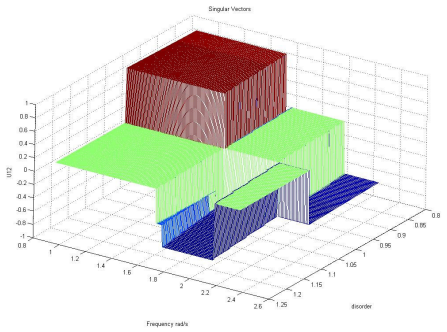

Figure E.10 : U12 component

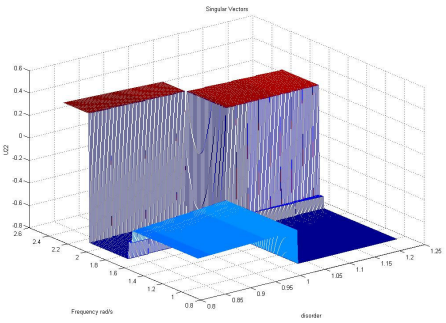

Figure E.11 : U22 component

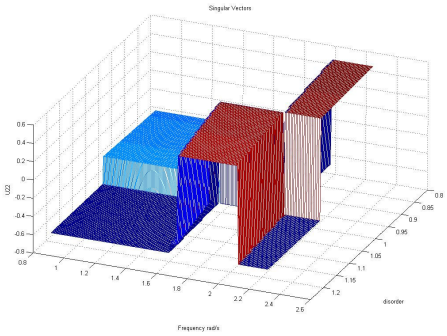

Figure E.12 : U22 component

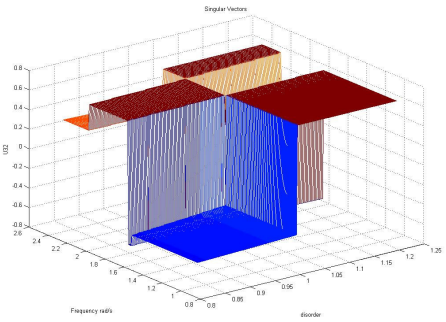

Figure E.13 : U32 component

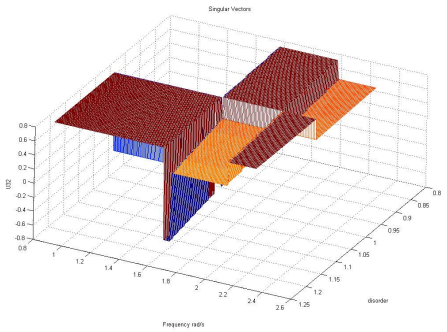

Figure E.14 : U32 component

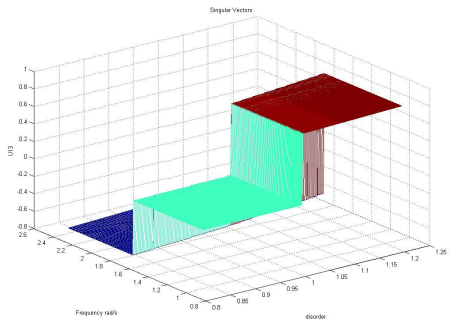

Figure E.15 : U13 component

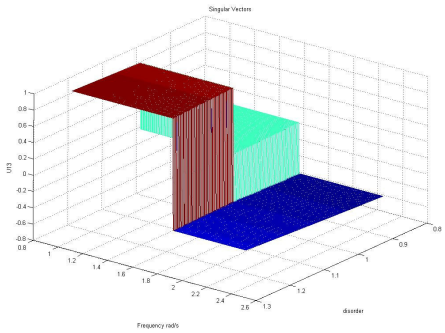

Figure E.16 : U13 component

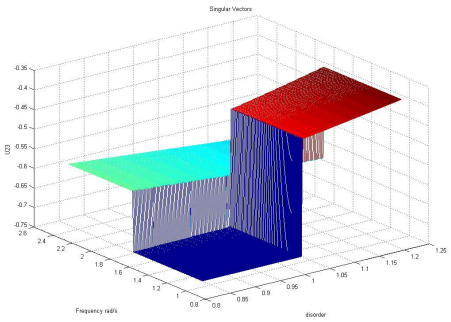

Figure E.17 : U23 component

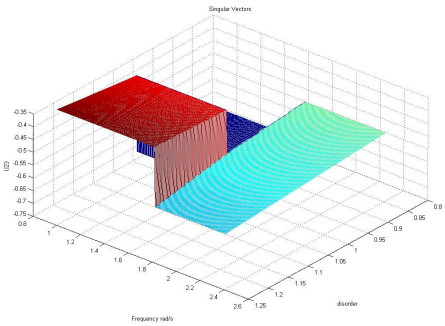

Figure E.18 : U23 component

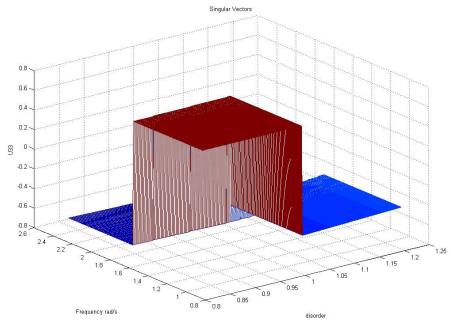

Figure E.19 : U33 component

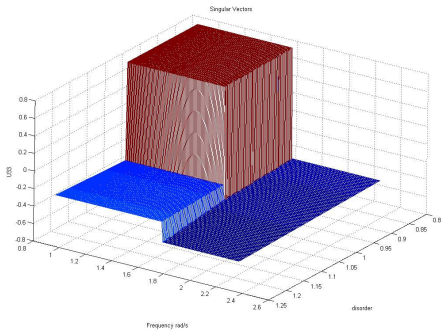

Figure E.20 : U33 component

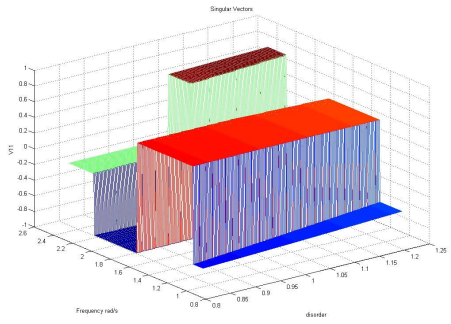

Figure E.21 : V11 component

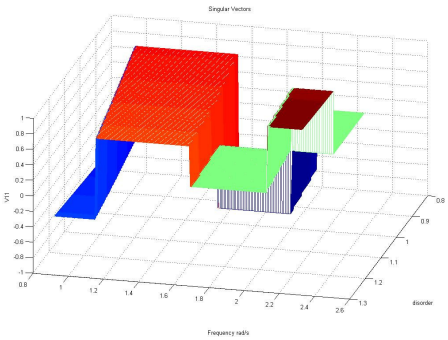

Figure E.22 : V11 component

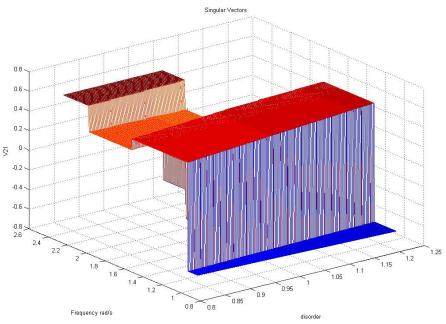

Figure E.23 : V21 component

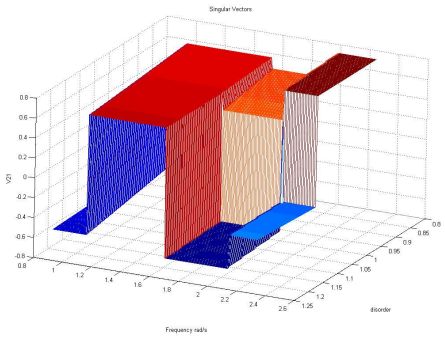

Figure E.24 : V21 component

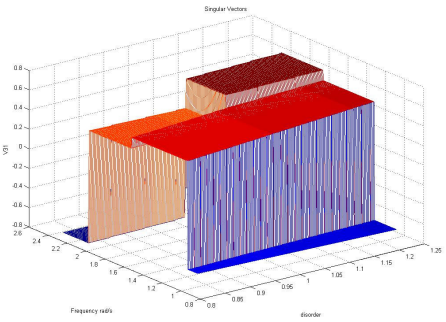

Figure E.25 : V31 component

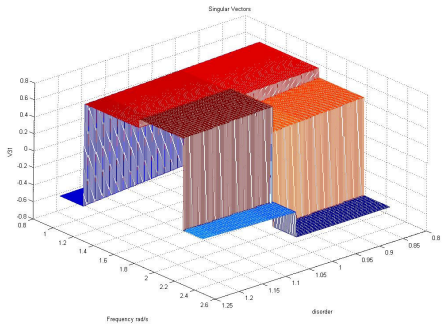

Figure E.26 : V31 component

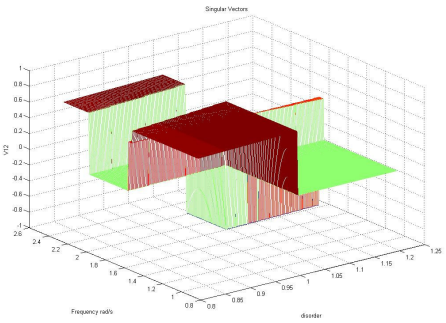

Figure E.27 : V12 component

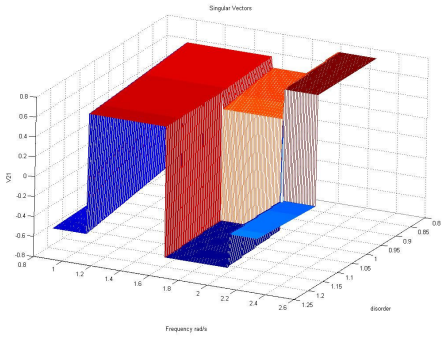

Figure E.28 : V12 component

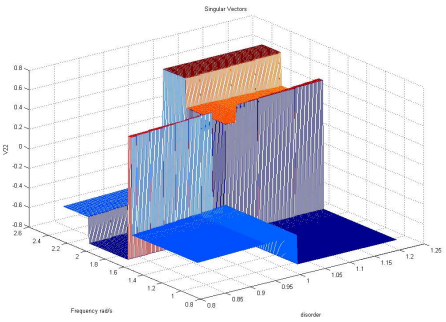

Figure E.29 : V22 component

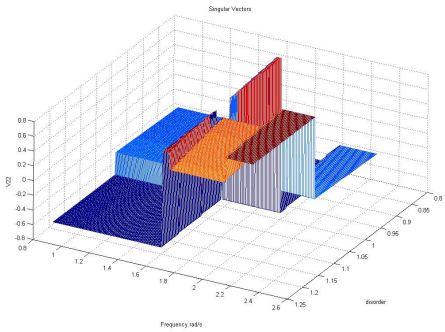

Figure E.30 : V22 component

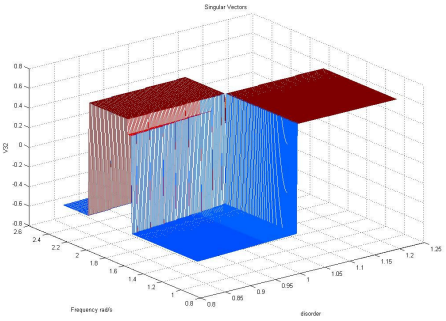

Figure E.31 : V32 component

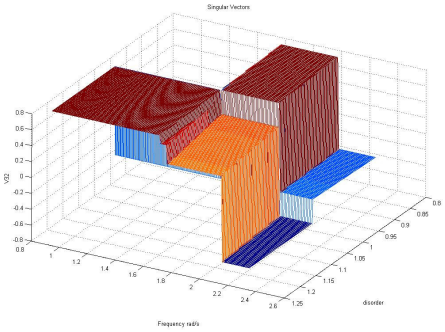

Figure E.32 : V32 component

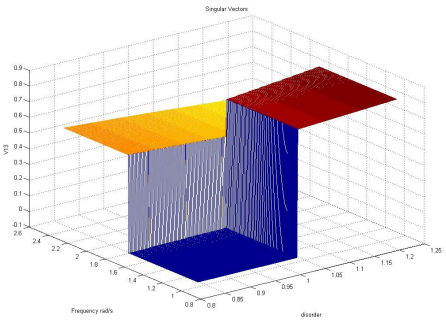

Figure E.33 : V13 component

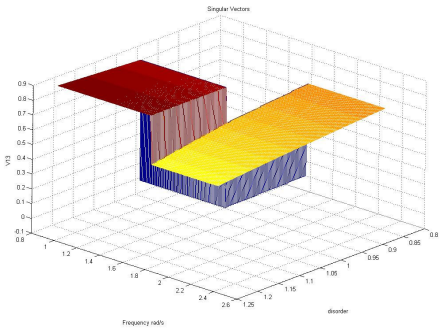

Figure E.34 : V13 component

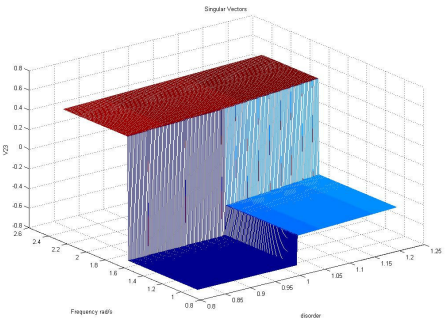

Figure E.35 : V23 component

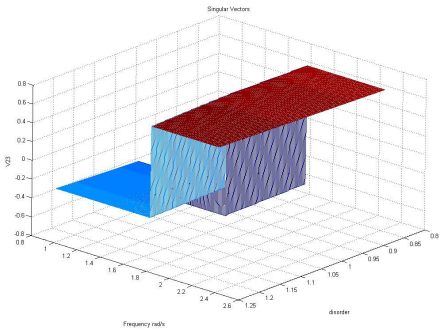

Figure E.36 : V23 component

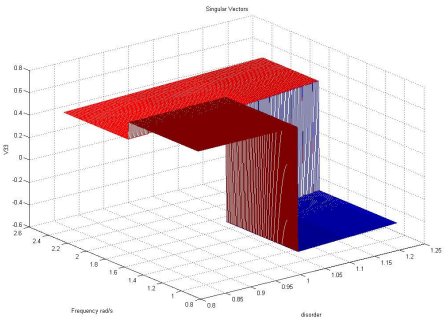

Figure E.37 : V33 component

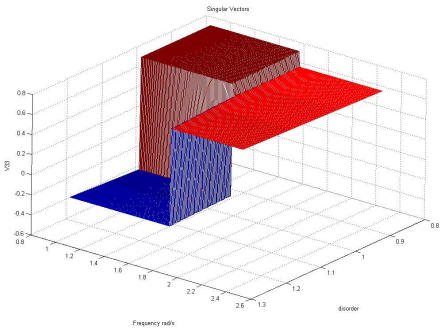

Figure E.38 : V33 component

AUTOBIOGRAPHY

Özgür Uyar was born in Eskişehir in 1978. He finished primary, secondary and high school educations in Eskişehir. In 1997 he started undergraduate education in Mechanical Engineering Department of Ege University. After finishing undergraduate education, he started graduate education in Solid Mechanics Program of Mechanical Engineering Department of İ.T.Ü.

He is stil working in THY Technic A.Ş. since July 2004.